BioMed Research International

Laboratory Medicine 2016

Guest Editors: Mina Hur, Patrizia Cardelli, and Giulio Mengozzi

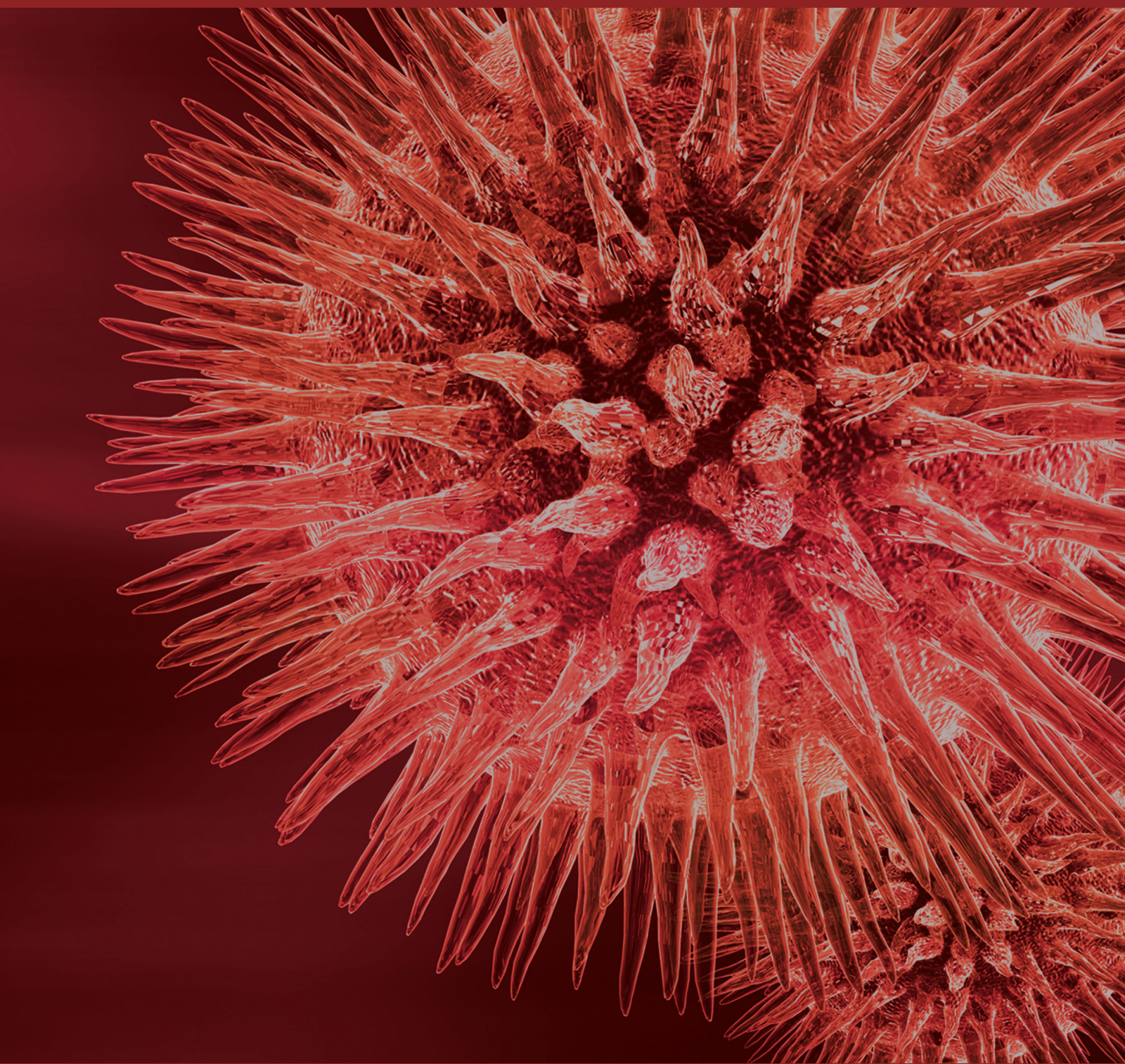

Laboratory Medicine 2016

BioMed Research International

Laboratory Medicine 2016

Guest Editors: Mina Hur, Patrizia Cardelli,
and Giulio Mengozzi

Contents

Hindawi Publishing Corporation
BioMed Research International
Volume 2016, Article ID 2913840, 2 pages
http://dx.doi.org/10.1155/2016/2913840

Editorial
Laboratory Medicine 2016

Mina Hur,[1] Patrizia Cardelli,[2] and Giulio Mengozzi[3]

[1]*Department of Laboratory Medicine, Konkuk University School of Medicine, 120-1 Neungdong-ro, Hwayang-dong, Gwangjin-gu, Seoul 05030, Republic of Korea*
[2]*Clinical and Molecular Medicine Department Azienda Ospedaliera Sant'Andrea, School of Medicine and Psychology, Sapienza University, Rome, Italy*
[3]*Laboratory Medicine Department, Clinical Biochemistry Laboratory, "Città della Salute e della Scienza" University Hospital of Turin, Turin, Italy*

Correspondence should be addressed to Mina Hur; dearmina@hanmail.net

Received 5 December 2016; Accepted 6 December 2016

Laboratory medicine is the bridging filed between basic research and clinical practice. Numerous candidate research findings and assays should be filtered, modified, and validated in terms of their analytical and clinical utility before being considered clinically useful. Clinical laboratory tests have essential roles in clinical decision-making from diagnosis to monitoring; accordingly, laboratory medicine is related to every specialty in clinical filed.

This is the third special issue on laboratory medicine, succeeding the issues of Laboratory Medicine and Laboratory Medicine 2014. This issue includes seven research papers covering a wide variety of interesting laboratory-related topics.

Three papers deal with the growing area of molecular diagnostic applications. The paper by Y. Chung et al. demonstrated the usefulness of multiplex real-time PCR for simultaneous pathogen detection and resistance profiling of Staphylococcal bacteremia. This direct multiplex real-time PCR assay of positive blood cultures containing Gram-positive cocci in clusters could provide essential information at the critical point of infection with a turnaround time of no more than 4 h. The paper by T. S. Kim et al. explored the significance of "not detected but amplified" (NDBA) results by real-time PCR method for human papilloma virus (HPV) DNA detection. They concluded that NDBA results in real-time PCR should be regarded as equivocal, not negative, and also addressed the adjustment of cut-off Ct value for HPV types for the appropriate result interpretation. Q.-Q. Zheng et al. performed a clinical and molecular study and identified a large *SLC25A13* deletion via sophisticated molecular analyses using peripheral blood lymphocytes in an infant with neonatal intrahepatic cholestasis caused by citrin deficiency.

The other three papers came from the conventional areas of hematology, immunoassay, and microbiology. M. Y. Lee et al. evaluated mean platelet volume (MPV) in tuberculosis (TB) patients and showed that MPV can be an inflammatory marker to determine the disease activity in TB patients. The paper by J. Samardzic et al. demonstrated that different vancomycin immunoassays contribute to the variability in vancomycin trough measurements in neonates. They suggested the impact of vancomycin immunoassays in neonatal matrix, supporting a switch to more advanced techniques (LC MS/MS). The other paper by S. H. Kim et al. explored the serotype distribution and antimicrobial resistance of *Streptococcus pneumoniae* isolates causing invasive and noninvasive pneumococcal diseases in Korea for seven years.

The last paper by J. S. Heo et al. covers the basic field of laboratory medicine. They demonstrated that poly-L-lysine provides favorable microenvironment for mesenchymal stem cells (MSCs) culture by reversing the replicative senescence that is typical of MSCs cultured in vitro. This method will

significantly contribute to effective preparation of MSCs for cellular therapy.

We hope that this special issue would solidify the unique value of this journal and contribute to the scientific development in this field.

Mina Hur
Patrizia Cardelli
Giulio Mengozzi

Hindawi Publishing Corporation
BioMed Research International
Volume 2016, Article ID 5170419, 7 pages
http://dx.doi.org/10.1155/2016/5170419

Research Article

Significance of "Not Detected but Amplified" Results by Real-Time PCR Method for HPV DNA Detection

Taek Soo Kim,[1] Mi Suk Lim,[2] Yun Ji Hong,[2] Sang Mee Hwang,[2] Kyoung Un Park,[2,3] Junghan Song,[2,3] and Eui-Chong Kim[1,3]

[1]*Department of Laboratory Medicine, Seoul National University Hospital, 101 Daehak-ro, Jongno-gu, Seoul 03080, Republic of Korea*
[2]*Department of Laboratory Medicine, Seoul National University Bundang Hospital, 82 Gumi-ro, 173 Beon-gil, Bundang-gu, Seongnam-si, Gyeonggi-do 13620, Republic of Korea*
[3]*Department of Laboratory Medicine, Seoul National University College of Medicine, 101 Daehak-ro, Jongno-gu, Seoul 03080, Republic of Korea*

Correspondence should be addressed to Kyoung Un Park; m91w95pf@snu.ac.kr

Received 24 March 2016; Accepted 21 November 2016

Academic Editor: Patrizia Cardelli

Human papillomavirus (HPV) infection is an important etiologic factor in cervical carcinogenesis. Various HPV DNA detection methods have been evaluated for clinicopathological level. For the specimens with normal cytological finding, discrepancies among the detection methods were frequently found and adequate interpretation can be difficult. 6,322 clinical specimens were submitted and evaluated for real-time PCR and Hybrid Capture 2 (HC2). 573 positive or "Not Detected but Amplified" (NDBA) specimens by real-time PCR were additionally tested using genetic analyzer. For the reliability of real-time PCR, 325 retests were performed. Optimal cut-off cycle threshold (C_T) value was evaluated also. 78.7% of submitted specimens showed normal or nonspecific cytological finding. The distributions of HPV types by real-time PCR were not different between positive and NDBA cases. For positive cases by fragment analysis, concordance rates with real-time PCR and HC2 were 94.2% and 84.2%. In NDBA cases, fragment analysis and real-time PCR showed identical results in 77.0% and HC2 revealed 27.6% of concordance with fragment analysis. Optimal cut-off C_T value was different for HPV types. NDBA results in real-time PCR should be regarded as equivocal, not negative. The adjustment of cut-off C_T value for HPV types will be helpful for the appropriate result interpretation.

1. Introduction

Persistent infection with one or more carcinogenic types of human papillomavirus (HPV) is an important etiologic factor in the development of cervical intraepithelial neoplasia and the progression to cervical cancer [1–3], the third common cause of cancer mortality in women worldwide [4]. HPV infection causes virtually all cases of cervical cancer and a less-defined, smaller fraction of vaginal, vulvar, penile, and anal cancers. Moreover, cervical infection with high risk HPV is associated with preterm birth and placental abnormalities in pregnant women [5]. Cytopathology has provoked the marked reduction of cervical cancer mortality, but its sensitivity is actually lower than that of HPV DNA assays [6]. Based upon this agreement, some researchers insisted that the screening interval could be extended to 6 years (10 years for women aged 50 and over) in HPV testing replaced cytology as the primary screening test [7].

Until now, more than 100 HPV types have been identified and fully sequenced [8]. Approximately 40 HPV types infect the anogenital tract and fifteen HPV types, 16, 18, 31, 33, 35, 39, 45, 51, 52, 56, 58, 59, 68, 73, and 82, are considered as highly oncogenic (high risk HPV) and HPV types 26, 53, and 66 as probably oncogenic, while HPV types 6, 11, 40, 42, 43, 44, 54, 61, 70, 72, 81, and CP6108 are classified as viruses with low oncogenic potential (low risk HPV) [9]. As well as in nearly all abnormal cytology samples, high risk HPV DNA has been detected in a high percent of cytological "negative for intraepithelial lesion or malignancy (NILM)" samples [10, 11]. In other words, HPV is known to be detectable in virtually all abnormal cervical samples; how about in NILM samples? So we evaluated "Not Detected but Amplified (NDBA)" results

that could be low-copy of high risk HPV DNA and/or cross-reaction with nonhigh risk HPV types, when using real-time PCR method compared with the results for other assays.

2. Materials and Methods

2.1. Study Population. From April 2010 to July 2012, 6,322 clinical specimens were submitted for HPV DNA test at Seoul National University Bundang Hospital. 814 specimens showing positive and NDBA results by real-time PCR method were evaluated in this study.

2.2. Papanicolaou (Pap) Tests. All women were first subjected to a conventional cervicovaginal Pap smear. Pap smear abnormalities were interpreted and classified by using the 2001 Bethesda System [12]. An additional sample for the detection of HPV DNA was taken from the cervix by using the sampling kit for the Hybrid Capture 2 (HC2; Qiagen, Hilden, Germany).

2.3. HPV Detection by Real-Time PCR. The Abbott RealTime High Risk HPV test (Abbott, Wiesbaden, Germany) was performed with the fully automated nucleic acid preparation instrument *m*2000sp (Abbott) and the real-time PCR instrument *m*2000rt (Abbott) by following the manufacturer's instructions as previously described [13]. The assay uses four channels for the detection of fluorescent signals: one for the detection of an internal control (136-bp region of human β-globin), a second one for the detection of HPV 16, a third one for the detection of HPV 18, and a fourth one for the detection of the high risk common 12 HPV types, that is, 31, 33, 35, 39, 45, 51, 52, 56, 58, 59, 66, and 68. PCR amplification of HPV targets was achieved using a modified GP5+/6+ primer mixture consisting of three forward and two reverse primers. The assay cut-off is set at a fixed cycle threshold (C_T) value of 32, which is already established by the manufacturer. On the interpretation of amplification curve, amplification above the target C_T value refers to new term "Not Detected but Amplified (NDBA)." For 325 of 814 specimens showing NDBA or positive results, the specimens were refrigerated at 4°C. After 2 or 4 days, DNA extraction and real-time PCR were repeated by the same technologist.

2.4. HR HPV Detection by HC2 Assay. HC2 test was also performed on the Digene Specimen Transport Medium (STM; Qiagen, Hilden, Germany) specimen throughout the study in accordance with the manufacturer's instructions and as previously described [14]. Specimens are stored in the STM tubes at 4°C until use. The hybridization RNA probes used were directed against high risk HPV types 16, 18, 31, 33, 35, 39, 45, 51, 52, 56, 58, 59, and 68, as described by the manufacturer. Samples were classified as high risk HPV DNA positive if the relative light unit/cut-off (RLU/CO) ratio reading obtained from the luminometer was 1.0 or greater.

2.5. HPV Detection Using Genetic Analyzer. Using 3130xl genetic analyzer (Applied Biosystems, Foster, USA), fragment analysis were performed. To detect the HPV type(s) present in a sample, the samples showing positive and NDBA results by real-time PCR were tested additionally and this method is capable of recognizing 18 different HPV types including 13 high risk (16, 18, 31, 33, 35, 39, 45, 51, 52, 56, 58, 59, and 68) and 5 low risk types. DNA was extracted using QIAamp viral RNA kit (Qiagen, Hilden, Germany) and amplified through 40 cycles consisting of 30 sec at 95°C, 90 sec at 60°C, and 90 sec at 72°C. PCR products were purified with 1 μL of shrimp alkaline phosphatase (SAP) under the condition of 35 min at 35°C followed by 15 min at 65°C. Purified PCR products were analyzed with GeneMapper software version 4.0 (Applied Biosystems, Foster, USA).

2.6. Statistical Analysis. Statistical analysis of the data was performed and included the 2-tailed chi-square test for comparison of NDBA results and positive results in real-time PCR. The statistics were calculated using Analyse-it (version 2.30, Analyse-it Software, Ltd., Leeds, UK). Statistical significance was set at a level of < 0.05.

3. Results

3.1. Specimen Demographics. Totally, 6,322 clinical specimens from health promotion center (6,036, 95.5%), the department of obstetrics and gynecology (272, 4.3%), and other departments (14, 0.2%) were submitted at the Department of Laboratory Medicine, Seoul National University Bundang Hospital. Through the chart reviews, Pap smear results were reported as "negative for intraepithelial lesion or malignancy (NILM)" in 4516 (71.4%) specimens, "reactive cellular change" in 117 (1.9%) specimens, "reactive cellular changes associated with inflammation (includes typical repair)" in 347 (5.5%) specimens, "high grade squamous intraepithelial lesion (HSIL)" in 7 (0.1%) specimens, "low grade squamous intraepithelial lesion (LSIL)" in 26 (0.4%) specimens, "atypical squamous cells of undetermined significance (ASC-US)" in 115 (1.8%) specimens, "atrophy" in 251 (3.0%) specimens, "chronic cervicitis" in 3 (0.1%) specimens, and the descriptive reports not mentioned above in 749 (11.9%) specimens. In 191 (3.0%) specimens, Pap smear results were not reported or tests were not performed.

3.2. Concordance among Multiple Methods. Positive or NDBA results in real-time PCR were shown in 816 (12.9%) specimens. For 763 (12.1%) specimens, fragment analysis was performed and high risk HPV types were identified in 582 (9.2%) specimens. Positivity for HC2 was shown in 544 (8.6%) specimens and high risk HPV types for real-time PCR were identified in 593 (9.4%) specimens. In 479 (7.6%) specimens, HC2 and real-time PCR revealed concordant results (positive in HC2 and high risk HPV types in real-time PCR).

In 593 (9.4%) and 221 (3.5%) out of 6,322 specimens, positive and NDBA results for high risk HPV types by real-time PCR were obtained and described with mean C_T value (Table 1). The distribution of high risk HPV type for positive and NDBA results are not significantly different ($p > 0.05$).

In NDBA results by real-time PCR, HC2 shows correspondence rate of 20.4% in HRC, 21.1% in type 16, and 38.1% in type 18, respectively. For 14 mixed HPV type, HC2 revealed

Table 1: Distribution of high risk HPV types for positive and NDBA results by real-time PCR.

	Type 16	Type 18	HRC	Type 16 & HRC	Type 18 & HRC	Types 16 & 18	Total
Positive	55	33	482	12	10	1	593
C_{T_Mean}	25.1	26.5	25.6	25.0/26.9	25.2/25.4	24.1/23.2	
NDBA	19	21	167	9	5	0	221
C_{T_Mean}	34.6	34.9	34.0	34.6/34.3	35.5/34.0	—	

negativity. In positive results by real-time PCR, HC2 revealed the positivity in 82.0% (HRC), 72.7% (type 16), 66.7% (type 18), and 95.7% (mixed type), respectively (Table 2).

For the results by fragment analysis, real-time PCR shows the detection rates of 79.7% (type 16), 92% (type 18), 96.4% (HRC), and 32.5% (mixed type) including NDBA. HC2 detected 57.6% (type 16), 68.0% (type 18), 78.4% (HRC), and 75.0% (mixed type) for types identified by fragmented analysis (Table 3). Overall, real-time PCR detects correctly 516 (90.1%) of 573 fragments analysis results. On the other hand, HC2 detects 433 (75.6%) of fragment analysis. For NDBA results identified as high risk HPV by fragment analysis, real-time PCR revealed 77.0% (67/87) of concordance rate, whereas HC2 showed 27.6% (24/87) (Table 4).

3.3. Result Interpretation by Cycle Threshold (C_T) Changes. Up to the change of cut-off C_T from 31 to 34, sensitivity and specificity of real-time PCR were described in Table 5. When drawing ROC decision plot, areas under the ROC curve (AUCs) were 0.86 for HPV type 16, 0.98 for HPV type 18, and 0.76 for HRC. Optimal cut-off C_T values were 35.58 in type 16, 34.01 in type 18, and 31.99 in high risk common types.

3.4. Repeatability. For evaluation of repeatability, retests were performed in 325 specimens showing the presence of type 16 HPV DNA, type 18 HPV DNA, or HRC HPV DNA including NDBA results. For type 16 HPV DNA, retests were done in 53 specimens and amplification curve was observed in 43 (81.1%) specimens. As shown in Figure 1, SD difference was 0.873 and upper and lower margins of 95% limits of agreement were 1.384 and −2.037, respectively. In 43 specimens showing amplification, 5 retest results showed C_T value larger than 32. For 10 specimens, no amplification curve was observed at repetition, and they showed initial C_T value larger than 32. In case of type 18, retests were performed in 22 specimens and 15 specimens showed amplification at repetition. No cases revealed C_T value larger than 32 and 7 cases did not show any amplification at repetition. The initial C_T values in 7 cases were larger than 32. In 15 specimens, SD difference was 0.842 and upper and lower margins of 95% limits of agreement were 1.558 and −1.744, respectively.

In case of HRC HPV DNA, 265 specimens showed amplification at repetition and SD of difference was 1.3. The upper and lower margins of 95% limits of agreement were 2.352 and −2.744, respectively. In 17 specimens, no amplification was observed at repetition. For 10 specimens showing initial C_T value larger than 32, 3 specimens showed C_T value under 32 at repetition. For 18 specimens larger than 32 C_T value at repetition, 11 specimens showed initial C_T value under 32. Ten of 17 specimens showing no amplification showed C_T values larger than 32 at initial test.

4. Discussion

Differently from other previous evaluation studies, our study population was mainly limited to the specimens showing the normal or nonspecific cytological findings (NILM, reactive cellular change, atrophy, etc.). So, the cytological or pathologic finding was not helpful for the prediction of HPV existence in this study. HPV load and cumulative incidence of cervical lesion are known to be significantly correlated [15, 16]. At the view of guideline change, the position of HPV DNA test moves from the adjunctive test method to cotest method. Although PCR has been the "gold standard" technique in HPV diagnostics, the disadvantages of PCR are its extremely high analytical sensitivity and potential for contamination, leading to false-positive results [14]. But, as revealed in NDBA results, real-time PCR results showing amplification curve above C_T were needed to be reconsidered carefully. The accuracy of detection of high risk HPV is known to be significantly higher with Abbott RealTime High Risk HPV than HC2 [17]. HC2 technology measures sensitivity versus defined clinical endpoints (CIN 3+/SCC) and ensures reporting of positive results only when risk of disease progression exists. The limit of detection of HC2 is 5,000 copies/mL; it is much lower when compared to less than 10 copies of PCR [18].

Also, in results showing specific HPV types by fragment analysis, real-time PCR shows higher concordance rate than HC2. Particularly, in specimens showing NDBA, HC2 tends to reveal negative results much more frequently. Considering the distributions of HPV types in NDBA and positive results, the concordance rates between fragment analysis and real-time PCR, and the results of repeatability tests, NDBA results should be regarded as equivocal or positive, not as negative.

According to AUC value for the C_T change, appropriate C_T was different for HPV types. In HRC, C_T of 32 is appropriate as described by manufacturer, but in types 16 and 18, C_T of 33 or 34 will be more suitable.

In 167 results with negative result by HC2 and NDBA by real-time PCR, 58 (34.7%) results were assigned to the specific high risk HPV types by fragment analysis. Out of 58 results, 52 (89.6%) high risk HPV types were detected by real-time PCR and fragment analysis. Using HC2 only, false-negative results can be reported in specimens with low level persistent infection. The clinical relevance and implications of low level persistence of HPV are not clearly known, nor is the cause of low level persistence. In a previous study by Collins et al., integration of HPV 16 resulted in a markedly lower viral copy

Table 2: Result comparison of real-time PCR with HC2 and fragment analysis.

Real-time PCR		HC2			Fragment analysis								Total
		Positive	Negative	Error	Type 16	Type 18	HRC[a]	Type 16 & HRC	Type 18 & HRC	Types 16 & 18	Not tested	Not detected	
Positive	Type 16	40 (72.7%)	14	1	39 (70.9%)	0	1	8	0	0	7	0	55
	Type 18	22 (66.7%)	10	1	0	22 (66.7%)	1	0	2	0	2	6	33
	HRC	395 (82.0%)	86	1	3	0	375 (77.8%)	12	1	0	38	53	482
	Type 16 & HRC	12 (100%)	0	0	4	0	1	7 (58.3%)	0	0	0	0	12
	Type 18 & HRC	9 (90.0%)	1	0	0	2	2	0	5 (50.0%)	0	1	0	10
	Types 16 & 18	1	0	0	0	0	0	0	0	1	0	0	1
	Total	479	111	3	46	24	380	27	8	1	48	59	593
NDBA	Type 16	4 (21.1%)	15	0	8 (42.1%)	0	6	0	0	0	0	5	19
	Type 18	8 (38.1%)	13	0	1	1 (4.8%)	1	0	2	0	2	14	21
	HRC	34 (20.4%)	127	6	2	0	58 (34.7%)	2	0	0	2	103	167
	Type 16 & HRC	0	9	0	1	0	2	0	0	0	0	6	9
	Type 18 & HRC	0	5	0	1	0	1	1	0	0	0	2	5
	Types 16 & 18	0	0	0	0	0	0	0	0	0	0	0	0
	Total	46	169	6	13	1	68	3	2	0	4	130	221

[a]High risk common.

Table 3: Result comparison of fragment analysis with real-time PCR and HC2 in positive results with real-time PCR.

Fragment analysis	Real-time PCR						HC2			Total
	Type 16	Type 18	HRC[a]	Type 16 & HRC	Type 18 & HRC	Types 16 & 18	Positive	Negative	Error	
Type 16	39 (84.8%)	0	3	4	0	0	31 (67.4%)	14	1	46
Type 18	0	22 (91.7%)	0	0	2	0	17 (70.8%)	6	1	24
HRC	1	1	375 (98.7%)	1	2	0	331 (87.1%)	48	1	380
Type 16 & HRC	8	0	12	7 (25.9%)	0	0	22 (81.4%)	5	0	27
Type 18 & HRC	0	2	1	0	5 (62.5%)	0	7 (87.5%)	1	0	8
Types 16 & 18	0	0	0	0	0	1	1	0	0	1
Total	48	25	391	12	9	1	409	74	3	486

[a]High risk common.

Table 4: Result comparison of fragment analysis with real-time PCR and HC2 in NDBA results with real-time PCR.

Fragment analysis	Real-time PCR						HC2			Total
	Type 16	Type 18	HRC[a]	Type 16 & HRC	Type 18 & HRC	Types 16 & 18	Positive	Negative	Error	
Type 16	8 (61.5%)	1	2	1	1	0	3 (23.1%)	9	1	13
Type 18	0	1	0	0	0	0	0	1	0	1
HRC	6	2	58 (84.1%)	2	1	0	21 (30.4%)	44	4	69
Type 16 & HRC	0	0	2	0	1	0	0	3	0	3
Type 18 & HRC	0	1	0	0	0	0	0	1	0	1
Types 16 & 18	0	0	0	0	0	0	0	0	0	0
Total	14	5	62	3	3	0	24	58	5	87

[a]High risk common.

Table 5: Comparison of four cut-off C_T values in real-time PCR to fragment analysis for detection of high risk HPV ($n = 763$).

HPV type	Cut-off C_T	Number of specimens with results				% Sensitivity	% Specificity
		TP[b]	FP[c]	TN[d]	FN[e]		
16	31	54	2	671	36	60.0	99.7
	32	59	2	671	31	65.6	99.7
	33	62	2	671	28	68.9	99.7
	34	65	6	667	25	72.2	99.1
18	31	31	7	721	4	88.6	99.0
	32	32	9	713	3	91.4	98.8
	33	33	10	718	2	94.3	98.6
	34	33	12	716	2	94.3	98.4
HRC[a]	31	369	49	218	127	74.4	81.6
	32	403	62	205	93	81.3	76.8
	33	424	81	186	72	85.5	69.7
	34	447	107	160	49	90.1	59.9

[a]High risk common.
[b]True positive.
[c]False positive.
[d]True negative.
[e]False negative.

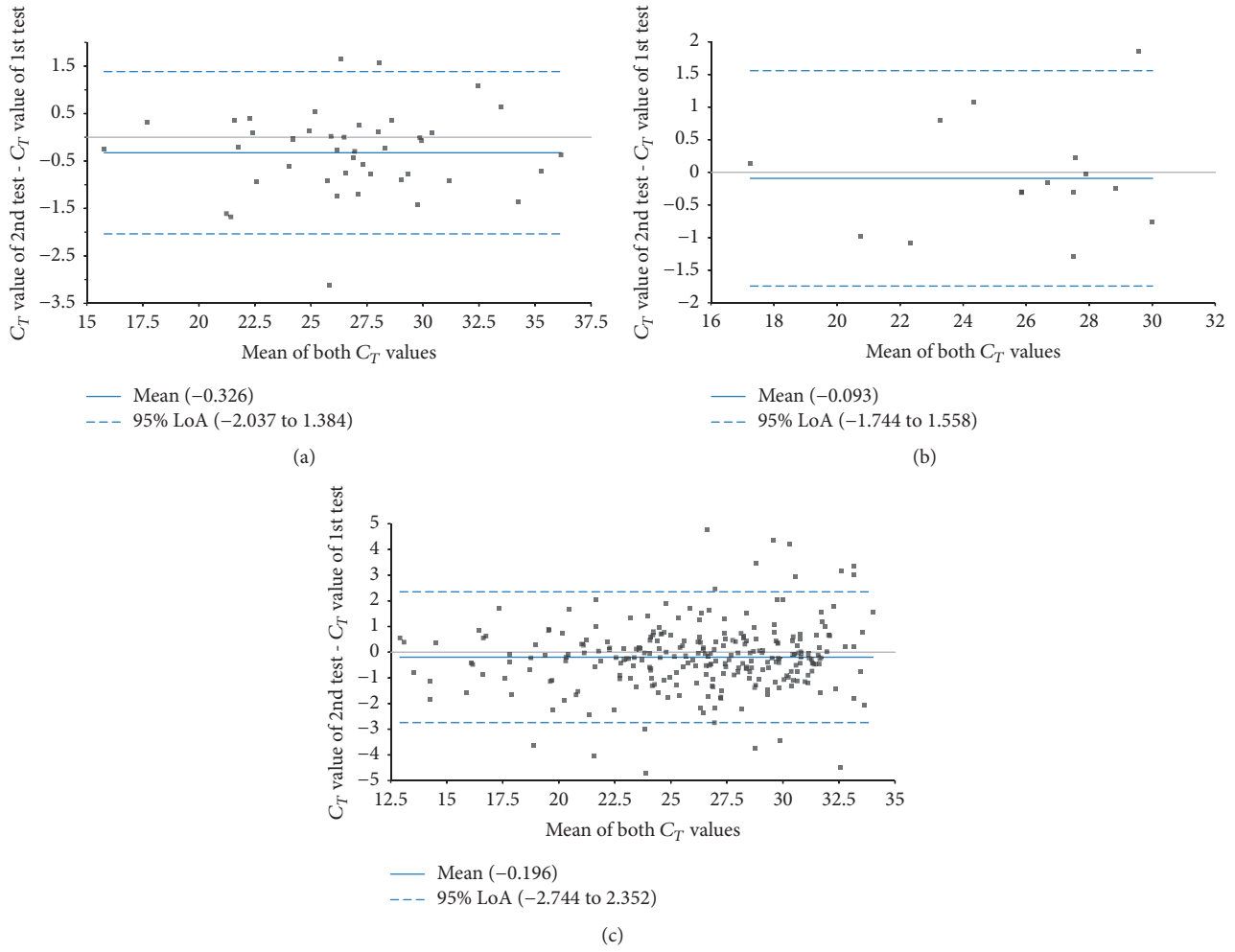

Figure 1: Difference plot in real-time PCR results for detection of specific HPV type. (a) Type 16: 43 specimens. (b) Type 18: 15 specimens. (c) High risk common: 265 specimens.

number per cell [19]. Integration seems to be an important event in the series of events leading to the development of cervical cancer [19, 20]. Alternatively, low level persistence may signify containment of HPV-infected cells by cellular immunity resulting in a small lesion that may be difficult to adequately sample by standard methods. Therefore, the clinical significance of low level persistent infection of HPV and the appropriate interpretation of low level HPV DNA existence become more important [21].

5. Conclusions

Other reports specifying NDBA do not exist at our level of knowledge. But there is a possibility that the NDBA is expected to be described as "undetected" in the published papers. According to a retrospective study, there were 14 (2.2%) undetected cases in 635 CIN III cases using HC2 [22]. In addition, as around 50% of ASC-US specimens will be tested high risk HPV positive, the accurate early detection of relevant infections by noninvasive and cost-effective tests is thought to be fundamental [23].

To figure out the accurate infection status of HPV (new infection, reinfection, or persistent infection), NDBA results by real-time PCR should not be overlooked and regarded as equivocal, not negative. Additionally, the adoption of different cut-off C_T value is recommended for each high risk HPV type. Large-scale research can be needed to be backed up, as HPV infection may disappear on its own in long-term follow-up through the actions of the immune system, may remain just persistent, or contribute to the occurrence of the cancerous lesions in some patients. Psychosocial stresses from further work up can be minimized through the counselling of physicians. Virtually, all cases of cervical cancer are caused by HPV and no test will be perfect [24].

Ethical Approval

This study was reviewed and approved by the Seoul National University Bundang Hospital Institutional Review Board (IRB nos. B-1207/164-304 and B-1501-284-116).

Competing Interests

The authors declare that there is no conflict of interests.

Acknowledgments

This study is funded by Seoul National University Bundang Hospital Research Fund (Grants nos. 11-2012-011 and 02-2013-068).

References

[1] G. Y. F. Ho, R. Bierman, L. Beardsley, C. J. Chang, and R. D. Burk, "Natural history of cervicovaginal papillomavirus infection in young women," *The New England Journal of Medicine*, vol. 338, no. 7, pp. 423–428, 1998.

[2] N. F. Schlecht, S. Kulaga, J. Robitaille et al., "Persistent human papillomavirus infection as a predictor of cervical intraepithelial neoplasia," *Journal of the American Medical Association*, vol. 286, no. 24, pp. 3106–3114, 2001.

[3] L. A. Koutsky, K. K. Holmes, C. W. Critchlow et al., "A cohort study of the risk of cervical intraepithelial neoplasia grade 2 or 3 in relation to papillomavirus infection," *The New England Journal of Medicine*, vol. 327, no. 18, pp. 1272–1278, 1992.

[4] M. Arbyn, X. Castellsagué, S. de sanjosé et al., "Worldwide burden of cervical cancer in 2008," *Annals of Oncology*, vol. 22, no. 12, pp. 2675–2686, 2011.

[5] Z. Zuo, S. Goel, and J. E. Carter, "Association of cervical cytology and HPV DNA status during pregnancy with placental abnormalities and preterm birth," *American Journal of Clinical Pathology*, vol. 136, no. 2, pp. 260–265, 2011.

[6] M. F. Evans, C. S.-C. Adamson, L. M. Schned et al., "HPV is detectable in virtually all abnormal cervical cytology samples after reinvestigation of HPV negatives with multiple alternative PCR tests," *Diagnostic Molecular Pathology*, vol. 19, no. 3, pp. 144–150, 2010.

[7] H. C. Kitchener, C. Gilham, A. Sargent et al., "A comparison of HPV DNA testing and liquid based cytology over three rounds of primary cervical screening: extended follow up in the ARTISTIC trial," *European Journal of Cancer*, vol. 47, no. 6, pp. 864–871, 2011.

[8] E.-M. De Villiers, C. Fauquet, T. R. Broker, H.-U. Bernard, and H. Zur Hausen, "Classification of papillomaviruses," *Virology*, vol. 324, no. 1, pp. 17–27, 2004.

[9] N. Muñoz, F. X. Bosch, S. de Sanjosé et al., "Epidemiologic classification of human papillomavirus types associated with cervical cancer," *The New England Journal of Medicine*, vol. 348, no. 6, pp. 518–527, 2003.

[10] A.-B. Moscicki, L. Widdice, Y. Ma et al., "Comparison of natural histories of human papillomavirus detected by clinician-and self-sampling," *International Journal of Cancer*, vol. 127, no. 8, pp. 1882–1892, 2010.

[11] S. de Sanjosé, M. Diaz, X. Castellsagué et al., "Worldwide prevalence and genotype distribution of cervical human papillomavirus DNA in women with normal cytology: a meta-analysis," *Lancet Infectious Diseases*, vol. 7, no. 7, pp. 453–459, 2007.

[12] D. Solomon, D. Davey, R. Kurman et al., "The 2001 bethesda system: terminology for reporting results of cervical cytology," *Journal of the American Medical Association*, vol. 287, no. 16, pp. 2114–2119, 2002.

[13] M. Poljak, A. Oštrbenk, K. Seme et al., "Comparison of clinical and analytical performance of the Abbott RealTime High Risk HPV test to the performance of hybrid capture 2 in population-based cervical cancer screening," *Journal of Clinical Microbiology*, vol. 49, no. 5, pp. 1721–1729, 2011.

[14] S.-M. Kulmala, S. Syrjänen, I. Shabalova et al., "Human papillomavirus testing with the hybrid capture 2 assay and PCR as screening tools," *Journal of Clinical Microbiology*, vol. 42, no. 6, pp. 2470–2475, 2004.

[15] S. Monnier-Benoit, V. Dalstein, D. Riethmuller, N. Lalaoui, C. Mougin, and J. L. Prétet, "Dynamics of HPV16 DNA load reflect the natural history of cervical HPV-associated lesions," *Journal of Clinical Virology*, vol. 35, no. 3, pp. 270–277, 2006.

[16] M. Schmitt, C. Depuydt, I. Benoy et al., "Multiple human papillomavirus infections with high viral loads are associated with cervical lesions but do not differentiate grades of cervical abnormalities," *Journal of Clinical Microbiology*, vol. 51, no. 5, pp. 1458–1464, 2013.

[17] S. Huang, B. Erickson, N. Tang et al., "Clinical performance of Abbott RealTime High Risk HPV test for detection of high-grade cervical intraepithelial neoplasia in women with abnormal cytology," *Journal of Clinical Virology*, vol. 45, supplement 1, pp. S19–S23, 2009.

[18] A. Molijn, B. Kleter, W. Quint, and L.-J. Van Doorn, "Molecular diagnosis of human papillomavirus (HPV) infections," *Journal of Clinical Virology*, vol. 32, supplement 1, pp. S43–S51, 2005.

[19] S. I. Collins, C. Constandinou-Williams, K. Wen et al., "Disruption of the E2 gene is a common and early event In the natural history of cervical human papillomavirus infection: a longitudinal cohort study," *Cancer Research*, vol. 69, no. 9, pp. 3828–3832, 2009.

[20] W. Li, W. Wang, M. Si et al., "The physical state of HPV16 infection and its clinical significance in cancer precursor lesion and cervical carcinoma," *Journal of Cancer Research and Clinical Oncology*, vol. 134, no. 12, pp. 1355–1361, 2008.

[21] B. Weaver, M. Shew, B. Qadadri et al., "Low-level persistence of human papillomavirus 16 DNA in a cohort of closely followed adolescent women," *Journal of Medical Virology*, vol. 83, no. 8, pp. 1362–1369, 2011.

[22] M. Motamedi, G. Böhmer, H. H. Neumann, and R. von Wasielewski, "CIN III lesions and regression: retrospective analysis of 635 cases," *BMC Infectious Diseases*, vol. 15, no. 1, article 541, 2015.

[23] M. F. Evans, C. S.-C. Adamson, J. L. Papilio, T. L. S. John, G. Leiman, and K. Cooper, "Distribution of human papillomavirus types in ThinPrep papanicolaou tests classified according to the Bethesda 2001 terminology and correlations with patient age and biopsy outcomes," *Cancer*, vol. 106, no. 5, pp. 1054–1064, 2006.

[24] W. Kinney, M. H. Stoler, and P. E. Castle, "Patient safety and the next generation of HPV DNA tests," *American Journal of Clinical Pathology*, vol. 134, no. 2, pp. 193–199, 2010.

Hindawi Publishing Corporation
BioMed Research International
Volume 2016, Article ID 1974972, 4 pages
http://dx.doi.org/10.1155/2016/1974972

Research Article

Different Vancomycin Immunoassays Contribute to the Variability in Vancomycin Trough Measurements in Neonates

Janko Samardzic,[1,2] Anne Smits,[3,4] Isabel Spriet,[5] Ivan Soldatovic,[6] Andrew Atkinson,[2] Milica Bajcetic,[1,7] John N. Van Den Anker,[2,8,9] and Karel Allegaert[3,9]

[1]*Institute of Pharmacology, Clinical Pharmacology and Toxicology, Medical Faculty, University of Belgrade, 11000 Belgrade, Serbia*
[2]*Division of Pediatric Pharmacology and Pharmacometrics, University of Basel Children's Hospital, 4056 Basel, Switzerland*
[3]*Department of Development and Regeneration, KU Leuven, 3000 Leuven, Belgium*
[4]*Neonatal Intensive Care Unit, University Hospitals Leuven, 3000 Leuven, Belgium*
[5]*Clinical Pharmacology and Pharmacotherapy, Department of Pharmaceutical and Pharmacological Sciences, KU Leuven and Pharmacy Department, University Hospitals Leuven, 3000 Leuven, Belgium*
[6]*Medical Faculty, University of Belgrade, 11000 Belgrade, Serbia*
[7]*Clinical Pharmacology Unit, University Children's Hospital, 11000 Belgrade, Serbia*
[8]*Division of Pediatric Clinical Pharmacology, Children's National Medical Center, Washington, DC 20010, USA*
[9]*Intensive Care and Department of Pediatric Surgery, Erasmus MC Sophia Children's Hospital, 3000 CB Rotterdam, Netherlands*

Correspondence should be addressed to Janko Samardzic; janko@med.bg.ac.rs

Received 18 February 2016; Accepted 31 July 2016

Academic Editor: Giulio Mengozzi

Substantial interassay variability (up to 20%) has been described for vancomycin immunoassays in adults, but the impact of neonatal matrix is difficult to quantify because of blood volume constraints in neonates. However, we provide circumstantial evidence for a similar extent of variability. Using the same vancomycin dosing regimens and confirming similarity in clinical characteristics, vancomycin trough concentrations measured by PETINIA (2011-2012, $n = 400$) were 20% lower and the mean difference was 1.93 mg/L compared to COBAS (2012–2014, $n = 352$) measurements. The impact of vancomycin immunoassays in neonatal matrix was hereby suggested, supporting a switch to more advanced techniques (LC-MS/MS).

1. Introduction

Vancomycin, a glycopeptide antibiotic, is commonly used in neonatal intensive care units (NICUs) for the treatment of late onset sepsis and catheter-related infections [1]. In adults, a ratio of the 24-hour area under the curve (AUC_{0-24}) divided by the minimum inhibitory concentration (MIC) for a given pathogen ≥ 400 is considered to be the optimal predictor of vancomycin efficacy for invasive methicillin-resistant staphylococci (MRSA) respiratory infections. Vancomycin serum concentrations are widely used as a surrogate marker for AUC, aiming to achieve target trough concentrations between 10 and 15 mg/L during intermittent intravenous administration [2].

Large interindividual variability in vancomycin pharmacokinetics (PK) within the neonatal population is well-known and is only in part explained by covariates such as weight, age, or serum creatinine [3, 4]. Since therapeutic drug monitoring (TDM) is clinically useful for drugs that have a known relationship between measured bodily fluid concentration and therapeutic effect, neonates with their rapid developmental changes in pharmacokinetic parameters will benefit from vancomycin TDM [5]. However, even if TDM is implemented, the immunoassays currently used to quantify vancomycin concentrations may differ because of differences in matrix. Cross-validation of different published PK models on vancomycin in neonates from different NICUs failed [6]. Clinicians do not take into account that routine

vancomycin quantification by commercial immunoassays can indeed show substantial differences, and this is an important clinical argument in support of a switch towards LC-MS/MS methodologies [7–10].

While this phenomenon is obviously not limited to neonatal matrix, the relevance may be population specific because of differences in plasma composition (e.g., concentration of albumin, immunoglobulins like IgA, and bilirubin) [7, 8]. Current recommendations do not take into account that routine plasma vancomycin quantification by commercial immunoassays can show substantial between-method differences. Next to standardization issues, immunoassays can also lack specificity. Cross-reacting substances such as vancomycin degradation products have been described to interfere with some immunoassays [7–10].

Unfortunately, there are no data on the interassay differences in neonatal matrix, likely due to blood volume constraints. Since the blood samples are of very limited quantity in neonates, it is not feasible to analyze different between-assay differences in a paired study design as applied in adult samples [7–9]. In an attempt to provide circumstantial evidence, we explored the impact of between-assay differences on the variability in vancomycin serum trough levels measured in neonates treated in a single neonatal intensive care unit (NICU) following a switch in immunoassay (PETINIA to COBAS).

2. Design and Methods

2.1. Study Population, Clinical Data Collection, and Ethics. Vancomycin trough concentrations measured in neonates and young infants treated with intravenous vancomycin, mainly for (suspected) late onset sepsis (>72 hours after birth), in the NICU of the University Hospitals Leuven, Belgium, between June 2011 and December 2014, were considered for inclusion in this retrospective study. Our patient population consisted of preterm and term neonates, who needed specialized care related to infections and prematurity. Clinical characteristics at birth (birth weight [BW] in grams; gestational age [GA] in weeks) and characteristics at the moment of TDM (postmenstrual age [PMA] in weeks, postnatal age [PNA] in days, weight at inclusion [WT] in grams, serum creatinine (mg/dL), serum albumin (g/L), and serum trough vancomycin concentration (mg/L)) were extracted from the patient files. Results were excluded if data regarding vancomycin prescription could not be obtained or in case of an administration or sampling time error. The ethics board of our hospital approved the study protocol.

2.2. Vancomycin Indication, Administration, TDM Collection, and TDM Assays. Vancomycin (Vancocin®, Elly Lilly, Brussels, Belgium) combined with amikacin is used as standard therapy for (suspected) late onset sepsis. Administration occurs as an intravenous infusion over 60 minutes. The vancomycin dosing regimen was based on PMA and serum creatinine, irrespective of the vancomycin assay used [4]. As part of routine clinical care trough samples for TDM were collected at the end of the dosing interval, in most cases 24–72 hours after treatment was initiated. Subsequent trough TDM samples during the same course were collected based on the decision of the attending physician. All samples during the first vancomycin treatment course are included.

During the study period, two different vancomycin immunoassays were applied consecutively. The vancomycin serum trough concentrations were measured either by a particle-enhanced turbidimetric inhibition immunoassay method (Siemens Dimension; Dade Behring, Deerfield, Illinois, PETINIA) or by an enzyme multiplied immunoassay technique (Cobas c702; Roche Diagnostics, Germany, COBAS). In November 2012, the assay was changed from PETINIA to COBAS throughout the entire hospital for logistic, nonclinical reasons. The hospital laboratory has a quality system that conforms to ISO15189. This implies that clinical interchangeability of results is verified when changing from one assay to another. To avoid censoring of concentrations below the lower limit of quantification (2 mg/L), these concentrations were replaced by a lower limit of quantification/2 (1 mg/L) [11]. Throughout this study interval, an enzymatic technique (Cobas c702 module) was used to quantify serum creatinine concentrations, so issues on Jaffe versus enzymatic creatinine assays do not apply [12].

2.3. Data Analysis and Statistics. The data were analyzed by Student's t-test and Mann-Whitney U test, as appropriate. General linear modelling was performed to assess significant differences between both groups, when adjusting for confounding factors. Since vancomycin serum concentrations had a small deviation of distribution, these were transformed using logarithmic transformation to obtain a normal distribution. Data were analyzed in SPSS 20.0 (IBM corp.) and a p value < 0.05 was considered statistically significant.

3. Results and Discussion

Our dataset comprised 313 patients with 752 vancomycin trough TDM observations: 400 observations were assayed with PETINIA and 352 with COBAS. Both cohorts had comparable clinical characteristics and only differences for serum albumin concentration were documented (Table 1).

We observed a significant difference between the vancomycin trough concentrations using two different immunoassays: PETINIA versus COBAS ($F = 7.695$; $p = 0.006$, Figure 1). When adjusting for serum albumin concentration and creatinine levels as critical covariates, the difference in vancomycin concentration between cohorts remained statistically significant ($F = 4.567$, $p = 0.033$; $F = 4.302$; $p = 0.038$, resp.). According to these results, it was shown that the vancomycin assay used was a significant predictor of vancomycin serum concentration. Overall, immunoassays PETINIA and COBAS yielded significantly different vancomycin trough concentrations when adjusting for covariates and the mean difference was 1.93 mg/L. The vancomycin serum trough concentrations measured by PETINIA were 20% lower than those measured by COBAS (Figure 1).

Table 1: Clinical characteristics of studied patients. Data are provided by mean and standard deviation (SD).

	Mean	SD	p value
Gestational age (weeks)			
PETINIA	31.91	5.17	0.635
COBAS	31.71	5.27	
Birth weight (g)			
PETINIA	1,779.48	991.96	0.182
COBAS	1,906.91	1,143.24	
Weight at inclusion (g)			
PETINIA	2,066.77	1,101.14	0.233
COBAS	2,220.59	1,288.11	
Postmenstrual age (weeks)			
PETINIA	34.77	5.98	0.766
COBAS	34.61	6.00	
Postnatal age (days)			
PETINIA	20.98	22.31	0.951
COBAS	22.13	23.38	
Creatinine (mg/dL)			
PETINIA	0.47	0.19	0.052
COBAS	0.52	0.24	
Albumin (g/dL)			
PETINIA	31.13	5.09	<0.001
COBAS	29.42	4.71	

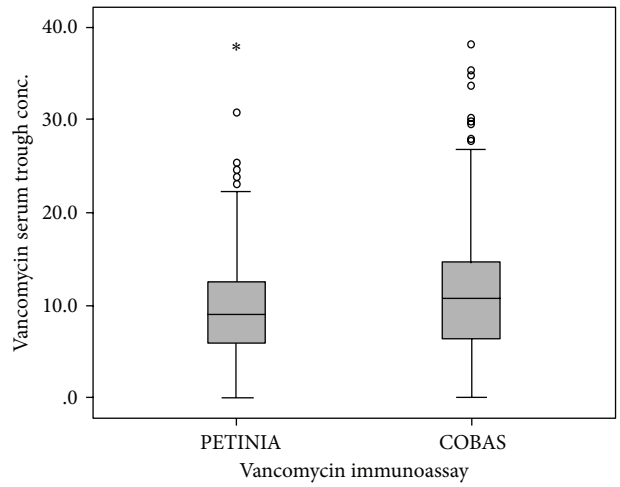

Figure 1: Vancomycin serum trough concentrations (mg/L) determined by two different immunoassays: PETINIA versus COBAS, presented as box plots (Mann-Whitney U test, $p < 0.05$).

Vancomycin dosing strategies in neonates are mostly based on postmenstrual and postnatal age, and they also take into account the developmental changes in volume of distribution and renal function as the most important covariates influencing vancomycin clearance [2]. However, the clinical significance of different analytical methods for serum vancomycin concentration was only recently suggested in neonates [6]. Between-assay studies in neonatal matrix are hampered by the blood volume needed to perform multiple between-assay studies, but we here provided circumstantial evidence of the relevance and the impact.

This provides further evidence that dosage individualization should not only consider clinical characteristics but also be tailored to the method of vancomycin quantification in neonates [6, 9]. We hereby speculate that this reflects the fact that immunoglobulin M (IgM) or IgA affects vancomycin concentration measured by PETINIA [10]. This might at least in part explain between-assay differences in the neonatal plasma matrix. Importantly, the relevance goes beyond our single institution, as illustrated by Zhao et al.: the transferability of published models of vancomycin pharmacokinetics to different clinical settings in part related to the use of conversion factors to "correct" for differences in vancomycin immune assays used [6].

The impact of vancomycin immunoassays in neonatal matrix was hereby suggested, providing additional support to switch to more advanced techniques (LC-MS/MS) to avoid both the matrix related differences between immunoassays and to lower the blood volume needed to quantify vancomycin in neonatal samples. Until then, clinicians taking care for neonates should consider the impact of immunoassays on vancomycin levels and targets. Similar, researchers should consider including neonatal samples in their assay comparison and assay development. Obviously and because of the limitations (sample volume) and ethical constrains in neonates, such studies should first be done using samples for adult patients. Matrix effects (ion suppression/enhancement) should hereby be considered, since this is a well-observed phenomenon in analyses of biological matrices by high-performance liquid chromatography-mass spectrometry (LC-MS) [13]. This should be followed by subsequent hypothesis testing, validation, or confirmation in neonatal matrix. Pooling of neonatal samples is hereby one of the approaches to further reduce this burden.

Competing Interests

The authors declare that there are no competing interests regarding the publication of this paper.

Acknowledgments

Janko Samardzic is supported by ERAWEB II scholarship for postdoctoral program at the KU Leuven, Belgium, Isabel Spriet by the Clinical Research Fund, University Hospitals Leuven, Milica Bajcetic by Ministry of Education, Science and Technological Development of the Republic of Serbia (Project no. 173014) and European Commission (LENA [602295]), and John N. Van Den Anker by NIH (K24DA027992, R01HD048689, and U54HD071601) and the European Commission (TINN [223614], TINN2 [260908], and NEUROSIS [223060]). Karel Allegaert was supported by the Fund for Scientific Research, Flanders (Fundamental Clinical Investigatorship 1800214N), while his research activities are further facilitated by the agency for innovation by Science and Technology in Flanders (IWT) through the SAFEPEDRUG project (IWT/SBO 130033).

References

[1] M. de Hoog, J. W. Mouton, and J. N. van den Anker, "Vancomycin: pharmacokinetics and administration regimens in neonates," *Clinical Pharmacokinetics*, vol. 43, no. 7, pp. 417–440, 2004.

[2] J. N. van den Anker, "Getting the dose of vancomycin right in the neonate," *International Journal of Clinical Pharmacology and Therapeutics*, vol. 49, no. 4, pp. 247–249, 2011.

[3] G. M. Pacifici and K. Allegaert, "Clinical pharmacokinetics of vancomycin in the neonate: a review," *Clinics*, vol. 67, no. 7, pp. 831–837, 2012.

[4] B. J. Anderson, K. Allegaert, J. N. van den Anker, V. Cossey, and N. H. G. Holford, "Vancomycin pharmacokinetics in preterm neonates and the prediction of adult clearance," *British Journal of Clinical Pharmacology*, vol. 63, no. 1, pp. 75–84, 2007.

[5] E. J. Begg, M. L. Barclay, and C. J. M. Kirkpatrick, "The therapeutic monitoring of antimicrobial agents," *British Journal of Clinical Pharmacology*, vol. 47, no. 1, pp. 23–30, 1999.

[6] W. Zhao, F. Kaguelidou, V. Biran et al., "External evaluation of population pharmacokinetic models of vancomycin in neonates: the transferability of published models to different clinical settings," *British Journal of Clinical Pharmacology*, vol. 75, no. 4, pp. 1068–1080, 2013.

[7] K. König, U. Kobold, G. Fink et al., "Quantification of vancomycin in human serum by LC-MS/MS," *Clinical Chemistry and Laboratory Medicine*, vol. 51, no. 9, pp. 1761–1769, 2013.

[8] M. Shipkova, D. T. Petrova, A. E. Rosler et al., "Comparability and imprecision of 8 frequently used commercially available immunoassays for therapeutic drug monitoring," *Therapeutic Drug Monitoring*, vol. 36, no. 4, pp. 433–441, 2014.

[9] M. Oyaert, N. Peersman, D. Kieffer et al., "Novel LC-MS/MS method for plasma vancomycin: comparison with immunoassays and clinical impact," *Clinica Chimica Acta*, vol. 441, pp. 63–70, 2015.

[10] D. F. Legatt, G. B. Blakney, T. N. Higgins et al., "The effect of paraproteins and rheumatoid factor on four commercial immunoassays for vancomycin: implications for laboratorians and other health care professionals," *Therapeutic Drug Monitoring*, vol. 34, no. 3, pp. 306–311, 2012.

[11] A. Vandendriessche, K. Allegaert, V. Cossey, G. Naulaers, V. Saegeman, and A. Smits, "Prospective validation of neonatal vancomycin dosing regimens is urgently needed," *Current Therapeutic Research—Clinical and Experimental*, vol. 76, pp. 51–57, 2014.

[12] K. Allegaert and J. N. van den Anker, "Creatinine-based vancomycin dosing regimens in neonates: there is more to consider than the variation in drug assay," *Pharmacotherapy*, vol. 32, no. 9, pp. e174–e175, 2012.

[13] E. Tudela, G. Muñoz, and J. A. Muñoz-Guerra, "Matrix effect marker for multianalyte analysis by LC-MS/MS in biological samples," *Journal of Chromatography B: Analytical Technologies in the Biomedical and Life Sciences*, vol. 901, pp. 98–106, 2012.

Hindawi Publishing Corporation
BioMed Research International
Volume 2016, Article ID 7508763, 4 pages
http://dx.doi.org/10.1155/2016/7508763

Research Article

Mean Platelet Volume in *Mycobacterium tuberculosis* Infection

Min Young Lee,[1,2] Young Jin Kim,[2] Hee Joo Lee,[2] Sun Young Cho,[2] and Tae Sung Park[2]

[1]*Department of Laboratory Medicine, Graduate School, Kyung Hee University, Seoul 02447, Republic of Korea*
[2]*Department of Laboratory Medicine, School of Medicine, Kyung Hee University, Seoul 02447, Republic of Korea*

Correspondence should be addressed to Sun Young Cho; untoyou@hanmail.net

Received 21 March 2016; Revised 30 May 2016; Accepted 1 June 2016

Academic Editor: Giulio Mengozzi

Introduction. Mean platelet volume (MPV) has been thought as a useful index of platelet activation. It is supposed that MPV is also associated with several inflammatory and infectious diseases. Korea still has a high incidence of tuberculosis (TB). The aim of this study was to investigate MPV as an inflammatory marker in TB patients. *Materials and Methods.* MPV were determined in 221 patients with TB and 143 individuals for control group. MPV was estimated by an Advia 2120 (Siemens Healthcare Diagnostics, Tarrytown, NY, USA). *Results.* In the TB patient group, a positive correlation was found between CRP and MPV. Age and MPV had a positive correlation in TB patient group. *Conclusions.* We conclude that there is a significant relation between MPV and inflammatory conditions. MPV can be an inflammatory marker to determine the disease activity in TB patients.

1. Introduction

Platelet is well known to be involved in the hemostasis. However nowadays, its different roles are attracting interest, such as actions on inflammation and immunity. Platelets have been widely studied in inflammation-induced atherosclerosis, as well as in thrombosis [1]. Due to the development of the automated complete blood count (CBC) analyzer, platelet indices have been one of the fastest and easiest tests to verify platelet function. Among various platelet indices, the mean platelet volume (MPV) reflects the size of platelets and has been suggested as a useful index of platelet activation [2].

MPV has been also investigated in several infectious diseases such as hepatitis B or mycobacterial infection [3, 4]. Tuberculosis (TB) is one of the most problematic and important diseases threatening public health in Korea. Korea still has a higher prevalence of mycobacterial infection than most other developed countries [5]. Annually, 90 individuals per 100,000 people are newly diagnosed with TB in Korea [6]. Early diagnosis, proper treatment regimen, and determining the activity of TB are important for the regulation of TB. There is no reliable parameter to determining the activity of TB except follow-up of the culture growth of mycobacteria bacilli. A few studies have investigated the relations between TB and MPV [7, 8]. The results were controversial. In this study, we evaluated the MPV in TB patients who were confirmed positive by culture and investigate the meaning of MPV in determining the activity of TB by comparing with C-reactive protein (CRP) as an inflammatory marker.

2. Materials and Methods

This study included 221 patients who had positive results on conventional culture tests for mycobacterial species seen at our hospital between January 2011 and April 2012. As the control group, we selected 143 individuals who visited the same hospital for medical check-ups. Extensive chart reviews were done to exclude any individuals with hypertension, diabetes, or smoking from the control group. To ensure that patients had *Mycobacterium tuberculosis* (MTB) infections, the patient group comprised nonoverlapping individuals so that positive results could be identified in a conventional culture study. For solid cultures, 3% Ogawa medium was used. Inoculated medium was incubated for at least 8 weeks at 37°C, in a MGIT 960 incubator (Becton, Dickinson and Company, MD, USA). Culture results were checked weekly. Blood was sampled by venipuncture at antecubital fossa and collected in tubes containing ethylenediaminetetraacetic acid (EDTA). MPV was measured in an Advia 2120 (Siemens

Table 1: Characteristics of the 221 patients with positive *Mycobacterium tuberculosis* cultures and 143 individuals for control.

Total number of patients	221	143
Mean age (range)	55.86 (11–96) years	44.00 (13–71) years
Correlation between MPV and age**	rho = −0.067, $P = 0.426$	rho = 0.235, $P = 0.002$
Male : female	138 : 83	72 : 71
Types of specimens cultured		N/A
Sputum	189	
Bronchial fluid	9	
Pleural fluid	8	
Urine	4	
Catheter	3	
Random	1	
Pericardial fluid	2	
Wound	2	
Others*	7	

*Cerebrospinal fluid, joint fluid, pus, and so forth.
**By Spearman's coefficient of rank correlation.
N/A, not applicable.

Healthcare Diagnostics, Tarrytown, NY, USA) within 2 hours from sampling.

Data were tested for normal distribution using the Kolmogorov-Smirnov test. Statistical comparison was calculated by an unpaired t-test. Spearman's coefficient of rank correlation and partial correlation coefficient were used to evaluate the association between MPV, platelet count, CRP, and age. Regression analysis was performed to make regression equation and calculate coefficient of determination. P values < 0.05 were considered to indicate statistical significance. The statistical analyses were performed using SPSS version 17.0 (SPSS Inc., Chicago, IL, USA) and Excel 2007 (Microsoft, Redmond, WA).

3. Results

The patients' characteristics are summarized in Table 1. The mean age of the TB subjects was 55.86 years, while the mean age of controls was 44.00 years, respectively. Male and female ratio is 1.66 in TB patient group and 1.01 in control group, respectively.

The mean MPV did not differ significantly between the patients (8.03 fL) and controls (7.96 fL). However the platelet count was significantly higher in the TB patients (303×10^9/L) than in the controls (258×10^9/L).

Among control group, no correlation was found between MPV and the individuals' age, while among TB patient group, positive correlation was found between MPV and patient age (correlation coefficient; rho = 0.235, $P = 0.002$) (Figure 1) and between MPV and CRP (correlation coefficient; rho = 0.206, $P = 0.002$) (Figure 2) by Spearman's coefficient of rank correlation. The partial correlation coefficients of MPV with CRP after adjusting for age are presented in Table 2. However there was no correlation between CRP and platelet count.

Table 2: Partial correlation of MPV with laboratory parameters after adjustment for age.

Variables	MPV (fL)	
	R	P value
CRP (mg/L)	0.207	0.007
Platelet count ($\times 10^9$/L)	−0.018	0.819

R, correlation coefficient.

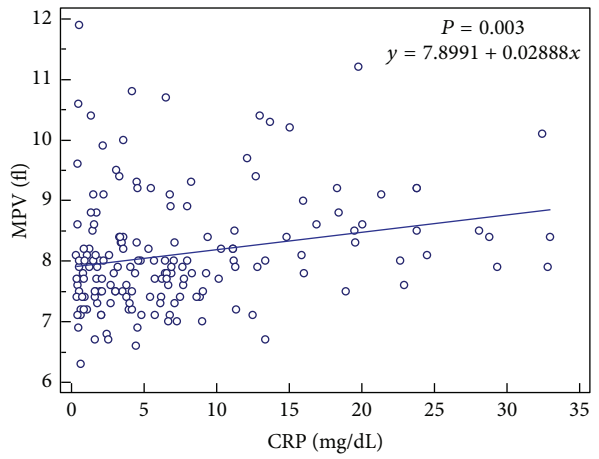

Figure 1: The correlation between mean platelet volume (MPV) and C-reactive protein (CRP) in patients with positive cultures for *Mycobacterium tuberculosis*.

4. Discussion

Although platelet indices such as MPV have been routinely tested in clinical laboratory using automated hematologic analyzer, their role in the diagnosis and management of diseases has not been fully investigated yet [4, 9]. In platelet

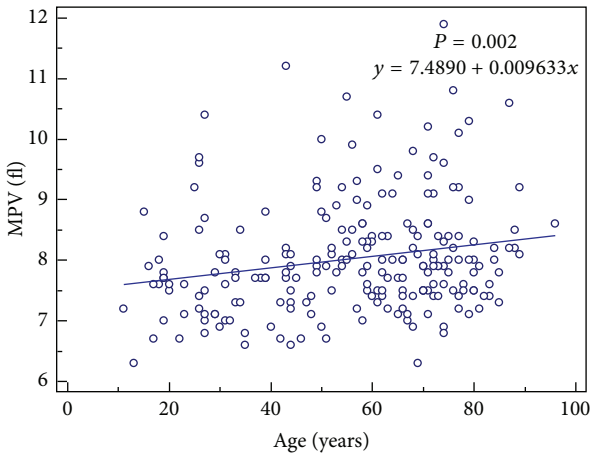

Figure 2: The correlation between mean platelet volume (MPV) and age in patients with positive cultures for *Mycobacterium tuberculosis*.

study, many investigations have focused on the change of platelet count such as thrombocytosis in inflammatory conditions or its role in hemostasis [10]. Although the function of platelets in hemostasis has been studied thoroughly, more recent evidence has been accumulated in an important role for platelets in the host inflammatory and immune responses [11]. As well as participating in blood coagulation, platelets can act as one of the inflammatory or immune effector cells by releasing inflammatory mediators, activating complement factors, interacting with foreign organisms such as parasites, viruses, and bacteria, and enhancing vascular permeability [1, 2, 10, 11]. Recently, many studies have suggested the importance of MPV as an inflammation marker in some chronic inflammatory disorders, such as rheumatoid arthritis (RA), ulcerative colitis (UC), and psoriasis [2]. However, the results have been controversial and only a few studies have investigated the role of MPV in infection and even fewer have studied the role of MPV specifically in TB infection. To the best of our knowledge, the present study is the largest study investigating MPV as an inflammatory marker in TB patients.

We have found direct relation between MPV and CRP in the TB patient group. As CRP is used commonly as an acute-phase reactant and an inflammatory marker, the result showed that MPV could be used as an inflammatory marker in disease activity assessment in TB. Platelets play a pathophysiological role in making multiple microthromboses around tuberculous cavities to prevent dissemination of the infection [12]. Increasing MPV can be explained by the fact that younger platelets being larger than mature ones are released from bone marrow to the peripheral blood circulation, as platelets are consumed [13]. Recently, it has been reported that various inflammatory conditions increase platelet size and activity [1, 2, 8, 14]. Contrary to our study, Zareifar et al. reported a negative relationship between MPV and serum CRP level. Contradictory results may be related to the characteristics of the studied groups of patients. In the study of Zareifar et al., the subjects were 100 children with all kinds of infectious and inflammatory diseases not defined as acute or chronic. In active phase or attacks of the chronic autoimmune inflammatory disorders, small platelets can circulate dominantly due to the excessively enhanced production of proinflammatory cytokines and acute-phase reactants which decreases the size of platelets [15]. It can also explain the phenomenon that MPV becomes higher after the anti-inflammatory treatment in RA. Gasparyan et al. explained this phenomenon by hypothesizing that high-grade inflammatory diseases, such as active rheumatoid arthritis or attacks of familial Mediterranean fever, result in low levels of MPV because of intensive consumption of large platelet, while low-grade inflammatory diseases or states, such as smoking, diabetes, psoriasis, Behcet's disease, or ankylosing spondylitis, have the opposite effect on MPV because the spleen contains approximately one-third of all the body's platelets which are relatively larger and hemostatically more active than platelets in the systemic circulation [16, 17]. Several studies investigating the relation between MPV and TB have controversial results. Tozkoparan et al. found that the MPV was higher in patients with active TB than in non-TB subjects [14], while Baynes et al. found MPV to be low in patients with active TB [18]. Şahin et al. reported that there was no statistical difference in MPV values between TB patients group and non-TB subjects [8]. However in all those studies, they just compared MPV values of TB patients and non-TB subjects and did not investigate the relation between MPV and CRP.

The effect of age on MPV remains controversial [10]. In this study, in contrast with control group, the increasing tendency of MPV with age was identified in the patient group. We excluded individuals with pathological conditions that may affect MPV values, such as hypertension and smoking from the subjects by means of an extensive chart review. The control group showed no association between MPV and age. This suggests that the platelets of older patients respond more readily to inflammatory or infectious conditions. Aging is known to be associated with increased levels of cytokines and proinflammatory markers. It can result from age-related changes in the immune system and increased secretion of cytokines by adipose tissue [19].

This study had several limitations. Our only inclusion criterion for the patient group was a positive MTB culture; other clinical data, such as medication and duration of disease, were not analyzed. In a future study, these clinical factors should be investigated to rule out their effect on platelet indices.

5. Conclusions

In our study we suggest that the changes in MPV are according to CRP and age in TB patients. We found a significant relation between MPV and inflammatory conditions. MPV can be an inflammatory marker measured by the easiest and fastest way to determine the disease activity in TB patients.

Disclosure

English editing was supported by textcheck.com in primary draft.

Competing Interests

The authors have no conflict of interests to report.

Authors' Contributions

Sun Young Cho and Tae Sung Park contributed equally to this work and both are considered senior authors. All of the authors contributed to this study as follows. Min Young Lee was involved in data collection, paper writing, and statistical analysis. Young Jin Kim and Hee Joo Lee provided opinions for interpreting results of infection markers in TB patients. Sun Young Cho and Tae Sung Park took part in the whole progress of this study such as data analysis, drawing conclusion, and writing and revising paper.

Acknowledgments

This research was supported by Basic Science Research Program through the National Research Foundation of Korea (NRF) funded by the Ministry of Education (2016R1A1A3A04004875).

References

[1] A. Y. Gasparyan, "Cardiovascular risk and inflammation: pathophysiological mechanisms, drug design, and targets," *Current Pharmaceutical Design*, vol. 18, no. 11, pp. 1447–1449, 2012.

[2] A. Y. Gasparyan, L. Ayvazyan, D. P. Mikhailidis, and G. D. Kitas, "Mean platelet volume: a link between thrombosis and inflammation?" *Current Pharmaceutical Design*, vol. 17, no. 1, pp. 47–58, 2011.

[3] S. Y. Cho, J. J. Yang, E. You et al., "Mean platelet volume/platelet count ratio in hepatocellular carcinoma," *Platelets*, vol. 24, no. 5, pp. 375–377, 2013.

[4] W.-Y. Shin, D.-H. Jung, J.-Y. Shim, and H.-R. Lee, "The association between non-alcoholic hepatic steatosis and mean platelet volume in an obese Korean population," *Platelets*, vol. 22, no. 6, pp. 442–446, 2011.

[5] World Health Organization, *Global Tuberculosis Report 2015*, WHO/HTM/TB/2015.22, World Health Organization, Geneva, Switzerland, 2015, http://apps.who.int/iris/bitstream/10665/191102/1/9789241565059_eng.pdf?ua=1.

[6] S. Y. Cho, M. J. Kim, J.-T. Suh, and H. J. Lee, "Comparison of diagnostic performance of three real-time PCR kits for detecting *Mycobacterium* species," *Yonsei Medical Journal*, vol. 52, no. 2, pp. 301–306, 2011.

[7] G. Gunluoglu, E. E. Yazar, N. S. Veske, E. C. Seyhan, and S. Altin, "Mean platelet volume as an inflammation marker in active pulmonary tuberculosis," *Multidisciplinary Respiratory Medicine*, vol. 9, no. 1, article 11, 2014.

[8] F. Şahin, E. Yazar, and P. Yıldız, "Prominent features of platelet count, plateletcrit, mean platelet volume and platelet distribution width in pulmonary tuberculosis," *Multidisciplinary Respiratory Medicine*, vol. 7, article 38, 2012.

[9] S. Y. Cho, J. J. Yang, Y.-S. Nam, J.-T. Suh, T. S. Park, and H. J. Lee, "Mean platelet volume in patients with increased procalcitonin level," *Platelets*, vol. 24, no. 3, pp. 246–247, 2013.

[10] H. Demirin, H. Ozhan, T. Ucgun et al., "Normal range of mean platelet volume in healthy subjects: Insight from a large epidemiologic study," *Thrombosis Research*, vol. 128, no. 4, pp. 358–360, 2011.

[11] C. N. Jenne, R. Urrutia, and P. Kubes, "Platelets: bridging hemostasis, inflammation, and immunity," *International Journal of Laboratory Hematology*, vol. 35, no. 3, pp. 254–261, 2013.

[12] C. Kuhn and F. Askin, "Lung and mediastinum," *Anderson's Pathology*, vol. 1, pp. 833–954, 1985.

[13] B. V. Kural, A. Örem, G. Çimşit, H. A. Uydu, Y. E. Yandi, and A. Alver, "Plasma homocysteine and its relationships with atherothrombotic markers in psoriatic patients," *Clinica Chimica Acta*, vol. 332, no. 1-2, pp. 23–30, 2003.

[14] E. Tozkoparan, O. Deniz, E. Ucar, H. Bilgic, and K. Ekiz, "Changes in platelet count and indices in pulmonary tuberculosis," *Clinical Chemistry and Laboratory Medicine*, vol. 45, no. 8, pp. 1009–1013, 2007.

[15] S. Zareifar, M. R. Farahmand Far, F. Golfeshan, and N. Cohan, "Changes in platelet count and mean platelet volume during infectious and inflammatory disease and their correlation with ESR and CRP," *Journal of Clinical Laboratory Analysis*, vol. 28, no. 3, pp. 245–248, 2014.

[16] A. Y. Gasparyan, A. Sandoo, A. Stavropoulos-Kalinoglou, and G. D. Kitas, "Mean platelet volume in patients with rheumatoid arthritis: the effect of anti-TNF-alpha therapy," *Rheumatology International*, vol. 30, no. 8, pp. 1125–1129, 2010.

[17] D. Bakovic, N. Pivac, D. Eterovic et al., "Changes in platelet size and spleen volume in response to selective and non-selective β-adrenoceptor blockade in hypertensive patients," *Clinical and Experimental Pharmacology and Physiology*, vol. 36, no. 4, pp. 441–446, 2009.

[18] R. D. Baynes, T. H. Bothwell, H. Flax et al., "Reactive thrombocytosis in pulmonary tuberculosis," *Journal of Clinical Pathology*, vol. 40, no. 6, pp. 676–679, 1987.

[19] Y. Feng, H. Yin, G. Mai et al., "Elevated serum levels of CCL17 correlate with increased peripheral blood platelet count in patients with active tuberculosis in China," *Clinical and Vaccine Immunology*, vol. 18, no. 4, pp. 629–632, 2011.

Hindawi Publishing Corporation
BioMed Research International
Volume 2016, Article ID 8196078, 13 pages
http://dx.doi.org/10.1155/2016/8196078

Research Article

Poly-L-lysine Prevents Senescence and Augments Growth in Culturing Mesenchymal Stem Cells *Ex Vivo*

June Seok Heo,[1] Hyun Ok Kim,[1,2] Seung Yong Song,[3] Dae Hyun Lew,[3] Youjeong Choi,[1] and Sinyoung Kim[2]

[1]*Cell Therapy Centre, Severance Hospital, Seoul 03722, Republic of Korea*
[2]*Department of Laboratory Medicine, Yonsei University College of Medicine, Seoul 03722, Republic of Korea*
[3]*Department of Plastic and Reconstructive Surgery, Yonsei University College of Medicine, Seoul 03722, Republic of Korea*

Correspondence should be addressed to Sinyoung Kim; sykim@yuhs.ac

Received 18 March 2016; Accepted 23 May 2016

Academic Editor: Giulio Mengozzi

Mesenchymal stem cells (MSCs) possess great therapeutic potential. Efficient *in vitro* expansion of MSCs is however necessary for their clinical application. The extracellular matrix (ECM) provides structural and biochemical support to the surrounding cells, and it has been used as a coating substrate for cell culture. In this study, we have aimed to improve the functionality and stemness of MSCs during culture using poly-L-lysine (PLL). Functionality of MSCs was analysed by cell cycle analysis, differentiation assay, β-galactosidase staining, and RT-PCR. Furthermore, we assessed the global gene expression profile of MSCs on uncoated and PLL-coated plates. MSCs on PLL-coated plates exhibited a faster growth rate with increased S-phase and upregulated expression of the stemness markers. In addition, their osteogenic differentiation potential was increased, and genes involved in cell adhesion, FGF-2 signalling, cell cycle, stemness, cell differentiation, and cell proliferation were upregulated, compared to that of the MSCs cultured on uncoated plates. We also confirmed that MSCs on uncoated plates expressed higher β-galactosidase than the MSCs on PLL-coated plates. We demonstrate that PLL provides favourable microenvironment for MSC culture by reversing the replicative senescence. This method will significantly contribute to effective preparation of MSCs for cellular therapy.

1. Introduction

The differentiation of mesenchymal stem cells (MSCs) into multiple cell lineages can be exploited as an attractive strategy for cell-based therapy and regenerative medicine [1]. MSCs can easily be obtained from various human tissue sources such as the bone marrow, cord blood, placenta, and adipose [2–5]. The clinical application of MSCs to tissue engineering has been introduced due to their numerous advantages including high expansion potential and extensive differentiation potential [6, 7]. However, MSCs need to be expanded *in vitro* in order to obtain sufficient cells for clinical trials since they are extremely rare in various tissues. Unlike embryonic stem cells, adult stem cells (MSCs) have a limited lifespan and stop proliferating during *in vitro* culture due to replicative senescence [8].

Cellular senescence, which is morphologically characterized by an enlarged and flattened cell shape, was first described by Hayflick [9]. Cellular senescence refers to active cells that eventually enter a state of irreversible growth arrest. Moreover, replicative senescence of MSCs exhibits reduced functionality, and cellular senescence might impair the regenerative potential of MSCs [10]. Studies investigating MSC senescence are therefore crucial for successful therapeutic application of MSCs. The mechanisms underlying the cellular senescence of MSCs are still poorly understood. Studies show that replicative senescence or cellular senescence is induced by intrinsic or extrinsic environmental factors [11]. The shortening of telomeres constitutes an intrinsic factor, whereas DNA damage is considered an extrinsic factor. Specifically, oxidative stress by reactive oxygen species (ROS) is the main extrinsic factor that induces senescence [12]. Cellular senescence is a complex process, and its molecular mechanisms are unknown. A number of studies demonstrated that hypoxia is beneficial to the senescence of MSC; however the precise understanding mechanism is not clear [13–15]. It was also

shown that inhibition of the p16 tumour suppressor gene delays growth arrest and therefore senescence of MSC [16]. Additionally, Abedin and King showed that FGF-2 suppresses the cellular senescence of human MSCs [17]. It is hard to preserve the important characteristics such as proliferation capacity and stemness of MSCs the inadequate cultivating microenvironment *in vitro*. Therefore, establishing an optimized culture condition that delays the senescence of MSCs is imperative.

MSCs naturally reside in a specialized niche *in vivo*, which mainly consists of the extracellular matrix (ECM). The ECM provides structural and biochemical support to the cells and has various other functions including cell adhesion, cell to cell communication, and differentiation [17, 18]. Poly-L-lysine (PLL) of extracellular matrix proteins is a small natural homopolymer of the essential amino acid L-lysine that is used to coat culture substrates. PLL functions as an attachment factor that enhances cell adherence due to its strong affinity for proteins and electrostatic interactions between the positive charges on the PLL molecule and the negative charges on the cell membrane [19, 20]. Park et al. showed that PLL increases the *ex vivo* expansion and erythroid differentiation of human hematopoietic stem cells [21]. It was also reported that PLL promoted neural progenitor cell function, and it is commonly used for MSC differentiation into neural lineages [22]. Recent studies suggest that neuroectodermal cells can generate MSCs, and they may arise in the neural crest, which is derived from embryonic neuroectoderm [23, 24]. These studies emphasized the interesting possibility that PLL could provide a favourable environment for MSC culture *in vitro*. We therefore hypothesized that PLL would be beneficial for MSC culture expansion and would preserve MSC properties *in vitro*. In this study, PLL-coated plates were used for MSC culture expansion. To the best of our knowledge, this study is the first to compare genome-wide expression profiles of MSCs cultured on PLL-coated plates with MSCs cultured on uncoated plates. In addition, we compared and analysed properties of MSCs cultured on PLL-coated plates with uncoated plates. The PLL-coated surface provided an excellent environment that improved the stemness of MSCs and delayed their senescence through upregulation of genes involved in cell adhesion, FGF-2 signaling, cell cycle, stemness, cell differentiation, and proliferation. This method could be useful for *in vitro* expansion of highly functional MSCs for cell-based therapeutic applications.

2. Materials and Methods

2.1. Reagents. Dulbecco's Modified Eagle Medium (DMEM), αMEM, foetal bovine serum (FBS), penicillin/streptomycin (P/S), 0.4% trypan blue stain, and TRIzol were obtained from Gibco (Invitrogen, Carlsbad, CA, USA). Mesenchymal stem cell growth medium (MSCGM), osteogenic differentiation medium, adipogenic differentiation medium, and chondrocyte differentiation medium were obtained from Cambrex (Lonza, Allendale, NJ, USA). Poly-L-lysine (PLL) and propidium iodide (PI) were purchased from Sigma-Aldrich (St. Louis, MO, USA). The senescence detection kit was obtained from BioVision Inc. Oligonucleotides for polymerase chain reaction (PCR), reverse transcription, and cDNA were synthesized by Bioneer (Bioneer Corporation, Daejeon, Korea). Silver nitrate, oil red O, and safranin O for differentiation staining were purchased from Sigma-Aldrich.

2.2. Cell Culture. MSCs were isolated from human bone marrow as previously described [25]. Cells after informed consent were collected from healthy three donors with approval from the Research Ethics Committee of Severance Hospital (Approval number 4-2014-0650). Primary cells of passage 0 were cultured and maintained in low glucose DMEM (DMEM-LG) supplemented with 10% FBS and 1% P/S at 37°C in 5% CO_2. Cells were harvested using 0.05% trypsin/EDTA (Invitrogen) when they reached 80–90% confluence for further experiment. Harvested 2×10^4 cells/well in 12-well plates were replated in 0.01% PLL-coated or uncoated plates for all experiments.

2.3. Flow Cytometry Analysis. For immunophenotyping, MSCs were stained with fluorescein isothiocyanate- (FITC-) or phycoerythrin- (PE-) conjugated monoclonal antibodies: CD14-FITC, CD29-FITC, CD31-PE, CD34-FITC, CD44-PE, CD45-PE, CD73-PE, CD90-FITC, CD105-PE, and CD106-FITC (all from BD Pharmingen, San Diego, CA, USA). Additionally, FITC- and PE-conjugated isotype controls were used as negative controls. Briefly, cultured MSCs were harvested and stained with the antibodies for 20 min at 4°C. Subsequently, the stained cells were washed with phosphate buffered saline (PBS) and fixed with 1% paraformaldehyde (Biosesang, Seongnam, Korea). The cells were analysed using a flow cytometer (Cytomics Flow Cytometer; Beckman Coulter, Fullerton, CA, USA).

2.4. Growth Characteristics. For analysis of cell proliferation, MSCs were plated at a density of 2×10^4 per well in uncoated or PLL-coated 12-well plates (Corning Inc., Corning 07-200-81, NY, USA) in MSC culture medium. Cultures were maintained for 5 days and then harvested for cell counting on days 3, 4, and 5. The proliferation rate of cells was determined using the trypan blue exclusion method. The population doubling time was calculated as the cumulative number of serial cells passaging until the cells reached senescence [26]. At passage 7, cells were photographed.

2.5. Cell Cycle Analysis. The cultured MSCs at passage 7 were removed from uncoated and PLL-coated plates. Harvested cells washed with PBS and fixed with cold 70% ethanol while minimizing clumping. After 30 min at 4°C, the cells were washed with PBS and stained with propidium iodide. Propidium iodide fluorescence was then examined using the Cytomics Flow Cytometer (Beckman Coulter).

2.6. β-Galactosidase Staining. β-galactosidase staining was performed using the senescence associated β-galactosidase staining kit (BioVision Inc.), according to the manufacturer's instructions. Briefly, passage 7 MSCs cultured on uncoated and PLL-coated plates were washed with PBS and fixed with 4% paraformaldehyde at room temperature. After washing

Table 1: Primer sequences.

Gene	Primer sequence (5′-3′)	Annealing temperature (°C)	Product size (bp)
$p16^{INK4a}$	Forward: CGAATAGTTACGGTCGGAGG Reverse: GCATGGTTACTGCCTCTGGT	62	309
$p21^{Cip1}$	Forward: GCGATGGAACTTCGACTTTG Reverse: CGTTTTCGACCCTGAGAGAGTC	60	285
SH3 (CD73)	Forward: TATTGCACTGGGACATTCGGGT Reverse: GGTTGCCCATGTTGCATTCTCT	62	443
SH2 (CD105)	Forward: CATCCTTGAAGTCCATGTCCTCTT Reverse: GCCAGGTGCCATTTTGCTT	62	95
VCAM-1 (CD106)	Forward: GCTTTCCTGCTCCGAAAATCCT Reverse: AACTGGGCCTTTCGGATGGTAT	62	367
Oct4	Forward: GACAACAATGAGAACCTTCAGGAGA Reverse: TTCTGGCGCCGGTTACAGAACCA	62	218
Sox2	Forward: AACCAAGACGCTCATGAAGAAG Reverse: GCGAGTAGGACATGCTGTAGGT	62	341
Nanog	Forward: ATAGCAATGGTGTGACGCAG Reverse: GATTGTTCCAGGATTGGGTG	62	219
GAPDH	Forward: GTGGTCTCCTCTGACTTCAACA Reverse: CTCTTCCTCTTGTGCTCTTGCT	62	210

with PBS, cells were incubated with senescence-associated β-galactosidase (SA-β-gal) staining solution for 24 h at 37°C. The number of β-galactosidase positive cells (blue colour) was evaluated under a light microscope (Olympus-IX71), as an indicator of the number of senescent cells.

2.7. Reverse Transcription PCR (RT-PCR). Total RNA was prepared using TRIzol reagent, and cDNA was synthesized using transcriptase II (Invitrogen). RT-PCR was performed with PCR primers under the conditions listed in Table 1 (Bioneer). Glyceraldehyde 3-phosphate dehydrogenase (GAPDH) was used as an internal standard. The signal intensity of the product was normalized to its respective GAPDH signal intensity.

2.8. Differentiation Assay. To assess the differentiation potential of MSCs, cells were seeded at 7×10^4/well in 12-well plates for the induction of osteogenesis and chondrogenesis and 1.5×10^5/well in 12-well plates for inducing adipogenesis. For differentiation, primary and passage 7 MSCs were maintained for 14 days in osteogenic, adipogenic, or chondrogenic differentiation medium (Lonza). For chondrogenesis, cells were treated with 10 ng/mL TGF- (transforming growth factor-) β3 (Lonza). After induction, Von Kossa staining was applied to analyse osteogenic differentiation, and calcium content was evaluated using the calcium (CPC) liquicolor kit (Stanbio Laboratory, Boerne, USA), based on a previously reported method [27]. Briefly, the cells were washed with PBS and treated 0.5 N HCl. After shaking for 3 h with an orbital shaker, the supernatant was transferred to a new tube for analysis. Ortho-cresolphthalein complexone (OCPC) was added to the sample, and absorbance was detected at 550 nm. After adipogenic differentiation, lipid droplets were detected by oil red O staining, and absorbance was measured at 500 nm after destaining with isopropanol for 30 min for quantitative analysis according to the previously reported method [27]. To evaluate chondrogenesis, cells were stained with safranin O solution, and the absorbance of sulphated glycosaminoglycan was detected at 656 nm using the Blyscan assay kit (Biocolor Ltd.) for quantitative analysis. Briefly, the supernatant of each sample was mixed with DMMB dye and reagents according to the manufacturer's protocols and reference [28]. Experiments were performed in triplicate.

2.9. Human Genome Microarray. The synthesis of target cRNA probes and hybridization were performed using Agilent's Low RNA Input Linear Amplification kit (Agilent Technology, USA), according to the manufacturer's instructions. Briefly, 1 μg of total RNA and T7 promoter primers were mixed and incubated at 65°C for 10 min. The cDNA master mix (5x first strand buffer, 0.1 M DTT, 10 mM dNTP mix, RNase-Out, and MMLV-RT) was prepared and added to the reaction mix. The samples were incubated at 40°C for 2 h and were then incubated at 65°C for 15 min to terminate RT and dsDNA synthesis. The transcription master mix was prepared according to the manufacturer's protocol (4x transcription buffer, 0.1 M DTT, NTP mix, 50% PEG, RNase-Out, inorganic pyrophosphatase, T7-RNA polymerase, and cyanine 3/5-CTP). Transcription of dsDNA was performed by adding the transcription master mix to dsDNA reaction samples and incubating at 40°C for 2 h. Amplified and labelled cRNA was purified using the cRNA Cleanup Module (Agilent Technology), according to the manufacturer's protocol. The labelled cRNA target was quantified using a ND-1000 spectrophotometer (NanoDrop Technologies, Inc., Wilmington, DE). After checking the labelling efficiency, fragmentation of cRNA was performed by adding 10x blocking agent and 25x fragmentation buffer and incubating at 60°C for 30 min. The

fragmented cRNA was resuspended with 2x hybridization buffer and directly pipetted onto assembled Agilent's Human Oligo Microarray (44 K). The arrays hybridized at 65°C for 17 h using an Agilent hybridization oven (Agilent Technology, USA). The hybridized microarrays were washed, according to the manufacturer's washing protocol (Agilent Technology, USA).

2.10. Data Acquisition and Analysis. All data normalization and selection of differentially expressed genes were performed using GeneSpringGX 7.3 (Agilent Technology, USA). The averages of normalized ratios were calculated by dividing the average normalized signal channel intensity by the average normalized control channel intensity. Functional annotation of genes was performed according to the Gene Ontology™ Consortium (http://www.geneontology.org/index.shtml) by GeneSpringGX 7.3. Gene classification was based on searches of the BioCarta (http://www.biocarta.com/), GenMAPP (http://www.genmapp.org/), DAVID (http://david.abcc.ncifcrf.gov/), and Medline databases (http://www.ncbi.nlm.nih.gov/).

2.11. Statistical Analysis. Statistical analysis was performed using Student's t-test. Quantitative data are expressed as means ± SD. Differences are considered statistically significant at $p < 0.05$.

3. Results

3.1. Characterization of Cultured MSCs. MSCs were isolated and cultured from human bone marrow of three different donors. Cultured MSCs displayed a fibroblast-like morphology, and they were differentiated into osteocyte, chondrocyte, and adipocyte under proper conditions (Figure 1(a)). For immunophenotyping of cultured MSCs, MSCs derived from different donors were analysed by flow cytometry. Figure 1(b) shows that MSCs were positive for MSC markers, including CD29, CD44, CD73, CD90, and CD105, whereas MSCs were negative for CD14, CD31, CD34, CD45, and CD106 known as hematopoietic and endothelial markers. The results of flow cytometry demonstrate that the cultured cells were typical MSCs.

3.2. Growth Kinetics of Cultured MSCs on Uncoated and PLL-Coated Plates. To determine the effect of PLL on *in vitro* culture of MSCs, we compared the proliferation activity of MSCs cultured on uncoated and PLL-coated plates. The optimal concentration of 0.01% PLL used for this study was determined empirically, since we observed that high concentrations greater than 0.01% hindered MSC adhesion and spread (data not shown). Bone marrow-derived MSCs at passage 3 were cultured for 5 days to determine whether PLL stimulates MSC proliferation in the short-term culture. The numbers of harvested cells at days 3, 4, and 5 were measured using the trypan blue exclusion method. An increase in cell numbers was detected in MSCs cultured on PLL-coated plates compared to cells grown in the absence of PLL-coating (Figure 1(c)).

3.3. PLL Suppressed MSC Replicative Senescence. Passage 7 MSCs cultured in DMEM on uncoated plates displayed the typical phenomenon of replicative senescence with morphological abnormalities (Figure 2(a)). MSCs are typically cultivated in DMEM-LG containing 10% FBS and 1% P/S. Additionally, αMEM and mesenchymal stem cell growth medium (MSCGM) are also used for MSC culture. MSCGM is a known specific medium for mesenchymal stem cell growth. To investigate morphological changes of replicative senescence of MSCs, cells were replated in αMEM and MSCGM with DMEM. MSCs grown in αMEM and MSCGM exhibited similar morphological patterns including cell aggregation as MSCs grown in DMEM (data not shown). Senescent cells were subsequently seeded on uncoated and PLL-coated plates to determine whether PLL could induce any changes during culture. Surprisingly, MSCs seeded on uncoated plates maintained an aggregated phenotype with growth arrest, whereas cells on the PLL-coated plates demonstrated an increased growth rate without aggregation (Figure 2(a)). The population doubling time of MSCs cultured on PLL-coated plates was decreased compared with that of MSCs on uncoated plates in culture (Figure 2(a)). Additionally, MSCs cultured on uncoated plates did not demonstrate further growth; however MSCs cultured on PLL-coated plates reached 100% confluence within several days. Furthermore, to examine whether PLL increased the S-phase, cell cycle analysis was carried out using flow cytometry. PLL increased the S-phase of MSCs compared to MSCs cultured in the absence of PLL (Figure 2(b)). We next investigated whether PLL suppressed MSC senescence. MSCs cultured on uncoated and PLL-coated plates were stained with β-galactosidase after the typical phenomenon of senescence was observed. MSCs cultured on uncoated plates showed a significant increase in the percentage of β-galactosidase positive cells compared to cells cultured on PLL-coated plates (Figure 2(c)).

3.4. PLL Induced Stemness Markers and Inhibited Senescence Related Genes. The gene expressions of known MSC markers *CD73, CD105*, and *CD106* in MSCs at passage 7 showing a senescent phenotype cultured on uncoated and PLL-coated plates were analysed using RT-PCR analysis. All MSCs, regardless of cell culture conditions, were positive for *CD105* and *CD106* (Figure 3(a)). Importantly, very low levels of *CD73* (ecto-5′-nucleotidase), a MSC specific marker, were detected in senescent MSCs cultured on uncoated plates, whereas it was distinctly expressed in MSCs cultured on PLL-coated plates (Figure 3(a)). *Oct4*, *Nanog,* and *Sox2* that regulate the maintenance of the pluripotency have been purported to play a similar role also in mesenchymal stem cells [29, 30]. To determine whether stemness was affected by PLL, we investigated the gene expression levels of stemness markers such as *Oct4*, *Sox2*, and *Nanog*. *Oct4* was undetectable in all MSCs regardless of culture conditions. However *Sox2* and *Nanog* were upregulated in MSCs cultured on PLL-coated plates compared to senescent MSCs cultured on uncoated plates (Figure 3(b)). These results indicate that MSC and stemness markers were affected by PLL. In addition, to confirm whether PLL affected cell proliferation, $p16^{INK4a}$ and

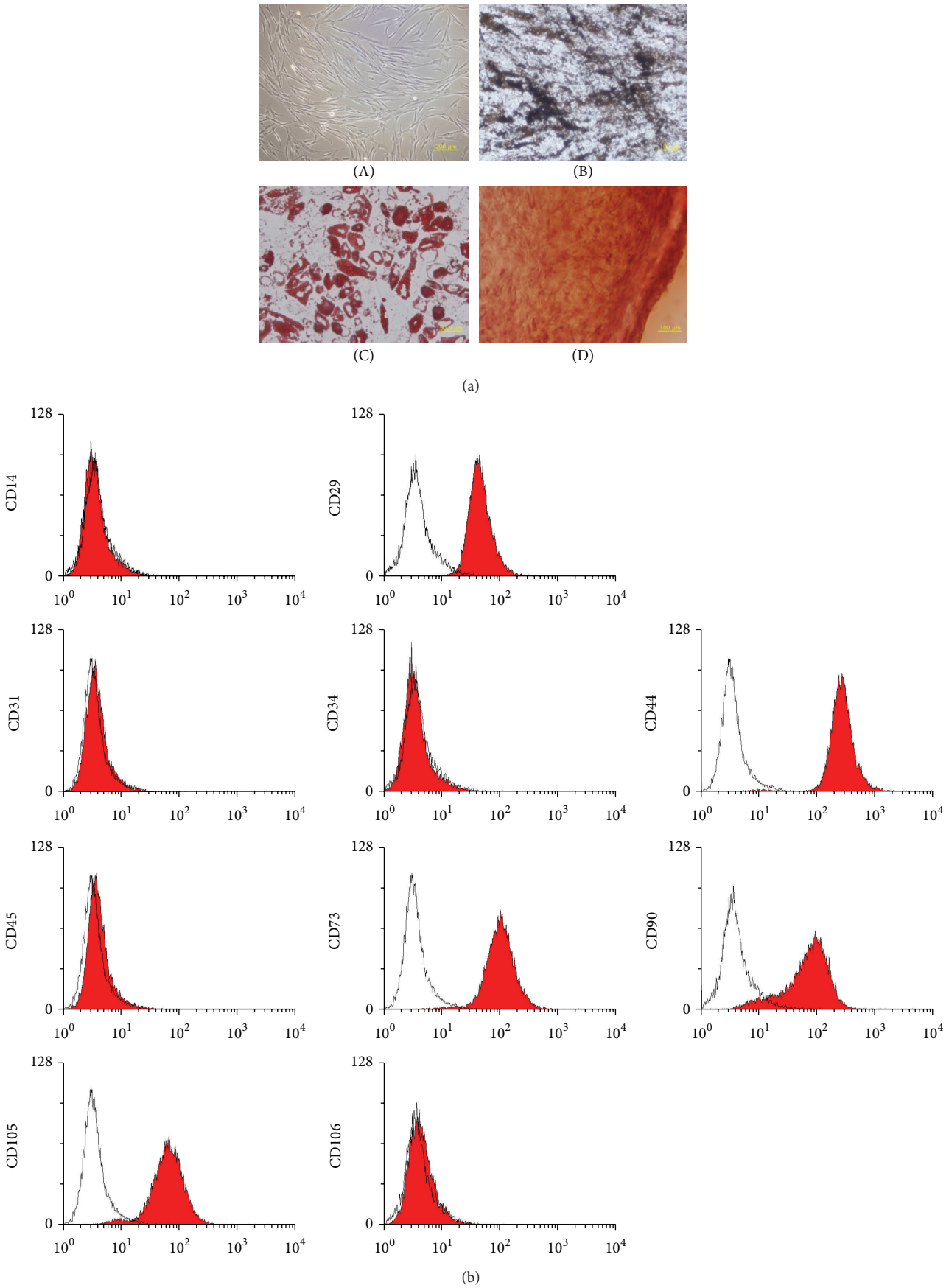

Figure 1: Continued.

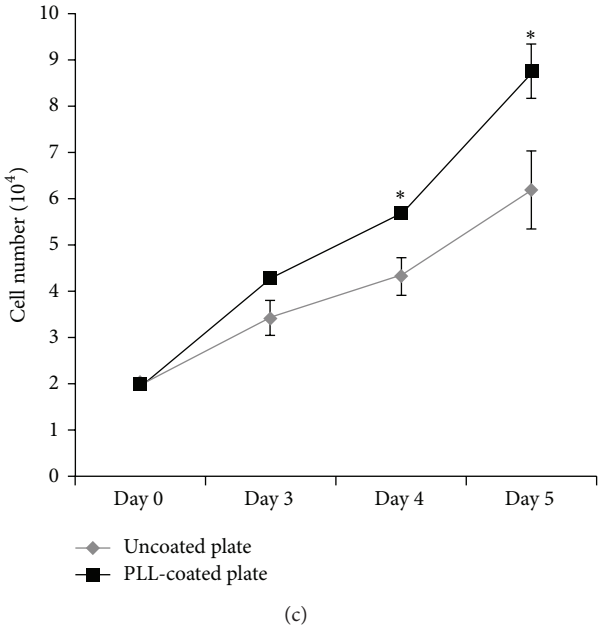

(c)

Figure 1: Characteristics and short-term culture of MSCs. (a) Cell morphology was observed under phase-contrast microscopy ((A) magnification: 100x) and differentiation potential was evaluated by Von Kossa, oil red O, and safranin O staining ((B) osteogenesis-magnification: 200x, (C) adipogenesis-magnification: 400x; (D) chondrogenesis-magnification: 200x). (b) The immunophenotype of bone marrow-derived MSCs. Flow cytometry histograms show that cultured MSCs were positive CD29, CD44, CD73, CD90, and CD105. These results show representative histograms of cultured MSCs. (c) Proliferative activity of cultured MSCs. MSCs were cultured on uncoated or poly-L-lysine- (PLL-) coated plates for 5 days. The number of harvested cells was measured by trypan blue staining. The data represent the mean ± standard deviation of three independent experiments ($n = 3$). $^*p < 0.05$.

$p21^{Cip1}$ genes associated senescence were analysed by RT-PCR. As shown in Figure 3(c), the mRNA expression levels of $p16^{INK4a}$ and $p21^{Cip1}$ were decreased in cells cultured on PLL-coated plates compared to the cells on uncoated plates. In particular, the decreasing of p21 is statistically significant in passage 7 of PLL-coated plate (Figure 3(c)). These results demonstrate that senescent MSCs can be cultured normally on PLL-coated plates and that PLL can inhibit MSC-replicative senescence.

3.5. Differentiation Potential of MSCs Cultured on PLL-Coated Plates. To assess the differentiation potential of MSCs, cells at passage 7 showing a senescent phenotype were cultured and induced to differentiate to osteocytes, adipocytes, and chondrocytes in specific differentiation media. Von Kossa staining was used to detect calcium-containing mineralized nodules indicating osteogenic induction. The results demonstrated that MSCs cultured on PLL-coated plates showed higher amounts of Von Kossa staining compared to cells on uncoated plates, and MSCs cultured on PLL-coated plates had higher calcium accumulation compared to cells on uncoated plates in the calcium content assay (Figure 4(a)). Adipogenic differentiation was analysed by oil red O staining. Both MSCs cultured on uncoated and PLL-coated plates showed lipid droplet formation, and the absorbance value for oil red O staining was similar between the two culture conditions (Figure 4(b)). The chondrogenic differentiation potential of MSCs was assessed using safranin O staining. Similar to the results of adipogenic differentiation, both MSCs had similar chondrogenic differentiation capacity, as sulphated glycosaminoglycan content was also similar between MSCs cultured under both conditions (Figure 4(c)).

3.6. Gene Expression Profiles. Genome-wide expression profiles of MSCs were analysed by human genome microarray. We analysed the expression patterns of senescent MSCs of the same donor cultured on uncoated and PLL-coated plates. The most significant differentially expressed genes are summarized in Tables 2 and 3. Differentially expressed genes (>twofold) in MSCs cultured on PLL and uncoated plates were sorted into 8 categories according to function: cell adhesion, FGF-2 signalling, cell cycle, oxidative stress, tumorigenicity, stemness, cell differentiation, and cell proliferation.

Upregulated genes included the following: calcium channel, voltage-dependent, L type, alpha 1C subunit (*CACNA1C*), which may play a role in the differentiation of stem cells [31]; delta-like 2 homolog (*DLK2*), a modulator of adipogenesis [32]; nuclear assembly factor 1 homolog (*NAF1*), which is required for telomerase function [33]; centromere protein I (*CENPI*), which is essential for mitosis [34]; apelin (*APLN*) that attenuates oxidative stress [35]; actinin, alpha 2 (*ACTN2*), which is involved in maintaining the cell spreading and motility [36]; ciliary neurotrophic factor receptor (*CNTFR*), which acts on neuronal populations in the developing and mature brain [37]; lethal giant larvae homolog 2 (*LLGL2*),

Table 2: Upregulated genes (>twofold) in MSCs on uncoated and poly-L-lysine- (PLL-) coated plates.

Gene name	Description	NCBI	PLL/UN
Calcium channel, voltage-dependent, L type, alpha 1C subunit	Homo sapiens calcium channel, voltage-dependent, L type, alpha 1C subunit (CACNA1C), transcript	NM_001129827	16.55
Delta-like 2 homolog (*Drosophila*)	Homo sapiens delta-like 2 homolog (*Drosophila*) (DLK2), transcript variant 2	NM_206539	10.97
Nuclear assembly factor 1 homolog (*S. cerevisiae*)	Homo sapiens nuclear assembly factor 1 homolog (*S. cerevisiae*) (NAF1), transcript variant 1	NM_138386	3.82
Centromere protein I	Homo sapiens centromere protein I (CENPI)	NM_006733	3.15
Apelin	Homo sapiens apelin (APLN)	NM_017413	3.07
Actinin, alpha 2	Homo sapiens actinin, alpha 2 (ACTN2)	NM_001103	2.89
Ciliary neurotrophic factor receptor	Homo sapiens ciliary neurotrophic factor receptor (CNTFR), transcript variant 1	NM_147164	2.84
Lethal giant larvae homolog 2 (*Drosophila*)	Homo sapiens lethal giant larvae homolog 2 (*Drosophila*) (LLGL2), transcript variant 3	NM_001031803	2.43
E2F transcription factor 8	Homo sapiens E2F transcription factor 8 (E2F8)	NM_024680	2.23
Tyrosine kinase, nonreceptor, 2	Homo sapiens tyrosine kinase, nonreceptor, 2 (TNK2), transcript variant 2	NM_001010938	2.20
Inhibin, beta B	Homo sapiens inhibin, beta B (INHBB)	NM_002193	2.07

Table 3: Downregulated genes (>twofold) in MSCs on uncoated and poly-L-lysine- (PLL-) coated plates.

Gene name	Description	NCBI	PLL/UN
Hairy/enhancer-of-split related with YRPW motif 1	Homo sapiens hairy/enhancer-of-split related to YRPW motif 1 (HEY1), transcript variant 2	NM_001040708	0.43
Thrombospondin 2	Homo sapiens thrombospondin 2 (THBS2)	NM_003247	0.45
Leucine rich repeat containing 17	Homo sapiens leucine rich repeat containing 17 (LRRC17), transcript variant 2	NM_005824	0.47
Collagen, type XI, alpha 1	Homo sapiens collagen, type XI, alpha 1 (COL11A1), transcript variant B	NM_080629	0.47
Chitinase 3-like 1 (cartilage glycoprotein-39)	Homo sapiens chitinase 3-like 1 (cartilage glycoprotein-39) (CHI3L1)	NM_001276	0.48
Sulfatase 2	Homo sapiens sulfatase 2 (SULF2), transcript variant 1	NM_018837	0.48
Neurotrophic tyrosine kinase, receptor, type 2	Homo sapiens neurotrophic tyrosine kinase, receptor, type 2 (NTRK2), transcript variant *c*	NM_001018064	0.50

involved in normal cell division [38]; E2F transcription factor 8 (*E2F8*), which plays an important role in the S-phase of the cell cycle [39]; tyrosine kinase, nonreceptor, 2 (*TNK2*), which inhibits the GTPase activity of p21 [40]; inhibin beta B (*INHBB*), which is involved in self-renewal of stem cells [41].

Downregulated genes included the following: hairy/enhancer-of-split related to YRPW motif 1 (*HEY1*), a tumour specific gene [42]; thrombospondin 2 (*THBS2*), which mediates focal adhesion disassembly [43]; leucine rich repeat containing 17 (*LRRC17*), a known negative regulator of osteogenesis [44]; collagen, type XI, alpha 1 (*COL11A1*), which is expressed in tumour cell lines [45]; chitinase 3-like 1 (cartilage glycoprotein-39, *CHI3L1*), which is involved in oxidative stress [46]; sulphates 2 (SULF2), which is upregulated in cancer [47, 48]; neurotrophic tyrosine kinase, receptor, type 2 (*NTRK2*), which stimulates focal adhesion disassembly and is involved in cancer [49, 50].

4. Discussion

Adult stem cells (MSCs) have many advantages, such as being less tumorigenic, and they do not trigger immune rejection. MSCs thus hold significant promise for future use in stem cell therapy and tissue engineering. However, there are also disadvantages that currently limit their clinical application. MSCs exist in low quantity from a variety of sources, and it is hard to culture them *in vitro* because they are sensitive to external stimuli and readily enter a state of replicative senescence. The culture and expansion of a large amount of MSCs from primary sources are very important for their successful clinical application. Therefore, the development of an easy and innovative method for cultivating MSCs is critical.

Generally, cells are exposed to complex and highly structured microenvironments regulated by multiple biophysical and biochemical factors such as soluble factors and ECM *in vivo* [51]. The fate of MSCs is controlled by cell to cell and cell to ECM interactions [52]. Similarly, *in vitro* culture conditions have a significant impact on the fate of MSCs with changes in gene and protein expression profiles. ECM proteins constitute a microenvironment that provides structural support and attachment to the cells and offer essential communication between cells and their surrounding environment [53]. In this study, we applied a

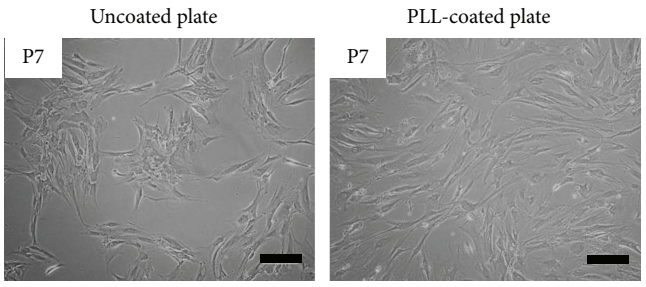

PDT (h)	
Uncoated plate	74.07 ± 12.24
PLL-coated plate	57.35 ± 10.34

(a)

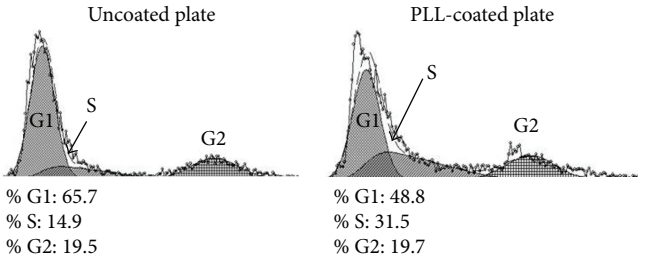

% G1: 65.7
% S: 14.9
% G2: 19.5

% G1: 48.8
% S: 31.5
% G2: 19.7

(b)

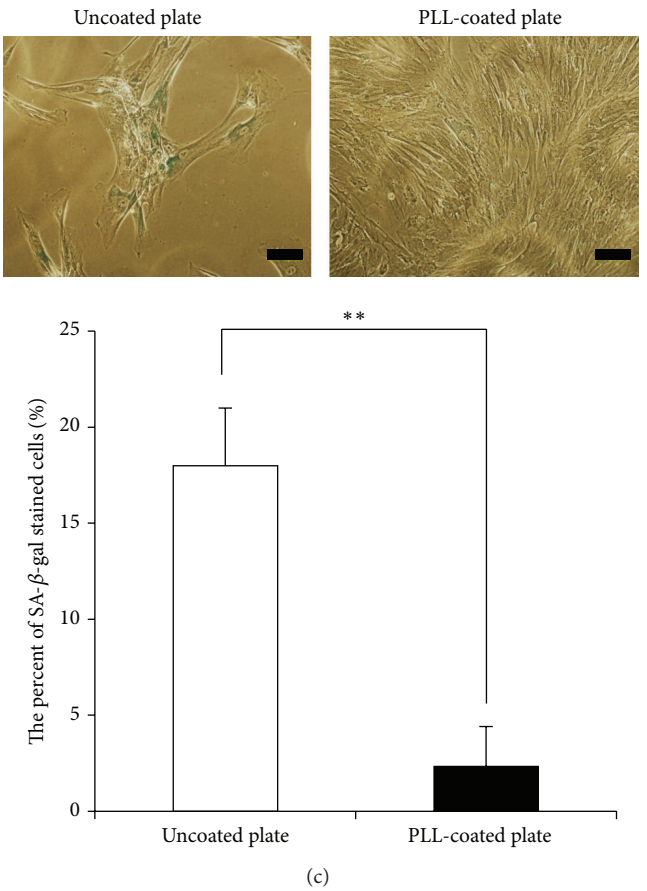

(c)

Figure 2: Changes in senescent cells induced by extracellular matrix (ECM) coating. (a) Morphological changes and population doubling time in senescent cells cultivated on a poly-L-lysine- (PLL-) coated plate were observed compared to cells cultured on an uncoated plate (magnification: 100x, scale bar = 200 μm). (b) Cell cycle analysis. Cells were removed from the culture well, stained for DNA with propidium iodide (PI), and analysed by flow cytometry. (c) Senescence associated β-gal assay of MSCs cultured on uncoated and PLL-coated plates. One representative of three independent experiments is shown. The number of β-gal positive cells was enumerated. The data represent the mean ± standard deviation of three experiments (magnification: 200x, scale bar = 100 μm). $^{**}p < 0.01$.

cell culture condition, in which MSCs were grown on plates coated with PLL, which is known to promote cell adhesion to solid substrates and to recreate the *in vivo* microenvironment. We observed an increase in the number of MSCs cultured on PLL-coated plates with activation of the S-phase of the cell cycle. These results indicate the positive effects of PLL on the proliferation of MSCs in *in vitro* culture. In addition, PLL retarded MSC replicative senescence, as determined by β-galactosidase staining, demonstrating that PLL-coated plates provide the necessary microenvironment for optimal growth of MSCs *in vitro*. Interestingly, CD73, ecto-5′-nucleotidase used as a marker for MSCs, was rarely

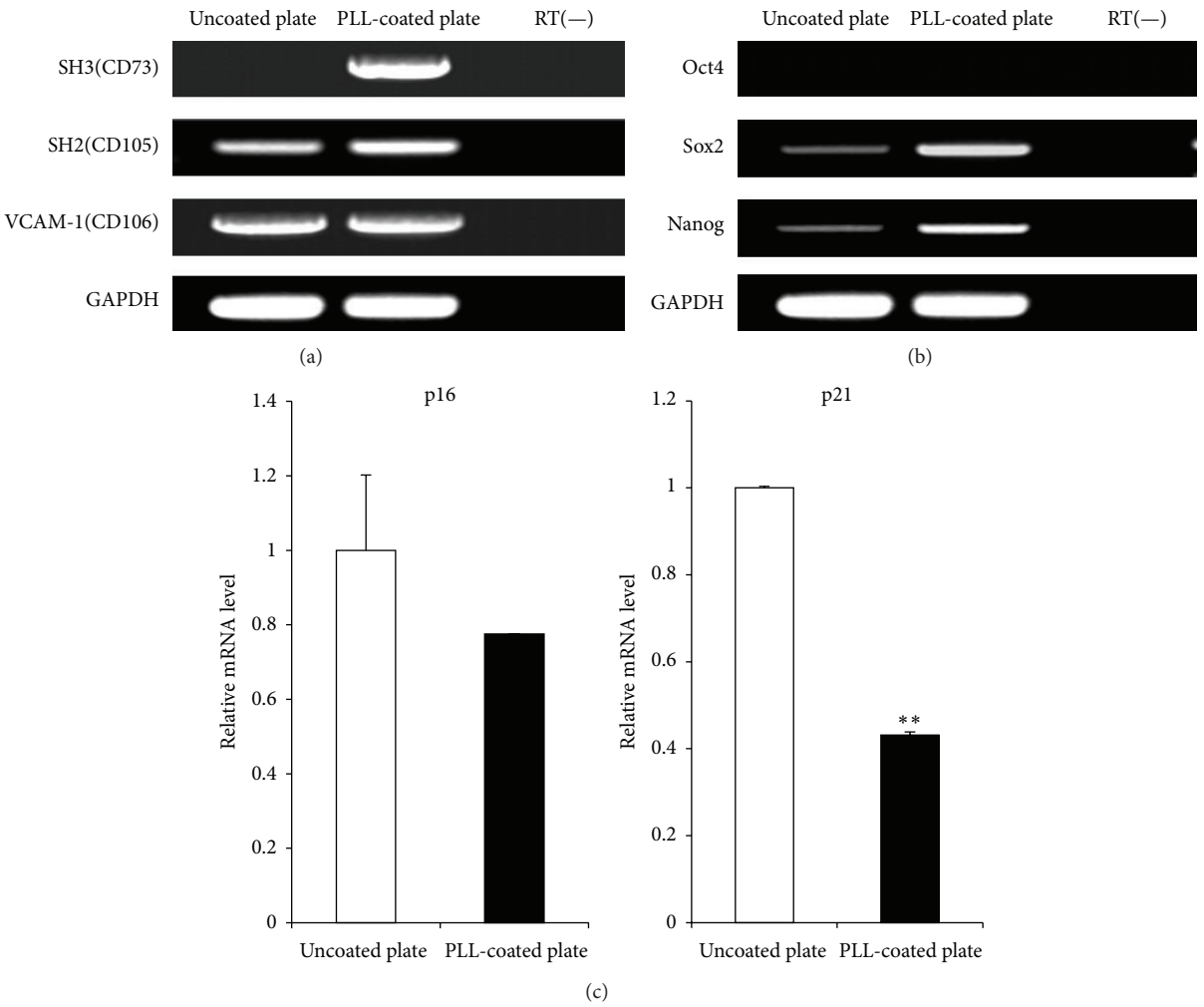

Figure 3: Gene expression of cells cultured on uncoated and poly-L-lysine- (PLL-) coated plates. Gene expression was analysed by RT-PCR for (a) MSC and (b) stemness markers. (c) $p16^{INK4a}$ and $p21^{Cip1}$ mRNA expression levels were evaluated using RT-PCR. Expression level relative to that of housekeeping gene GAPDH is shown. $^{**}p < 0.01$.

expressed in senescent MSCs, whereas MSCs cultured on PLL-coated plates strongly expressed this marker. It is known that most cells that express CD73 are responsible for the production of extracellular adenosine; however its specific function in MSCs is not fully understood. CD73 may be associated with replicative senescence and be a marker of MSC senescence as indicated by our findings (Figure 3(a)). *Oct4*, *Sox2*, and *Nanog*, which are known pluripotency and stemness markers, are very important for self-renewal of stem cells, and they play an essential role in generating induced pluripotent stem cells [54]. *Sox2* is also recently known that it is important in maintenance of cell proliferation and multipotency of MSC [55]. Normally, *Oct4* that is a key transcription factor essential for survival and self-renewal is expressed in adult stem cells. However, the expression of *Oct4* easily disappears during culture *in vitro* [56]. *Oct4* was in our study undetectable because genes concerning pluripotency including *Oct4*, *Sox2*, and *Nanog* were analysed in passage 7 MSCs. Our results demonstrated that *Sox2* and *Nanog* are significantly upregulated in MSCs cultured on PLL-coated plates compared with MSCs cultured on uncoated plates. Upregulation of those stemness factors may play a crucial role in increasing MSC proliferation and delaying replicative senescence of MSCs. Moreover, our results suggest that PLL can significantly improve osteogenic differentiation of MSCs. MSCs could not ordinarily differentiate into osteocytes due to cell aggregation and inhibition of proliferation in osteogenic induction environment. However, PLL had no effect on the adipogenic and chondrogenic differentiation capacity of MSCs.

In this study, we present for the first time an analysis of the global gene expression profiles of senescent MSCs cultured on uncoated versus PLL-coated plates, using human genome microarray to gain insight into the molecular characteristics of senescence. Functional classification of differentially expressed genes, according to the Gene Ontology (GO), demonstrated that genes associated with the cell cycle (GO:0007049), cell division (GO:0051301), cell proliferation (GO:0008283), transcription factor activity (GO:0003700), extracellular region (GO:0005576), positive

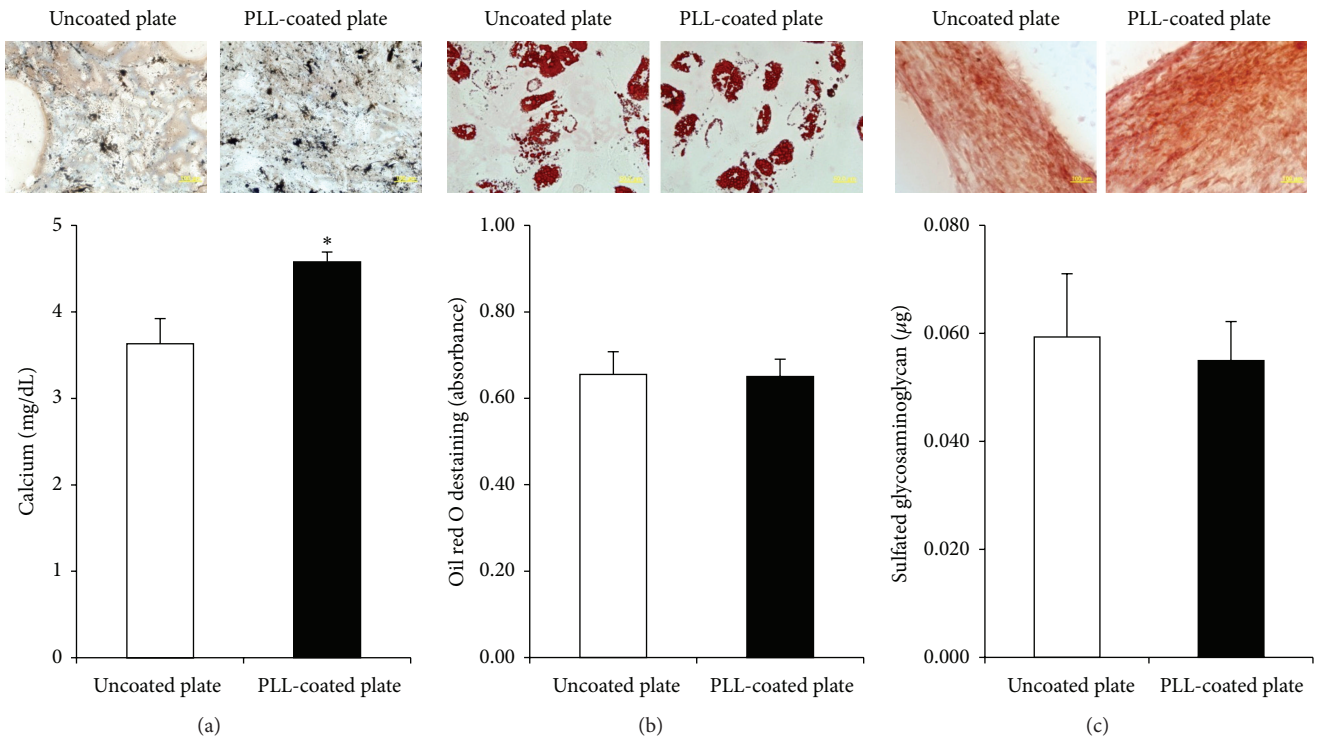

FIGURE 4: Differentiation potential of cells cultured on uncoated and poly-L-lysine- (PLL-) coated plates. (a) Osteogenesis was determined by Von Kossa staining and calcium quantification. (b) Adipogenesis was examined by oil red O staining. For quantitative analysis, absorbance was detected after destaining. (c) Chondrogenesis was analysed by safranin O staining and glycosaminoglycan quantification. The data represent the mean ± standard deviation of three independent experiments. $^{*}p < 0.05$.

regulation of cell proliferation (GO:0008284), and focal adhesion (GO:0005925) were upregulated in MSCs cultured on PLL-coated plates compared to MSCs cultured on uncoated plates. These findings are in line with the increased proliferation potential of MSCs cultured on PLL-coated plates. Several genes related to cell proliferation might also act as inhibitors of MSC senescence. However, to determine the role of individual genes on MSC, additional studies will be required.

Several studies have reported that MSCs undergo a typical phenomenon of replicative senescence with changing cell morphology and decreasing proliferation under *in vitro* culture. We determined that senescence of bone marrow-derived MSCs occurred after 6 passages. Such senescence is considered to be associated with the accumulation of intracellular reactive oxygen species (ROS) and shortening of telomere length [57]. High levels of ROS are associated with the loss of stemness, and growth arrest is triggered by the p53 and p21 pathways [58, 59]. In this study, we showed that the cell senescence was inhibited by PLL through the suppression of $p16^{INK4a}$ and $p21^{Cip1}$ mRNA expression levels. Based on those mechanisms, it was recently reported that cellular senescence of MSCs could be inhibited via FGF-2 mediated suppression of p53 and p21 [60]. Overall, our study showed that PLL induces the upregulation of genes involved in cell adhesion, FGF-2 signalling, cell cycle regulation, stemness, cell differentiation, and cell proliferation with downregulation of genes associated with oxidative stress and tumorigenicity. Changes in those genes corresponded to significant suppression of MSC senescence by PLL. The genes affected by PLL are summarized in Tables 2 and 3. Our results require further investigation as to the specific genes that have functional implications on senescent MSCs.

Cellular senescence is generally considered an irreversible cellular change. In our study, the proliferation capacity and functionality of senescent MSCs were improved by PLL; however this effect of PLL was reversed when these cells were recultured in the absence of PLL on uncoated plates (data not shown). PLL as a coating substrate affects senescent MSCs when the cells attached on PLL through cell to ECM interaction. Therefore, senescent MSCs on uncoated plates could return to a senescence phenotype if they were not maintained on PLL-coated culture vessels. Previously, Yocum et al. reported that infusing cells labeled with ferumoxides-PLL complex does not affect hematologic or biochemical measures [61]. MSCs cultured on and mixed with PLL may be useful for clinical application because PLL definitely enhances functionality, and it does not alter biochemical and hematologic measurements *in vivo*.

In conclusion, we established an easy and simple culture system for culturing MSCs. Our system enhanced the proliferation rates of MSCs and evokes consistent changes in gene expression associated with MSC stemness markers and differentiation potential. We conclude that senescent MSCs can

be converted to a normal-like state using PLL. Improvement of the MSC culture system *in vitro* will contribute greatly to the development of cell-based therapy and regenerative medicine.

Competing Interests

The authors declare that there is no conflict of interests regarding the publication of this paper.

Acknowledgments

This research was supported by Basic Science Research Program through the National Research Foundation of Korea (NRF) funded by the Ministry of Education (2013R1A1A2061722) and Grant HI15C0942 from the Korea Health Technology R&D Project through the Korea Health Industry Development Institute (KHIDI), funded by the Ministry of Health & Welfare, Republic of Korea.

References

[1] M. F. Pittenger, A. M. Mackay, S. C. Beck et al., "Multilineage potential of adult human mesenchymal stem cells," *Science*, vol. 284, no. 5411, pp. 143–147, 1999.

[2] S. A. Wexler, C. Donaldson, P. Denning-Kendall, C. Rice, B. Bradley, and J. M. Hows, "Adult bone marrow is a rich source of human mesenchymal 'stem' cells but umbilical cord and mobilized adult blood are not," *British Journal of Haematology*, vol. 121, no. 2, pp. 368–374, 2003.

[3] G. Kögler, S. Sensken, and P. Wernet, "Comparative generation and characterization of pluripotent unrestricted somatic stem cells with mesenchymal stem cells from human cord blood," *Experimental Hematology*, vol. 34, no. 11, pp. 1589–1595, 2006.

[4] S. Barlow, G. Brooke, K. Chatterjee et al., "Comparison of human placenta- and bone marrow-derived multipotent mesenchymal stem cells," *Stem Cells and Development*, vol. 17, no. 6, pp. 1095–1107, 2008.

[5] H. Busser, C. De Bruyn, F. Urbain et al., "fIsolation of adipose-derived stromal cells without enzymatic treatment: expansion, phenotypical, and functional characterization," *Stem Cells and Development*, vol. 23, no. 19, pp. 2390–2400, 2014.

[6] P. H. Lee, J. E. Lee, H.-S. Kim et al., "A randomized trial of mesenchymal stem cells in multiple system atrophy," *Annals of Neurology*, vol. 72, no. 1, pp. 32–40, 2012.

[7] L. Mazzini, K. Mareschi, I. Ferrero et al., "Autologous mesenchymal stem cells: clinical applications in amyotrophic lateral sclerosis," *Neurological Research*, vol. 28, no. 5, pp. 523–526, 2006.

[8] W. Wagner, P. Horn, M. Castoldi et al., "Replicative senescence of mesenchymal stem cells: a continuous and organized process," *PLoS ONE*, vol. 3, no. 5, Article ID e2213, 2008.

[9] L. Hayflick, "The limited in vitro lifetime of human diploid cell strains," *Experimental Cell Research*, vol. 37, no. 3, pp. 614–636, 1965.

[10] M. M. Bonab, K. Alimoghaddam, F. Talebian, S. H. Ghaffari, A. Ghavamzadeh, and B. Nikbin, "Aging of mesenchymal stem cell in vitro," *BMC Cell Biology*, vol. 7, article 14, 2006.

[11] K. Itahana, J. Campisi, and G. P. Dimri, "Mechanisms of cellular senescence in human and mouse cells," *Biogerontology*, vol. 5, no. 1, pp. 1–10, 2004.

[12] S. Loft, P. H. Danielsen, L. Mikkelsen, L. Risom, L. Forchhammer, and P. Møller, "Biomarkers of oxidative damage to DNA and repair," *Biochemical Society Transactions*, vol. 36, no. 5, pp. 1071–1076, 2008.

[13] W. L. Grayson, F. Zhao, B. Bunnell, and T. Ma, "Hypoxia enhances proliferation and tissue formation of human mesenchymal stem cells," *Biochemical and Biophysical Research Communications*, vol. 358, no. 3, pp. 948–953, 2007.

[14] W. L. Grayson, F. Zhao, R. Izadpanah, B. Bunnell, and T. Ma, "Effects of hypoxia on human mesenchymal stem cell expansion and plasticity in 3D constructs," *Journal of Cellular Physiology*, vol. 207, no. 2, pp. 331–339, 2006.

[15] H. Ren, Y. Cao, Q. Zhao et al., "Proliferation and differentiation of bone marrow stromal cells under hypoxic conditions," *Biochemical and Biophysical Research Communications*, vol. 347, no. 1, pp. 12–21, 2006.

[16] K. R. Shibata, T. Aoyama, Y. Shima et al., "Expression of the p16INK4A gene is associated closely with senescence of human mesenchymal stem cells and is potentially silenced by DNA methylation during in vitro expansion," *STEM CELLS*, vol. 25, no. 9, pp. 2371–2382, 2007.

[17] M. Abedin and N. King, "Diverse evolutionary paths to cell adhesion," *Trends in Cell Biology*, vol. 20, no. 12, pp. 734–742, 2010.

[18] G. Michel, T. Tonon, D. Scornet, J. M. Cock, and B. Kloareg, "The cell wall polysaccharide metabolism of the brown alga *Ectocarpus siliculosus*. Insights into the evolution of extracellular matrix polysaccharides in Eukaryotes," *New Phytologist*, vol. 188, no. 1, pp. 82–97, 2010.

[19] B. de Kruijff and P. R. Cullis, "The influence of poly(L-lysine) on phospholipid polymorphism. Evidence that electrostatic polypeptide-phospholipid interactions can modulate bilayer/non-bilayer transitions," *Biochimica et Biophysica Acta*, vol. 601, no. 1, pp. 235–240, 1980.

[20] K. Pachmann and W. Leibold, "Insolubilization of protein antigens on polyacrylic plastic beads using poly-l-lysine," *Journal of Immunological Methods*, vol. 12, no. 1-2, pp. 81–89, 1976.

[21] K.-S. Park, J. Ahn, J. Y. Kim, H. Park, H. O. Kim, and S.-H. Lee, "Poly-L-lysine increases the *ex vivo* expansion and erythroid differentiation of human hematopoietic stem cells, as well as erythroid enucleation efficacy," *Tissue Engineering Part A*, vol. 20, no. 5-6, pp. 1072–1080, 2014.

[22] L. Cai, J. Lu, V. Sheen, and S. Wang, "Optimal poly(l-lysine) grafting density in hydrogels for promoting neural progenitor cell functions," *Biomacromolecules*, vol. 13, no. 5, pp. 1663–1674, 2012.

[23] A. I. Caplan and D. Correa, "The MSC: an injury drugstore," *Cell Stem Cell*, vol. 9, no. 1, pp. 11–15, 2011.

[24] P. Charbord, "Bone marrow mesenchymal stem cells: historical overview and concepts," *Human Gene Therapy*, vol. 21, no. 9, pp. 1045–1056, 2010.

[25] H.-S. Kim, D.-Y. Choi, S. J. Yun et al., "Proteomic analysis of microvesicles derived from human mesenchymal stem cells," *Journal of Proteome Research*, vol. 11, no. 2, pp. 839–849, 2012.

[26] M. S. Choudhery, M. Khan, R. Mahmood, A. Mehmood, S. N. Khan, and S. Riazuddin, "Bone marrow derived mesenchymal stem cells from aged mice have reduced wound healing, angiogenesis, proliferation and anti-apoptosis capabilities," *Cell Biology International*, vol. 36, no. 8, pp. 747–753, 2012.

[27] Y. H. Kim, D. S. Yoon, H. O. Kim, and J. W. Lee, "Characterization of different subpopulations from bone marrow-derived mesenchymal stromal cells by alkaline phosphatase expression," *Stem Cells and Development*, vol. 21, no. 16, pp. 2958–2968, 2012.

[28] L.-X. Tay, C.-K. Lim, A. Mansor, and T. Kamarul, "Differential protein expression between chondrogenic differentiated MSCs, undifferentiated MSCs and adult chondroctyes derived from *Oryctolagus cuniculus* in vitro," *International Journal of Medical Sciences*, vol. 11, no. 1, pp. 24–33, 2013.

[29] E. Pierantozzi, B. Gava, I. Manini et al., "Pluripotency regulators in human mesenchymal stem cells: expression of NANOG but not of OCT-4 and SOX-2," *Stem Cells and Development*, vol. 20, no. 5, pp. 915–923, 2011.

[30] C.-C. Tsai, P.-F. Su, Y.-F. Huang, T.-L. Yew, and S.-C. Hung, "Oct4 and nanog directly regulate Dnmt1 to maintain self-renewal and undifferentiated state in mesenchymal stem cells," *Molecular Cell*, vol. 47, no. 2, pp. 169–182, 2012.

[31] J. Ge, Y. Ju, Z. Xue et al., "Distal C terminus of CaV1.2 channels plays a crucial role in the neural differentiation of dental pulp stem cells," *PLoS ONE*, vol. 8, no. 11, Article ID e81332, 2013.

[32] M.-L. Nueda, V. Baladrón, J.-J. García-Ramírez et al., "The novel gene *EGFL9/Dlk2*, highly homologous to *Dlk1*, functions as a modulator of adipogenesis," *Journal of Molecular Biology*, vol. 367, no. 5, pp. 1270–1280, 2007.

[33] C. Hoareau-Aveilla, M. Bonoli, M. Caizergues-Ferrer, and Y. Henry, "hNaf1 is required for accumulation of human box H/ACA snoRNPs, scaRNPs, and telomerase," *RNA*, vol. 12, no. 5, pp. 832–840, 2006.

[34] S.-T. Liu, J. C. Hittle, S. A. Jablonski, M. S. Campbell, K. Yoda, and T. J. Yen, "Human CENP-I specifies localization of CENP-F, MAD1 and MAD2 to kinetochores and is essential for mitosis," *Nature Cell Biology*, vol. 5, no. 4, pp. 341–345, 2003.

[35] A. Than, X. Zhang, M. K.-S. Leow, C. L. Poh, S. K. Chong, and P. Chen, "Apelin attenuates oxidative stress in human adipocytes," *The Journal of Biological Chemistry*, vol. 289, no. 6, pp. 3763–3774, 2014.

[36] H. Shao, J. H. Wang, M. R. Pollak, and A. Wells, "α-actinin-4 is essential for maintaining the spreading, motility and contractility of fibroblasts," *PLoS ONE*, vol. 5, no. 11, Article ID e13921, 2010.

[37] M.-Y. Lee, H.-D. Hofmann, and M. Kirsch, "Expression of ciliary neurotrophic factor receptor-α messenger RNA in neonatal and adult rat brain: an in situ hybridization study," *Neuroscience*, vol. 77, no. 1, pp. 233–246, 1997.

[38] M. Yasumi, T. Sakisaka, T. Hoshino et al., "Direct binding of Lgl2 to LGN during mitosis and its requirement for normal cell division," *Journal of Biological Chemistry*, vol. 280, no. 8, pp. 6761–6765, 2005.

[39] J. Christensen, P. Cloos, U. Toftegaard et al., "Characterization of E2F8, a novel E2F-like cell-cycle regulated repressor of E2F-activated transcription," *Nucleic Acids Research*, vol. 33, no. 17, pp. 5458–5470, 2005.

[40] E. Manser, T. Leung, H. Salihuddin, L. Tan, and L. Lim, "A non-receptor tyrosine kinase that inhibits the GTPase activity of p21cdc42," *Nature*, vol. 363, no. 6427, pp. 364–367, 1993.

[41] S. Diecke, A. Quiroga-Negreira, T. Redmer, and D. Besser, "FGF2 signaling in mouse embryonic fibroblasts is crucial for self-renewal of embryonic stem cells," *Cells Tissues Organs*, vol. 188, no. 1-2, pp. 52–61, 2008.

[42] R. Nakayama, Y. Miura, J. Ogino et al., "Detection of *HEY1-NCOA2* fusion by fluorescence in-situ hybridization in formalin-fixed paraffin-embedded tissues as a possible diagnostic tool for mesenchymal chondrosarcoma," *Pathology International*, vol. 62, no. 12, pp. 823–826, 2012.

[43] S. Goicoechea, A. W. Orr, M. A. Pallero, P. Eggleton, and J. E. Murphy-Ullrich, "Thrombospondin mediates focal adhesion disassembly through interactions with cell surface calreticulin," *The Journal of Biological Chemistry*, vol. 275, no. 46, pp. 36358–36368, 2000.

[44] T. Kim, K. Kim, S. H. Lee et al., "Identification of LRRc17 as a negative regulator of receptor activator of NF-κB ligand (RANKL)-induced osteoclast differentiation," *Journal of Biological Chemistry*, vol. 284, no. 22, pp. 15308–15316, 2009.

[45] H. Yoshioka and F. Ramirez, "Pro-alpha 1(XI) collagen. Structure of the amino-terminal propeptide and expression of the gene in tumor cell lines," *The Journal of Biological Chemistry*, vol. 265, no. 11, pp. 6423–6426, 1990.

[46] L. Zhang, M. Wang, X. Kang et al., "Oxidative stress and asthma: proteome analysis of chitinase-like proteins and FIZZ1 in lung tissue and bronchoalveolar lavage fluid," *Journal of Proteome Research*, vol. 8, no. 4, pp. 1631–1638, 2009.

[47] A. Khurana, H. McKean, H. Kim et al., "Silencing of HSulf-2 expression in MCF10DCIS.com cells attenuate ductal carcinoma in situ progression to invasive ductal carcinoma in vivo," *Breast Cancer Research*, vol. 14, no. 2, article R43, 2012.

[48] M. Morimoto-Tomita, K. Uchimura, A. Bistrup et al., "Sulf-2, a proangiogenic heparan sulfate endosulfatase, is upregulated in breast cancer," *Neoplasia*, vol. 7, no. 11, pp. 1001–1010, 2005.

[49] A. W. Orr, M. A. Pallero, and J. E. Murphy-Ullrich, "Thrombospondin stimulates focal adhesion disassembly through Gi- and phosphoinositide 3-kinase-dependent ERK activation," *Journal of Biological Chemistry*, vol. 277, no. 23, pp. 20453–20460, 2002.

[50] K. Tanaka, Y. Okugawa, Y. Toiyama et al., "Brain-Derived Neurotrophic Factor (BDNF)-induced Tropomyosin-related kinase B (Trk B) signaling is a potential therapeutic target for peritoneal carcinomatosis arising from colorectal cancer," *PLoS ONE*, vol. 9, no. 5, article e96410, 2014.

[51] J. You, D. S. Shin, D. Patel, Y. Gao, and A. Revzin, "Multilayered heparin hydrogel microwells for cultivation of primary hepatocytes," *Advanced Healthcare Materials*, vol. 3, no. 1, pp. 126–132, 2014.

[52] Y. Xu, X. Zhu, H. S. Hahm et al., "Revealing a core signaling regulatory mechanism for pluripotent stem cell survival and self-renewal by small molecules," *Proceedings of the National Academy of Sciences of the United States of America*, vol. 107, no. 18, pp. 8129–8134, 2010.

[53] N. Z. Kuhn and R. S. Tuan, "Regulation of stemness and stem cell niche of mesenchymal stem cells: Implications in tumorigenesis and metastasis," *Journal of Cellular Physiology*, vol. 222, no. 2, pp. 268–277, 2010.

[54] D. J. Rodda, J.-L. Chew, L.-H. Lim et al., "Transcriptional regulation of Nanog by OCT4 and SOX2," *Journal of Biological Chemistry*, vol. 280, no. 26, pp. 24731–24737, 2005.

[55] D. S. Yoon, Y. H. Kim, H. S. Jung, S. Paik, and J. W. Lee, "Importance of Sox2 in maintenance of cell proliferation and multipotency of mesenchymal stem cells in low-density culture," *Cell Proliferation*, vol. 44, no. 5, pp. 428–440, 2011.

[56] T. M. Liu, Y. N. Wu, X. M. Guo, J. H. P. Hui, E. H. Lee, and B. Lim, "Effects of Ectopic Nanog and Oct4 overexpression on mesenchymal stem cells," *Stem Cells and Development*, vol. 18, no. 7, pp. 1013–1022, 2009.

[57] K. Ksiazek, "A comprehensive review on mesenchymal stem cell growth and senescence," *Rejuvenation Research*, vol. 12, no. 2, pp. 105–116, 2009.

[58] U. Herbig, W. A. Jobling, B. P. C. Chen, D. J. Chen, and J. M. Sedivy, "Telomere shortening triggers senescence of human cells through a pathway involving ATM, p53, and p21CIP1, but not p16INK4a," *Molecular Cell*, vol. 14, no. 4, pp. 501–513, 2004.

[59] Z. Tothova, R. Kollipara, B. J. Huntly et al., "FoxOs are critical mediators of hematopoietic stem cell resistance to physiologic oxidative stress," *Cell*, vol. 128, no. 2, pp. 325–339, 2007.

[60] T. Ito, R. Sawada, Y. Fujiwara, Y. Seyama, and T. Tsuchiya, "FGF-2 suppresses cellular senescence of human mesenchymal stem cells by down-regulation of TGF-β2," *Biochemical and Biophysical Research Communications*, vol. 359, no. 1, pp. 108–114, 2007.

[61] G. T. Yocum, L. B. Wilson, P. Ashari, E. K. Jordan, J. A. Frank, and A. S. Arbab, "Effect of human stem cells labeled with ferumoxides-poly-L-lysine on hematologic and biochemical measurements in rats," *Radiology*, vol. 235, no. 2, pp. 547–552, 2005.

Hindawi Publishing Corporation
BioMed Research International
Volume 2016, Article ID 6913860, 7 pages
http://dx.doi.org/10.1155/2016/6913860

Research Article

Usefulness of Multiplex Real-Time PCR for Simultaneous Pathogen Detection and Resistance Profiling of Staphylococcal Bacteremia

Yousun Chung,[1] Taek Soo Kim,[2] Young Gi Min,[2] Yun Ji Hong,[3] Jeong Su Park,[3] Sang Mee Hwang,[3] Kyoung-Ho Song,[4] Eu Suk Kim,[4] Kyoung Un Park,[1,3] Hong Bin Kim,[4] Junghan Song,[1,3] and Eui-Chong Kim[1,2]

[1]*Department of Laboratory Medicine, Seoul National University College of Medicine, 101 Daehak-ro, Jongno-gu, Seoul 03080, Republic of Korea*
[2]*Department of Laboratory Medicine, Seoul National University Hospital, 101 Daehak-ro, Jongno-gu, Seoul 03080, Republic of Korea*
[3]*Department of Laboratory Medicine, Seoul National University Bundang Hospital, 82 Gumi-ro, 173 Beon-gil, Bundang-gu, Seongnam-si, Gyeonggi-do 13620, Republic of Korea*
[4]*Department of Internal Medicine, Seoul National University Bundang Hospital, 82 Gumi-ro, 173 Beon-gil, Bundang-gu, Seongnam-si, Gyeonggi-do 13620, Republic of Korea*

Correspondence should be addressed to Kyoung Un Park; m91w95pf@snu.ac.kr

Received 24 March 2016; Accepted 23 May 2016

Academic Editor: Giulio Mengozzi

Staphylococci are the leading cause of nosocomial blood stream infections. Fast and accurate identification of staphylococci and confirmation of their methicillin resistance are crucial for immediate treatment with effective antibiotics. A multiplex real-time PCR assay that targets *mecA*, *femA* specific for *S. aureus*, *femA* specific for *S. epidermidis*, *16S rRNA* for universal bacteria, and *16S rRNA* specific for staphylococci was developed and evaluated with 290 clinical blood culture samples containing Gram-positive cocci in clusters (GPCC). For the 262 blood cultures identified to the species level with the MicroScan WalkAway system (Siemens Healthcare Diagnostics, USA), the direct real-time PCR assay of positive blood cultures showed very good agreement for the categorization of staphylococci into methicillin-resistant *S. aureus* (MRSA), methicillin-susceptible *S. aureus* (MSSA), methicillin-resistant *S. epidermidis* (MRSE), methicillin-susceptible *S. epidermidis* (MSSE), methicillin-resistant non-*S. epidermidis* CoNS (MRCoNS), and methicillin-susceptible non-*S. epidermidis* CoNS (MSCoNS) ($\kappa = 0.9313$). The direct multiplex real-time PCR assay of positive blood cultures containing GPCC can provide essential information at the critical point of infection with a turnaround time of no more than 4 h. Further studies should evaluate the clinical outcome of using this rapid real-time PCR assay in glycopeptide antibiotic therapy in clinical settings.

1. Introduction

Staphylococci are the most commonly isolated organisms in clinical laboratories, accounting for almost 30% of all nosocomial infections and 50% of nosocomial bloodstream infections [1]. *Staphylococcus aureus* is the leading cause of nosocomial infections [2], and methicillin-resistant *S. aureus* (MRSA) infections result in significant morbidity, mortality, and longer hospital stays if not treated early with effective antibiotics [3]. Coagulase-negative staphylococci (CoNS) are the most common isolates from blood culture, and more than 70% are resistant to oxacillin [4]. Although they are known to contaminate blood cultures as a result of their colonization on the skin and mucous membranes, they have recently become important pathogens causing nosocomial infections with the increasing use of invasive procedures and prosthetic devices [5, 6]. Fast and accurate identification of staphylococci and confirmation of their methicillin resistance are crucial for immediate treatment with effective antibiotics, which will result in decreased morbidity and mortality rates [7].

The conventional culture method for the identification and susceptibility testing of positive blood cultures has

Table 1: PCR primers and TaqMan probes for *mecA*, *femA* specific for *S. aureus* (*femA*-SA), *femA* specific for *S. epidermidis* (*femA*-SE), and universal *16S rRNA* and PCR primers for staphylococcal *16S rRNA*.

Target genes	Sequence
mecA	5′-CATTGATCGCAACGTTCAATTT-3′
	5′-TGGTCTTTCTGCATTCCTGGA-3′
	5′-FAM-TGGAAGTTAGATTGGGATCATAGCGTCAT-TAMRA-3′
femA-SA	5′-TGCCTTTACAGATAGCATGCCA-3′
	5′-AGTAAGTAAGCAAGCTGCAATGACC-3′
	5′-JOE-TCATTTCACGCAAACTGTTGGCCACTATG-BHQ1-3′
femA-SE	5′-CAACTCGATGCAAATCAGCAA-3′
	5′-GAACCGCATAGCTCCCTGC-3′
	5′-JOE-TACTACGCTGGTGGAACTTCAAATCGTTATCG-BHQ1-3′
Universal *16S rRNA*	5′-TCCTACGGGAGGCAGCAGT-3′
	5′-GGACTACCAGGGTATCTAATCCTGTT-3′
	5′-FAM-CGTATTACCGCGGCTGCTGGCAC-TAMRA-3′
Staphylococcal *16S rRNA*	5′-GCAAGCGTTATCCGGATTT-3′
	5′-CTTAATGATGGCAACTAAGC-3′

some disadvantages, including long turnaround time and potential false-negative results when samples are obtained after antimicrobial therapy. Real-time PCR is significantly faster than conventional PCR and other detection methods, and its excellent sensitivity and specificity, low contamination risk, ease of use, and high speed have made real-time PCR technology appealing to clinical microbiology laboratories [8].

The aim of this study was to develop and evaluate a multiplex real-time PCR assay for the rapid detection and identification of MRSA, methicillin-susceptible *S. aureus* (MSSA), methicillin-resistant *S. epidermidis* (MRSE), methicillin-susceptible *S. epidermidis* (MSSE), methicillin-resistant non-*S. epidermidis* CoNS (MRCoNS), and methicillin-susceptible non-*S. epidermidis* CoNS (MSCoNS) directly from positive blood cultures containing Gram-positive cocci in clusters (GPCC) by targeting *mecA* for determining methicillin resistance, *femA* specific for *S. aureus* (*femA*-SA), *femA* specific for *S. epidermidis* (*femA*-SE), *16S rRNA* for universal bacteria, and *16S rRNA* specific for staphylococci.

2. Materials and Methods

2.1. Blood Culture. This study evaluated 290 blood cultures containing GPCC obtained from March 2013 to December 2013 at Seoul National University Bundang Hospital. Two or more pairs of culture bottles for aerobes or anaerobes were incubated in BacT/Alert 3D (bioMérieux Inc., Durham, NC, USA) or BACTEC FX (BD Diagnostics, Sparks, MD, USA) blood culture systems for 5 days after inoculation for blood drawn from the patient. If bacterial growth was not detected within 5 days, then the blood culture result was considered negative. When bacterial growth was noted, blood from the positive bottles was Gram-stained, and samples containing GPCC (230 specimens in BacT/Alert 3D (bioMérieux Inc.) and 60 specimens in BACTEC FX (BD Diagnostics)) were inoculated onto blood agar plates and cultured overnight at 35°C in a 5% CO_2 incubator. Isolates were identified by colony morphology, Gram-staining, catalase, and coagulase tests. Final identification according to phenotypic characteristics and antimicrobial susceptibility tests was performed using the MicroScan WalkAway system (Siemens Healthcare Diagnostics, Deerfield, IL, USA) with Pos Combo Panel Type 1A.

2.2. DNA Extraction. A 100 μL aliquot of blood was drawn directly from the positive blood culture bottles, collected on filter paper, and dried for 15 min at room temperature. The blood spot was lysed with 2 mL of lysis buffer for 30 min at room temperature. Next, the paper was removed, and 2 μL of lysozyme-Tris-EDTA buffer was added to 500 μL of the eluate and incubated for 30 min at 37°C. The sample was incubated again for 10 min in 2 mL of lysis buffer, and the final eluate was used for nucleic acid extraction with the NucliSENS easyMAG platform (bioMérieux Inc.).

2.3. Multiplex Real-Time PCR Assay Targeting mecA, femA-SA, femA-SE, and Universal 16S rRNA. The double duplex real-time PCR TaqMan assay was performed with two tubes in one reaction. One tube corresponded to the targets *femA*-SA and *mecA* and the other to the targets *femA*-SE and universal *16S rRNA*. The primers and probes for each target were designed as described by previously published studies [9, 10] (Table 1). Real-time PCR was conducted in a total volume of 20 μL, including 2.0 μL of 10x LightCycler FastStart DNA Master HybProbe (Roche Diagnostics, Mannheim, Germany), 2.4 μL of 15 mM $MgCl_2$ (Takara Bio, Shiga, Japan), 0.2 μM of each primer, and 0.1 μM of each probe with 3.0 μL of DNA template. The amplification conditions used by the m2000rt instrument (Abbott Diagnostic, Chicago, IL, USA) were as follows: 95°C for 10 min followed by 35 cycles of 95°C for 15 sec and 60°C for 1 min in a single real-time PCR assay. Positive controls with MRSA, MSSA, and MRSE and a negative control with sterile distilled water (DW) were included throughout the procedures.

2.4. Additional Real-Time PCR Assay Targeting Staphylococcal 16S rRNA. A real-time PCR assay targeting staphylococcal *16S rRNA* was performed using a LightCycler 2.0 system

Table 2: Interpretation of results by real-time PCR assays.

	mecA	*femA*-SA[a]	*femA*-SE[b]	Universal *16S rRNA*	Staphylococcal *16S rRNA*
MRSA	P[c]	P	N[d]	P	P
MSSA	N	P	N	P	P
MRSE	P	N	P	P	P
MSSE	N	N	P	P	P
MRCoNS	P	N	N	P	P
MSCoNS	N	N	N	P	P
Nonstaphylococci	P or N	N	N	P	N

[a]*femA* specific for *S. aureus*.
[b]*femA* specific for *S. epidermidis*.
[c]Positive.
[d]Negative.

(Roche Diagnostics) for the detection of staphylococci. Primers targeting staphylococcal *16S rRNA* were designed as described in a previously published study [11] (Table 1). Amplification reactions were performed in a 20 μL volume containing 2 μL of DNA template, 0.25 μM of each primer, and 10 μL of 2x SYBR Premix Ex Taq (Takara Bio). The conditions consisted of an initial denaturation at 95°C for 10 min followed by amplification program for 30 cycles of 10 sec at 95°C, 20 sec at 58°C, and 20 sec at 74°C with fluorescence acquisition at the end of each cycle. The amplification program was followed by a melting program consisting of heating to 95°C with a 0 sec hold and 15 sec at 60°C and a gradual increase to 99°C at a rate of 0.1°C/sec with fluorescence acquisition at each temperature transition. Positive controls with MRSA, MSSA, and MRSE and a negative control with sterile DW were included throughout the procedure. The existence of the target was confirmed by melting curve analysis. If the melting temperature (Tm) of the samples was within 0.5°C of the Tm of the positive control's product, they were regarded as positive.

All the above-mentioned real-time PCR assays were repeated with DNA extracted with subcultured colonies for comparison with the direct specimens.

2.5. Categorization of Real-Time PCR Results. Using a double duplex real-time PCR assay, the detection of *femA*-SA and universal *16S rRNA* indicated the presence of MSSA, while the detection of *femA*-SA, *mecA*, and universal *16S rRNA* indicated the presence of MRSA. If *femA*-SE and universal *16S rRNA* were detected, the presence of MSSE was inferred, while the detection of *femA*-SE, *mecA,* and universal *16S rRNA* indicated the presence of MRSE. The detection of *mecA* and universal *16S rRNA* was interpreted as indicating the presence of MRCoNS or methicillin-resistant nonstaphylococci, while the detection of universal *16S rRNA* alone was interpreted as indicating the presence of MSCoNS or methicillin-susceptible nonstaphylococci. The additional PCR test targeting staphylococcal *16S rRNA* confirmed whether the isolate was staphylococci. The detection of universal *16S rRNA*, but not staphylococcal *16S rRNA*, was interpreted as indicating the presence of bacteria other than staphylococci (Table 2). The real-time PCR results were compared with MicroScan identification and susceptibility results as a reference.

3. Results

3.1. Identification Results Obtained with the MicroScan Walk-Away System (Siemens Healthcare Diagnostics). Of the 290 positive blood cultures with GPCC, 262 cultures were identified to the species level by MicroScan as follows: 89 *S. aureus*, 96 *S. epidermidis*, 27 *S. hominis*, 26 *S. capitis*, 9 *S. haemolyticus*, 5 *S. capitis* subsp. *urealyticus*, 2 *Staphylococcus saprophyticus*, 2 *S. lugdunensis*, 2 *S. hominis* subsp. *hominis*, 1 *S. cohnii*, 1 *S. auricularis*, 1 *S. schleiferi*, and 1 *S. schleiferi* subsp. *coagulans*. Fifteen isolates showed low-probability identification, with multiple possible staphylococcal species, and the remaining 13 isolates were nonstaphylococci, including 12 *Micrococcus* species and 1 *Enterococcus faecalis*.

3.2. Comparison of Results Obtained by Real-Time PCR with Direct Specimens and the Results of the MicroScan WalkAway System (Siemens Healthcare Diagnostics). The real-time PCR identification of MRSA correlated with the MicroScan results for 46 out of 47 specimens. The discordant one was identified as MSSA by MicroScan. The real-time PCR identification of MSSA correlated with the MicroScan results for all 42 isolates.

Eighty-five out of 96 blood cultures identified as containing MRSE by real-time PCR were confirmed by MicroScan, while four isolates were identified as MRCoNS and two as MSSE. The MicroScan results for the remaining five isolates were low-probability identifications with multiple possible staphylococcal species that were all resistant to methicillin. The real-time PCR identification of MSSE correlated with the MicroScan results for seven out of eight isolates; the discordant isolate was identified as MSCoNS by MicroScan.

A total of 50 out of 58 blood cultures containing MRCoNS, as determined by real-time PCR, were confirmed to be MRCoNS with MicroScan, while one isolate was identified as MRSE and another as MSCoNS. The MicroScan results for the remaining six isolates were low-probability identifications with multiple possible staphylococcal species that were all resistant to methicillin. Eighteen out of 26

Table 3: Comparison of results by real-time PCR with direct specimen and results by MicroScan WalkAway system (thirteen isolates of nonstaphylococci are excluded.).

MicroScan WalkAway system	Real-time PCR assays with direct specimen					
	MRSA[a]	MSSA[b]	MRSE[c]	MSSE[d]	MRCoNS[e]	MSCoNS[f]
MRSA	46	—	—	—	—	—
MSSA	1	42	—	—	—	—
MRSE	—	—	85	—	1	—
MSSE	—	—	2	7	—	1
MRCoNS	—	—	4	—	50	3
MSCoNS	—	—	—	1	1	18
Unidentified staphylococci*	—	—	5	—	6	4

*All the results of *mecA* were in concordance with phenotypic methicillin resistance.
[a]Methicillin-resistant *S. aureus*.
[b]Methicillin-susceptible *S. aureus*.
[c]Methicillin-resistant *S. epidermidis*.
[d]Methicillin-susceptible *S. epidermidis*.
[e]Methicillin-resistant non-*S. epidermidis* CoNS.
[f]Methicillin-susceptible non-*S. epidermidis* CoNS.

blood cultures containing MSCoNS by real-time PCR were confirmed by MicroScan, while three were identified as MRCoNS and one as MSSE. The MicroScan results for the remaining four isolates were low-probability identifications with multiple possible staphylococcal species that were all sensitive to methicillin. Thirteen isolates that were interpreted as nonstaphylococci by real-time PCR were confirmed as 12 *Micrococcus* species and 1 *Enterococcus faecalis* by MicroScan system.

For the 262 blood cultures identified to the species level by MicroScan, the results agreed very well with those obtained by real-time PCR for staphylococcal species categorization into MRSA, MSSA, MRSE, MSSE, MRCoNS, and MSCoNS (Cohen's unweighted kappa coefficient $\kappa = 0.9313$) (Table 3). The sensitivity and specificity of *mecA*, *femA*-SA, *femA*-SE, universal *16S rRNA*, and staphylococcal *16S rRNA* were evaluated with the 262 blood cultures according to the MicroScan results. The sensitivity and specificity were, respectively, 98.4% and 94.5% for the *mecA* gene, 100.0% and 100.0% for *femA*-SA, 97.9% and 97.0% for *femA*-SE, 100.0% and 100.0% for universal *16S rRNA,* and 100.0% and 100.0% for staphylococcal *16S rRNA* (Table 4).

3.3. Comparison of the Results Obtained by Real-Time PCR with Direct Specimens and Real-Time PCR with Subcultured Colonies. The real-time PCR results of direct specimens correlated with the PCR results of subcultured colonies for 282 of 290 samples. The results for 14 out of the 282 concordant samples were discordant with the MicroScan results. Of the seven samples that were interpreted as MRSE by both real-time PCR techniques, three were identified by MicroScan as MSCoNS, three as methicillin-resistant staphylococci (not identified to the species level), and one as MSSE. In two samples identified as MRCoNS by both real-time PCR techniques, the MicroScan identifications were MRSE and MSCoNS. Of the four samples identified as MSCoNS by both real-time PCR techniques, one was identified by MicroScan as MSSE and the other three were identified as MRCoNS. The remaining sample identified as MSSE by both real-time PCR techniques was identified as MSCoNS by MicroScan.

Table 4: Sensitivity and specificity of *mecA*, *femA* specific for *S. aureus* (*femA*-SA), *femA* specific for *S. epidermidis* (*femA*-SE), universal *16S rRNA*, and staphylococcal *16S rRNA*.

Target genes	Sensitivity (%)	Specificity (%)
mecA	98.4	94.5
femA-SA	100.0	100.0
femA-SE	97.9	97.0
Universal *16S rRNA*	100.0	100.0
Staphylococcal *16S rRNA*	100.0	100.0

There were eight discordant results between real-time PCR with direct specimens and real-time PCR with subcultured colonies. In two samples that were identified as MSSA and MSSE by MicroScan, only real-time PCR with direct specimens detected *mecA*. In one sample, identified as MRCoNS by MicroScan, only real-time PCR with direct specimens detected *femA*-SE. In another sample, identified as MRSA by MicroScan, only real-time PCR with colonies failed to detect *femA*-SA. Finally, in the remaining four samples, which were identified as MRSE by MicroScan, only real-time PCR with colonies failed to detect *femA*-SE. The discordant results for the three methods are shown in Table 5.

4. Discussion

In this study, a multiplex real-time PCR assay that targets *mecA*, *femA*-SA, *femA*-SE, universal bacterial 16S rRNA, and staphylococci-specific 16S rRNA was developed and evaluated with clinical samples for the rapid identification of GPCC and determination of methicillin susceptibility. Overall, there was very good agreement between the real-time PCR with direct specimens and the MicroScan system for the 290 blood cultures, indicating reliable categorization

Table 5: The discordant results between real-time PCR with direct specimen, real-time PCR with subcultured colonies, and MicroScan WalkAway system.

Real-time PCR with direct specimen	Real-time PCR with subcultured colonies	MicroScan Walkaway system	Number
MRSE[a]	MRSE	MRCoNS[b]	3
MRSE	MRSE	MSSE[c]	1
MRSE	MRSE	MR staphylococci	3
MSSE	MSSE	MSCoNS[d]	1
MRCoNS	MRCoNS	MRSE	1
MRCoNS	MRCoNS	MSCoNS	1
MSCoNS	MSCoNS	MSSE	1
MSCoNS	MSCoNS	MRCoNS	3
MRSA[e]	MSSA[f]	MSSA	1
MRSA	MRCoNS	MRSA	1
MRSE	MSSE	MSSE	1
MRSE	MRCoNS	MRCoNS	1
MRSE	MRCoNS	MRSE	4

[a]MRSE, methicillin-resistant *S. epidermidis*.
[b]MRCoNS, methicillin-resistant non-*S. Epidermidis* CoNS.
[c]MSSE, methicillin-susceptible *S. epidermidis*.
[d]MSCoNS, methicillin-susceptible non-*S. epidermidis* CoNS.
[e]MRSA, methicillin-resistant *S. aureus*.
[f]MSSA, methicillin-susceptible *S. aureus*.

as MRSA, MSSA, MRSE, MSSE, MRCoNS, MSCoNS, and nonstaphylococci.

Real-time PCR correctly identified all 46 positive blood cultures, which were confirmed as MRSA by MicroScan. Of the 43 blood cultures identified as MSSA by MicroScan, all but one were identified as MSSA by real-time PCR; the discordant culture was identified as MRSA by real-time PCR and as MSSA by additional PCR with subcultured colonies. This result could be due to nonspecific amplification of the *mecA* gene, but the presence of the *mecA* gene at a very low level in the positive blood bottle is also a potential explanation. There were no *S. aureus* isolates that were identified as *mecA* negative by real-time PCR but methicillin-resistant by MicroScan. It would be more troublesome if methicillin-resistant strains were not detected by PCR because these cases are likely to result in treatment failures.

In two out of 96 cultures identified as *S. epidermidis* by MicroScan, the *femA*-SE gene was not detected by real-time PCR with direct specimens or real-time PCR with subcultured colonies. As suggested by the manufacturers of MicroScan, we used a cut-off of 85% for identification at the species level as indicating a high probability and no additional tests required. However, previous studies have reported the misidentification of staphylococci by MicroScan, and misidentification by MicroScan is also a possibility in these cases [12, 13].

The *mecA* gene was detected by real-time PCR in all 86 blood cultures that were identified as MRSE by MicroScan. In two samples out of 10 blood cultures identified as MSSE by MicroScan, *mecA* was detected by real-time PCR. PCR testing using DNA from the subcultured colonies was positive for *mecA* in one sample but negative in the other sample. In the case of positive *mecA* identification by both PCR assays (direct specimen and subcultured colonies) but identification as methicillin-susceptible by MicroScan, there is a possibility of false oxacillin susceptibility results due to the heteroresistance phenomenon, which is a consequence of the complex regulation of the phenotypic expression of the *mecA* gene [14, 15].

Among the 57 isolates identified as MRCoNS by MicroScan, three were negative in *mecA* using real-time PCR directly from the blood culture bottles and additional PCR with subcultured colonies. This result could be attributed to false-negatives due to the possible limitations of PCR assays, such as the presence of PCR inhibitors. However, another possible explanation is a resistance mechanism other than *mecA*. Strains without the *mecA* gene can acquire methicillin resistance modification of normal PBP genes or overproduction of staphylococcal β-lactamase, resulting in methicillin resistance [16–18]. There were two discordant results out of 20 blood cultures identified as MSCoNS by MicroScan. In one sample, *mecA* was detected by both real-time PCR assays (direct specimen and subcultured colonies), while *femA*-SE genes were detected in the other sample by both real-time PCR assays.

For the fifteen staphylococci that were not identified to the species level by MicroScan, the *mecA* results were all in concordance with phenotypic methicillin resistance. And for the thirteen isolates identified as *Micrococci* and *Enterococci* by MicroScan, only universal *16S rRNA* genes were detected by real-time PCR assays.

One limitation of this assay is that it cannot determine methicillin resistance of *S. aureus* when staphylococci other than *S. aureus* are also detected as mixed culture with positive

mecA. Unlike conventional identification and susceptibility testing, multiplex real-time PCR assay is unable to indicate methicillin resistance to each of the staphylococci when it comes to mixed culture [19, 20]. It would be important to incorporate the multiplex real-time PCR assay alongside conventional identification and susceptibility testing.

In a clinical laboratory setting, the rapid and reliable identification of staphylococci and the determination of their methicillin susceptibility are important for effective antibiotic therapy and avoidance of the inappropriate use of glycopeptides [21]. Conventional identification and susceptibility testing of positive blood cultures based on phenotypic characteristics can take up to 48 h after the GPCC are recognized by Gram-staining. For prompt initiation with optimal antibiotic therapy, clinical laboratories are incorporating molecular diagnostic methods, such as real-time PCR assays, which provide rapid, sensitive, and specific detection of microbial pathogens within a few hours [22–24]. Recently, real-time PCR assays have been developed for the detection of staphylococci directly from positive blood culture bottles in clinical microbiology laboratories [25–33]. However, these assays are limited in that although they are able to rapidly identify staphylococci and determine methicillin susceptibility, they only allow the identification of staphylococci and cannot discriminate Gram-positive cocci other than staphylococci. We hypothesized that the addition of a PCR assay targeting staphylococcal *16S rRNA* might mitigate this limitation and target both universal *16S rRNA* and staphylococcal *16S rRNA*. In this study, thirteen isolates that were recognized as GPCC by preliminary Gram-staining were confirmed as *Micrococci* and *Enterococci* by MicroScan system; without an assay targeting the staphylococci-specific 16S rRNA, they would have been interpreted as MSCoNS by real-time PCR.

5. Conclusions

The direct multiplex real-time PCR assay of positive blood cultures containing GPCC can provide essential information for prompt initiation of appropriate antibiotic treatment at the critical point of infection with a turnaround time of no more than 4 h, which includes 2 h for DNA extraction and 1.5 h for PCR. Further studies should evaluate the clinical outcome and benefit of using this rapid real-time PCR assay incorporated with conventional culture methods for glycopeptide antibiotic therapy in the case of positive blood cultures growing GPCC in clinical settings.

Additional Points

(i) We developed multiplex real-time PCR assay for rapid categorization of staphylococci. (ii) The targets were *mecA*, *femA*, universal *16S rRNA,* and staphylococcal *16S rRNA*. (iii) The results directly from positive blood culture bottles were compared with MicroScan. (iv) The assay rapidly detected methicillin-resistant staphylococci with good agreement.

Competing Interests

The authors declare that they have no competing interests.

Authors' Contributions

The first two authors, Yousun Chung and Taek Soo Kim, contributed equally to this work.

References

[1] Á. Skow, K. A. Mangold, M. Tajuddin et al., "Species-level identification of staphylococcal isolates by real-time PCR and melt curve analysis," *Journal of Clinical Microbiology*, vol. 43, no. 6, pp. 2876–2880, 2005.

[2] E. Gradelski, L. Valera, L. Aleksunes, D. Bonner, and J. Fung-Tomc, "Correlation between genotype and phenotypic categorization of staphylococci based on methicillin susceptibility and resistance," *Journal of Clinical Microbiology*, vol. 39, no. 8, pp. 2961–2963, 2001.

[3] T. P. Lodise, P. S. McKinnon, L. Swiderski, and M. J. Rybak, "Outcomes analysis of delayed antibiotic treatment for hospital-acquired *Staphylococcus aureus* bacteremia," *Clinical Infectious Diseases*, vol. 36, no. 11, pp. 1418–1423, 2003.

[4] R. B. R. Ferreira, N. L. P. Iorio, K. L. Malvar et al., "Coagulase-negative staphylococci: comparison of phenotypic and genotypic oxacillin susceptibility tests and evaluation of the agar screening test by using different concentrations of oxacillin," *Journal of Clinical Microbiology*, vol. 41, no. 8, pp. 3609–3614, 2003.

[5] T. G. Krediet, E. M. Mascini, E. Van Rooij et al., "Molecular epidemiology of coagulase-negative staphylococci causing sepsis in a neonatal intensive care unit over an 11-year period," *Journal of Clinical Microbiology*, vol. 42, no. 3, pp. 992–995, 2004.

[6] B. Favre, S. Hugonnet, L. Correa, H. Sax, P. Rohner, and D. Pittet, "Nosocomial bacteremia: clinical significance of a single blood culture positive for coagulase-negative staphylococci," *Infection Control and Hospital Epidemiology*, vol. 26, no. 8, pp. 697–702, 2005.

[7] E. L. Munson, D. J. Diekema, S. E. Beekmann, K. C. Chapin, and G. V. Doern, "Detection and treatment of bloodstream infection: laboratory reporting and antimicrobial management," *Journal of Clinical Microbiology*, vol. 41, no. 1, pp. 495–497, 2003.

[8] M. J. Espy, J. R. Uhl, L. M. Sloan et al., "Real-time PCR in clinical microbiology: applications for routine laboratory testing," *Clinical Microbiology Reviews*, vol. 19, no. 1, pp. 165–256, 2006.

[9] P. Francois, D. Pittet, M. Bento et al., "Rapid detection of methicillin-resistant *Staphylococcus aureus* directly from sterile or nonsterile clinical samples by a new molecular assay," *Journal of Clinical Microbiology*, vol. 41, no. 1, pp. 254–260, 2003.

[10] M. A. Nadkarni, F. E. Martin, N. A. Jacques, and N. Hunter, "Determination of bacterial load by real-time PCR using a broad-range (universal) probe and primers set," *Microbiology*, vol. 148, no. 1, pp. 257–266, 2002.

[11] H. Al-Talib, C. Y. Yean, A. Al-Khateeb et al., "A pentaplex PCR assay for the rapid detection of methicillin-resistant *Staphylococcus aureus* and Panton-Valentine Leucocidin," *BMC Microbiology*, vol. 9, article 113, 2009.

[12] M. Kim, S. R. Heo, S. H. Choi et al., "Comparison of the MicroScan, VITEK 2, and Crystal GP with 16S rRNA sequencing and MicroSeq 500 v2.0 analysis for coagulase-negative staphylococci," *BMC Microbiology*, vol. 8, article 233, 2008.

[13] A. N. Olendzki, E. M. Barros, M. S. Laport, K. R. N. Dos Santos, and M. Giambiagi-Demarval, "Reliability of the MicroScan

WalkAway PC21 panel in identifying and detecting oxacillin resistance in clinical coagulase-negative staphylococci strains," *European Journal of Clinical Microbiology & Infectious Diseases*, vol. 33, no. 1, pp. 29–33, 2014.

[14] G. L. Archer, D. M. Niemeyer, J. A. Thanassi, and M. J. Pucci, "Dissemination among staphylococci of DNA sequences associated with methicillin resistance," *Antimicrobial Agents and Chemotherapy*, vol. 38, no. 3, pp. 447–454, 1994.

[15] F. Martineau, F. J. Picard, N. Lansac et al., "Correlation between the resistance genotype determined by multiplex PCR assays and the antibiotic susceptibility patterns of *Staphylococcus aureus* and *Staphylococcus epidermidis*," *Antimicrobial Agents and Chemotherapy*, vol. 44, no. 2, pp. 231–238, 2000.

[16] E. Galdiero, G. Liguori, M. D'Isanto, N. Damiano, and L. Sommese, "Distribution of mecA among methicillin-resistant clinical staphylococcal strains isolated at hospitals in Naples, Italy," *European Journal of Epidemiology*, vol. 18, no. 2, pp. 139–145, 2003.

[17] J. L. Gerberding, C. Miick, H. H. Liu, and H. F. Chambers, "Comparison of conventional susceptibility tests with direct detection of penicillin-binding protein 2a in borderline oxacillin-resistant strains of *Staphylococcus aureus*," *Antimicrobial Agents and Chemotherapy*, vol. 35, no. 12, pp. 2574–2579, 1991.

[18] A. Jain, A. Agarwal, and R. K. Verma, "Cefoxitin disc diffusion test for detection of meticillin-resistant staphylococci," *Journal of Medical Microbiology*, vol. 57, no. 8, pp. 957–961, 2008.

[19] L. Jukes, J. Mikhail, N. Bome-Mannathoko et al., "Rapid differentiation of *Staphylococcus aureus*, *Staphylococcus epidermidis* and other coagulase-negative staphylococci and meticillin susceptibility testing directly from growth-positive blood cultures by multiplex real-time PCR," *Journal of Medical Microbiology*, vol. 59, no. 12, pp. 1456–1461, 2010.

[20] A. Kilic, K. L. Muldrew, Y.-W. Tang, and A. C. Basustaoglu, "Triplex real-time polymerase chain reaction assay for simultaneous detection of *Staphylococcus aureus* and coagulase-negative staphylococci and determination of methicillin resistance directly from positive blood culture bottles," *Diagnostic Microbiology and Infectious Disease*, vol. 66, no. 4, pp. 349–355, 2010.

[21] Y.-W. Tang, A. Kilic, Q. Yang et al., "StaphPlex system for rapid and simultaneous identification of antibiotic resistance determinants and Panton-Valentine leukocidin detection of staphylococci from positive blood cultures," *Journal of Clinical Microbiology*, vol. 45, no. 6, pp. 1867–1873, 2007.

[22] S. Klaschik, L. E. Lehmann, A. Raadts et al., "Detection and differentiation of in vitro-spiked bacteria by real-time PCR and melting-curve analysis," *Journal of Clinical Microbiology*, vol. 42, no. 2, pp. 512–517, 2004.

[23] T. Mohammadi, H. W. Reesink, C. M. J. E. Vandenbroucke-Grauls, and P. H. M. Savelkoul, "Optimization of real-time PCR assay for rapid and sensitive detection of eubacterial 16S ribosomal DNA in platelet concentrates," *Journal of Clinical Microbiology*, vol. 41, no. 10, pp. 4796–4798, 2003.

[24] H. Sakai, G. W. Procop, N. Kobayashi et al., "Simultaneous detection of *Staphylococcus aureus* and coagulase-negative staphylococci in positive blood cultures by real-time PCR with two fluorescence resonance energy transfer probe sets," *Journal of Clinical Microbiology*, vol. 42, no. 12, pp. 5739–5744, 2004.

[25] A. Huletsky, P. Lebel, F. J. Picard et al., "Identification of methicillin-resistant *Staphylococcus aureus* carriage in less than 1 hour during a hospital surveillance program," *Clinical Infectious Diseases*, vol. 40, no. 7, pp. 976–981, 2005.

[26] W. C. Lindsey, E. S. Woodruff, D. Weed, D. C. Ward, and R. D. Jenison, "Development of a rapid diagnostic assay for methicillin-resistant *Staphylococcus aureus* and methicillin-resistant coagulase-negative *Staphylococcus*," *Diagnostic Microbiology and Infectious Disease*, vol. 61, no. 3, pp. 273–279, 2008.

[27] N. K. Shrestha, M. J. Tuohy, G. S. Hall, C. M. Isada, and G. W. Procop, "Rapid identification of *Staphylococcus aureus* and the mecA gene from BacT/ALERT blood culture bottles by using the LightCycler system," *Journal of Clinical Microbiology*, vol. 40, no. 7, pp. 2659–2661, 2002.

[28] T. Y. Tan, S. Corden, R. Barnes, and B. Cookson, "Rapid identification of methicillin-resistant *Staphylococcus aureus* from positive blood cultures by real-time fluorescence PCR," *Journal of Clinical Microbiology*, vol. 39, no. 12, pp. 4529–4531, 2001.

[29] C. Palomares, M. J. Torres, A. Torres, J. Aznar, and J. C. Palomares, "Rapid detection and identification of *Staphylococcus aureus* from blood culture specimens using real-time fluorescence PCR," *Diagnostic Microbiology and Infectious Disease*, vol. 45, no. 3, pp. 183–189, 2003.

[30] S. M. Paule, A. C. Pasquariello, R. B. Thomson Jr., K. L. Kaul, and L. R. Peterson, "Real-time PCR can rapidly detect methicillin-susceptible and methicillin-resistant *Staphylococcus aureus* directly from positive blood culture bottles," *American Journal of Clinical Pathology*, vol. 124, no. 3, pp. 404–407, 2005.

[31] S. Gröbner and V. A. J. Kempf, "Rapid detection of methicillin-resistant staphylococci by real-time PCR directly from positive blood culture bottles," *European Journal of Clinical Microbiology & Infectious Diseases*, vol. 26, no. 10, pp. 751–754, 2007.

[32] L. C. Thomas, H. F. Gidding, A. N. Ginn, T. Olma, and J. Iredell, "Development of a real-time *Staphylococcus aureus* and MRSA (SAM-) PCR for routine blood culture," *Journal of Microbiological Methods*, vol. 68, no. 2, pp. 296–302, 2007.

[33] J. Stratidis, F. J. Bia, and S. C. Edberg, "Use of real-time polymerase chain reaction for identification of methicillin-resistant *Staphylococcus aureus* directly from positive blood culture bottles," *Diagnostic Microbiology and Infectious Disease*, vol. 58, no. 2, pp. 199–202, 2007.

Hindawi Publishing Corporation
BioMed Research International
Volume 2016, Article ID 6950482, 7 pages
http://dx.doi.org/10.1155/2016/6950482

Research Article

Serotype Distribution and Antimicrobial Resistance of *Streptococcus pneumoniae* Isolates Causing Invasive and Noninvasive Pneumococcal Diseases in Korea from 2008 to 2014

Si Hyun Kim,[1,2] Il Kwon Bae,[3] Dongchul Park,[1,2] Kyungmin Lee,[1,2] Na Young Kim,[1,2] Sae Am Song,[1] Hye Ran Kim,[1] Ga Won Jeon,[4] Sang-Hwa Urm,[5] and Jeong Hwan Shin[1,2]

[1]*Department of Laboratory Medicine, Inje University College of Medicine, Busan 47392, Republic of Korea*
[2]*Paik Institute for Clinical Research, Inje University College of Medicine, Busan 47392, Republic of Korea*
[3]*Department of Dental Hygiene, College of Health and Welfare, Silla University, Busan 46958, Republic of Korea*
[4]*Department of Pediatrics, Inje University College of Medicine, Busan 47392, Republic of Korea*
[5]*Preventive Medicine, Inje University College of Medicine, Busan 47392, Republic of Korea*

Correspondence should be addressed to Jeong Hwan Shin; jhsmile@inje.ac.kr

Received 18 February 2016; Revised 24 April 2016; Accepted 8 May 2016

Academic Editor: Patrizia Cardelli

Introduction. *Streptococcus pneumoniae* is an important pathogen with high morbidity and mortality rates. The aim of this study was to evaluate the distribution of common serotypes and antimicrobial susceptibility of *S. pneumoniae* in Korea. *Methods*. A total of 378 pneumococcal isolates were collected from 2008 through 2014. We analyzed the serotype and antimicrobial susceptibility for both invasive and noninvasive isolates. *Results*. Over the 7 years, 3 (13.5%), 35 (10.8%), 19A (9.0%), 19F (6.6%), 6A (6.1%), and 34 (5.6%) were common serotypes/serogroups. The vaccine coverage rates of PCV7, PCV10, PCV13, and PPSV23 were 21.4%, 23.3%, 51.9%, and 62.4% in all periods. The proportions of serotypes 19A and 19F decreased and nonvaccine serotypes increased between 2008 and 2010 and 2011 and 2014. Of 378 *S. pneumoniae* isolates, 131 (34.7%) were multidrug resistant (MDR) and serotypes 19A and 19F were predominant. The resistance rate to levofloxacin was significantly increased (7.2%). *Conclusion*. We found changes of pneumococcal serotype and antimicrobial susceptibility during the 7 years after introduction of the first pneumococcal vaccine. It is important to continuously monitor pneumococcal serotypes and their susceptibilities.

1. Introduction

Streptococcus pneumoniae is one of the most common causes of pneumonia, sepsis, and meningitis and is the leading cause of morbidity and death worldwide in adults and children [1–3]. Ninety-two capsular serotypes of *S. pneumoniae* exist, and the prevalence of serotypes differs according to age, region, and time of the surveillance [4, 5]. The 92 serotypes differ in virulence; a minority of serotypes is involved in most of invasive pneumococcal diseases and antimicrobial resistances.

The 23-valent polysaccharide vaccine (PPV23) and a 7-valent pneumococcal conjugate vaccine (PCV7) were recommended for the elderly (≥65 years old) and children (≤5 years old), respectively. In Korea, PCV7, which protects against the important invasive serotypes (4, 6B, 9V, 14, 18C, 19F, and 23F), was introduced in 2003 for infants and young children. The introduction of PCV7 in the United States produced a decrease in both invasive and noninvasive pneumococcal diseases caused by these vaccine serotypes [6, 7]. However, use of PCV7 has led to changes in prevalent serotypes; it tended to increase the PCV7 nonvaccine serotypes, especially 19A, worldwide [8–10]. A second pneumococcal conjugate vaccine (PCV10 and PCV7 with serotypes 1, 5, and 7F added) and a 13-valent vaccine (PCV13 and PCV10 with serotypes 3, 6A, and 19A added) were introduced in Korea in 2010. Since May 2014, pneumococcal vaccination has been provided for

free as a routine national vaccine program, including PCV10, PCV13, and PPSV23 in South Korea.

Since the first detection of *S. pneumoniae* with high resistance to penicillin and other antibiotics in 1977, high rates of antimicrobial resistance in *S. pneumoniae* have been a serious concern worldwide [11–13]. In Asian countries, beta-lactam and macrolide resistance are very high, and multidrug resistance (MDR) also is common [4, 14–16]. In 2008, the Clinical Laboratory and Standard Institute (CLSI) guideline changed the resistance breakpoint of nonmeningitis *S. pneumoniae* for penicillin from ≥2 μg/mL to ≥8 μg/mL [17]. Later, the resistance rate to penicillin decreased significantly; however, the high resistance rates to other antimicrobial agents have continued [18–20]. The aim of this study was to evaluate the changes in the prevalence of serotypes and their antimicrobial resistance during the past 7 years in Korea since the introduction of the vaccines.

2. Materials and Methods

2.1. Clinical Isolates. All 378 *S. pneumoniae* isolates collected from patients at a tertiary-care hospital in Korea from January 2008 to June 2014 were included. The isolates were identified by colony morphology, gram staining, optochin susceptibility, and other biochemical reactions using VITEK2 system. All isolates were stored at −70°C using 10% skim-milk until use.

2.2. Serotyping. Serotyping was performed by capsular swelling (Quellung reaction) using Pneumotest antisera kit (Statens Serum Institut, Copenhagen, Denmark). For determining the serotype, pool antisera were used as recommended by the manufacturer. In order to determine additional serotypes, some factor antisera and serotype-specific polymerase chain reaction (PCR) recommended by the U.S. Centers for Disease Control and Prevention (CDC, http://www.cdc.gov/streplab/downloads/pcr-oligonucleotide-primers.pdf) were used [21]. Serotypes were classified into vaccine serotype (VT) and nonvaccine serotype (NVT). Vaccine serotype means a serotype included in PCV7 (serotypes 4, 6B, 9V, 14, 18C, 19F, and 23F), PCV10 (serotypes 1, 5, and 7F added to PCV7), PCV13 (serotypes 3, 6A, and 19A added to PCV10), and PPSV23 (serotypes 2, 8, 9N, 10A, 11A, 12F, 15B, 17F, 20, 22F, and 33F added to PCV13, except for 6A). Nonvaccine serotype is the serotype which is not covered by PCV7, PCV10, PCV13, and PPSV23.

2.3. Antimicrobial Susceptibility. Antimicrobial susceptibilities were determined using the Microscan system, and the susceptibility interpretive criteria were those published in the relevant guidelines of the Clinical and Laboratory Standards Institute (CLSI). Separate interpretive breakpoints were used to define the resistance to penicillin, cefepime, cefotaxime, and ceftriaxone for meningeal isolates. The following antimicrobial agents were tested: amoxicillin, azithromycin, cefaclor, cefepime, cefotaxime, ceftriaxone, cefuroxime, chloramphenicol, clindamycin, erythromycin, levofloxacin, meropenem, penicillin, tetracycline, sulfamethoxazole/trimethoprim (SXT), and vancomycin. The Food and Drug Administration defines multiresistance as resistance to two or more of the five classes of antibacterial agents represented by erythromycin, cefuroxime, SXT, penicillin, and tetracycline [22]. The resistance to cefotaxime and ceftriaxone was analyzed instead of that to cefuroxime and SXT. Macrolide resistance was defined by the erythromycin susceptibility test results.

We assessed differences in serotypes by age group, clinical specimens, surveillance periods, and resistance types. The data was analyzed with the software IBM SPSS version 22, using chi-square test.

3. Results

3.1. Characteristics of S. pneumoniae Isolates. The numbers of *S. pneumoniae* isolates by period are as follows: 198 isolates (52.4%) were obtained between 2008 and 2010 (period I) and 180 isolates (47.6%) between 2011 and 2014 (period II). Of the 378 isolates, 265 (70.1%) and 113 (29.9%) were from male and female patients, respectively. A majority (197; 52.1%) were obtained from the elderly (>65 years old) and 16 (4.2%) from children (≤5 years old). The mean age (±SD) of the patients was 60.8 ± 19 years (range 0–107 years). Of these isolates, 68 (18.0%) were invasive and 310 (82.0%) were noninvasive. The most common source of invasive isolates was blood (N = 60; 88.2%), followed by cerebrospinal fluid (N = 5; 7.4%), pleural fluid (N = 2; 1.5%), and ascitic fluid (N = 1; 1.5%). The sources of noninvasive isolates were the respiratory specimens (N = 281) including sputum and bronchial washing, pus (N = 26), and others (N = 3).

3.2. Distribution of Pneumococcal Serotypes. The most frequently isolated serotypes were 3 (13.5%), 35 (10.8%), 19A (9.0%), 19F (6.6%), 6A (6.1%), and 34 (5.6%), which together accounted for 51.6% of all isolates (Table 1). In children ≤ 5 years old, nine serotypes were identified, and 19A, 11A, and 23A were major serotypes, accounting for 37.5%, 12.5%, and 12.5% of the isolates, respectively. However, a diversity of serotypes was identified: more than 30 in the adults (≥65 years and 6–64 years old). However, serotypes 3 (14.2%, 13.9%) and 35 (11.2%, 10.9%) were most frequent.

The coverage rates of PCV7, PCV10, PCV13, and PPSV23 were 21.4%, 23.3%, 51.9%, and 62.4%, respectively. In children ≤ 5 years old, both PCV7 and PCV10 serotype coverages were same at 12.5%, whereas PCV13 covered 50.0%. For the elderly, PCV13 and PPV23 serotype coverages were 52.8% and 64.0%, respectively. Overall, vaccine serotypes were identified in 259 isolates (68.5%). Serotype 3 (19.7%) was the most common vaccine serotype, followed by 19A (13.1%), 19F (9.7%), and 6A (8.9%). Among nonvaccine serotypes, 35 (34.5%) was the most common, followed by 34 (17.6%), 6D (10.1%), and 6C (8.4%). We also compared the serotypes by dividing them as invasive and noninvasive isolates. For invasive isolates, the major serotypes were 3 (20.6%), 19A (10.3%), 35 (7.4%), 22F (5.9%), and 6A (5.9%), accounting for 50.0% of all invasive isolates. Serotype 19F was more common among noninvasive isolates (7.7%) than invasive isolates (1.5%). Ten serotypes

Table 1: Distribution of pneumococcal serotypes by patient's age group.

Serotype	Total (378) N (%)	Age group N (%)		
		≤5 years (N = 16)	≥65 years (N = 197)	6–64 years (N = 165)
3	51 (13.5)		28 (14.2)	23 (13.9)
35	41 (10.8)	1 (6.3)	22 (11.2)	18 (10.9)
19A	34 (9.0)	6 (37.5)	18 (9.1)	10 (6.1)
19F	25 (6.6)	1 (6.3)	15 (7.6)	9 (5.5)
6A	23 (6.1)		13 (6.6)	10 (6.1)
34	21 (5.6)	1 (6.3)	10 (5.1)	10 (6.1)
11A	15 (4.0)	2 (12.5)	9 (4.6)	4 (2.4)
6B	15 (4.0)		9 (4.6)	6 (3.6)
9V	15 (4.0)		8 (4.1)	7 (4.2)
15B	12 (3.2)		6 (3.0)	6 (3.6)
6D	12 (3.2)		8 (4.1)	4 (2.4)
23F	11 (2.9)	1 (6.3)	2 (1.0)	8 (4.8)
22F	10 (2.6)		7 (3.6)	3 (1.8)
6C	10 (2.6)	1 (6.3)	4 (2.0)	5 (3.0)
14	9 (2.4)		4 (2.0)	5 (3.0)
23A	9 (2.4)	2 (12.5)	2 (1.0)	5 (3.0)
7B	2 (0.5)	1 (6.3)	1 (0.5)	
Others*	63 (16.7)		31 (15.7)	32 (19.4)
7-valent	81 (21.4)	2 (12.5)	41 (20.8)	38 (23.0)
10-valent	88 (23.3)	2 (12.5)	45 (22.8)	41 (24.8)
13-valent	196 (51.9)	8 (50.0)	104 (52.8)	84 (50.9)
23-valent	236 (62.4)	10 (62.5)	126 (64.0)	100 (60.6)
VTs	259 (68.5)	10 (62.5)	139 (70.6)	110 (66.7)
NVTs	119 (31.5)	6 (37.5)	58 (29.4)	55 (33.3)

VTs: vaccine serotypes; NVTs: nonvaccine serotypes.
*Others include 15A, 13, 20, 33F, 10A, 4, 9N, 1, 16, 12F, 5, 24, 18C, 7F, 8, 37, 11B, 17A, 17F, and 23B.

were detected only among noninvasive isolates, accounting for 9.7%, and serotype 12F (4.4%) was detected only among invasive isolates (Table 2).

We analyzed the changes in serotypes over time by dividing the 7 years into two periods based on the introduction of PCV10 and PCV13 in Korea (period I: 2008–2010, N = 198, and period II: 2011–2014, N = 180) (Table 3). In period I, the major serotypes were 3 (12.1%), 19A (11.1%), 35 (9.1%), and 19F (8.6%), a total of 40.9%. In period II, serotypes 3, 35, 19A, and 6A were the most frequent and accounted for 41.1%. The number of nonvaccine serotypes increased to 37.2% in period II versus 26.3% in period I. In particular, serotype 35 showed a significant increase in the elderly. Among the vaccine serotypes, 19A, 19F, and 23F were decreased from 11.1% to 6.7%, 8.6% to 4.4%, and 4.5% to 1.1%, respectively. Serotype 3 was remarkably increased in the elderly (9.9% to 17.9%). However, it showed a decrease in patients 6–64 years old (15.5% to 11.8%). In children, the proportion of PCV13 serotypes decreased from 70% (N = 7) in period I to 16.7% (N = 1) in period II, which was attributable primarily to a decrease in serotype 19A.

3.3. Antimicrobial Resistance. The antimicrobial susceptibility of the *S. pneumoniae* is shown in Table 4. The resistance rates to erythromycin, tetracycline, azithromycin, cefaclor, cefuroxime, and clindamycin were high: 73.3%, 72.7%, 72.0%, 68.7%, 66.1%, and 56.9%, respectively.

The nonsusceptibility rate to penicillin was 26.8%, including 9.0% resistant and 17.8% intermediate. In children, the rates of penicillin resistance and intermediate susceptibility (20.0% and 46.7%, resp.) were significantly higher than in the elderly (8.5% and 17.1%) and younger adults (8.5% and 15.5%). In invasive *S. pneumoniae* isolates, the resistant and intermediate rates for penicillin were 6.7% and 16.7%, respectively. The rate of resistance of cefuroxime was high as 66.1%, and the resistance rates to cefotaxime and ceftriaxone were low, 4.1% and 4.7%, respectively. The resistance rate to levofloxacin was 7.2%, with the highest rate being 10.3% in the elderly. Also we found that the resistance rate to levofloxacin increased from 3.6% in period I to 11.7% in period II among all isolates (p value = 0.003).

Among the major serotypes, serotype 3 expressed low-level resistance to nine major antimicrobial agents. Serotypes

Table 2: Comparison of pneumococcal serotypes between invasive and noninvasive organisms according to patient's age.

Serotype	Total *N* (%)	Invasive (age)			Noninvasive (age)		
		≤5	≥65	6–64	≤5	≥65	6–64
3	51 (13.5)		7	7		21	16
19A	34 (9.0)	1	3	3	5	15	7
35	41 (10.8)		1	4	1	21	14
22F	10 (2.6)		2	2		5	1
6A	23 (6.1)		1	3		12	7
11A	15 (4.0)		1	2	2	8	2
12F	3 (0.8)			3			
9V	15 (4.0)			3		8	4
4	4 (1.1)		1	1		1	1
16	3 (0.8)		1	1			1
20	6 (1.6)		1	1		1	3
34	21 (5.6)		2		1	8	10
23A	9 (2.4)	2				2	5
6D	12 (3.2)		1	1		7	3
5	2 (0.5)		1			1	
13	7 (1.9)			1		4	2
14	9 (2.4)		1			3	5
24	2 (0.5)			1		1	
10A	5 (1.3)			1		4	
15B	12 (3.2)			1		6	5
19F	25 (6.6)			1	1	15	8
33F	6 (1.6)		1			4	1
6B	15 (4.0)		1			8	6
6C	10 (2.6)		1		1	3	5
7B	2 (0.5)	1				1	
7F	2 (0.5)			1		1	
9N	4 (1.1)			1		1	2
1	3 (0.8)					1	2
8	1 (0.3)					1	
37	1 (0.3)						1
11B	1 (0.3)						1
15A	8 (2.1)					5	3
17A	1 (0.3)						1
17F	1 (0.3)						1
18C	2 (0.5)					1	1
23B	1 (0.3)						1
23F	11 (2.9)				1	2	8
Total	378	4	26	38	12	171	127

19A and 19F showed high resistance to most antimicrobial agents. For penicillin, serotypes 35, 19A, and 19F expressed high resistance (16.7%, 28.1%, and 19.0%, resp.) and serotypes 3 and 6B showed low resistance (2.4% and 7.7%). Serotypes 34, 11A, 6A, and 9V all were susceptible to penicillin. For levofloxacin, the resistance rates of serotypes 34, 5, 11A, and 9V were high: 15.8%, 15.8%, 23.1%, and 15.4%, respectively, whereas serotype 19A showed 100% susceptibility.

Of the total 378 isolates, 131 (34.7%) were multidrug resistant (MDR). The serotypes of most MDR *S. pneumoniae* isolates were vaccine serotypes (74.0%) consisting of 19A (20.6%), 19F (14.5%), 6A (7.6%), and so on. The rate of MDR *S. pneumoniae* was very high (68.8%) in children compared with those in the elderly (36.5%) and younger adults (29.1%). In period I, 78 isolates (39.4%) were identified as MDR; however, the prevalence of MDR *S. pneumoniae*

Table 3: Prevalence of common serotypes during two periods by patient's age.

Serotype	Total (378)		≤5 years (N = 16)		≥65 years (N = 197)		6–64 years (N = 165)	
	Period (P) I (198)	Period II (180)	P I (10)	P II (6)	P I (91)	P II (106)	P I (97)	P II (68)
3	24 (12.1)	27 (15.0)			9	19	15	8
34	12 (6.0)	9 (5.0)		1	6	4	6	4
35	18 (9.0)	23 (12.8)		1	8	14	10	8
19A	22 (11.1)	12 (6.7)	5	1	11	7	6	4
19F	17 (8.6)	8 (4.4)	1		10	5	6	3
23F	9 (4.5)	2 (1.1)	1		2		6	2
6A	11 (5.6)	12 (6.7)			4	9	7	3
7-valent	51 (25.8)	30 (16.7)	2		22	19	27	11
10-valent	57 (28.8)	31 (17.2)	2		26	19	29	12
13-valent	114 (57.6)	82 (45.6)	7	1	50	54	57	27
23-valent	135 (68.2)	101 (56.1)	8	2	63	63	64	36
VTs	146 (73.7)	113 (62.8)	8	2	67	72	71	39
NVTs	52 (26.3)	67 (37.2%)	2	4	24	34	26	29

VTs: vaccine serotypes; NVTs: nonvaccine serotypes.

Table 4: Resistance rates to antimicrobial agents by age.

Antibiotic	Total (378)			≤5 years (N = 16)			≥65 years (N = 197)			6–64 years (N = 165)		
	I	R	S	I	R	S	I	R	S	I	R	S
Amoxicillin	30 (8.2)	61 (16.8)	273 (75.0)	3	6	7	18	37	138	9	18	128
Azithromycin	11 (3.2)	244 (72.0)	84 (24.8)		13	2	7	126	39	4	105	43
Cefaclor	12 (3.7)	222 (68.7)	89 (27.6)		12	3	7	115	45	5	95	41
Cefepime	73 (22.0)	22 (6.6)	237 (71.4)	4	4	8	36	12	123	33	6	106
Cefotaxime	30 (9.4)	13 (4.1)	277 (86.6)	6	2	7	13	8	143	11	3	127
Ceftriaxone	33 (10.2)	15 (4.7)	274 (85.1)	6	3	6	13	10	142	14	2	126
Cefuroxime IV	11 (3.7)	199 (66.1)	91 (30.2)		12	2	8	101	46	3	86	43
Chloramphenicol	3 (0.9)	91 (26.7)	247 (72.4)		1	14	3	50	120		40	113
Clindamycin		193 (56.9)	146 (43.1)		13	2		106	71		74	73
Erythromycin	5 (1.4)	258 (73.3)	89 (25.3)		13	2	4	135	42	1	110	45
Levofloxacin	2 (0.6)	26 (7.2)	331 (92.2)			16	2	19	164		7	151
Meropenem	114 (32.9)	91 (26.2)	142 (40.9)	7	6	3	53	50	74	54	35	65
Penicillin IV	57 (17.8)	29 (9.0)	235 (73.2)	7	3	5	28	14	122	22	12	108
Tetracycline	5 (1.4)	256 (72.7)	91 (25.9)		13	2	2	130	49	3	113	40
Trimethoprim/sulfa	38 (10.3)	141 (38.3)	189 (51.4)	1	11	4	17	78	96	20	52	89
Vancomycin			352 (100)			15			181			156

I: intermediate; R: resistant; S: susceptible.

was decreased to 53 isolates (29.4%) in period II when the vaccines were available. Although the resistance rate to penicillin was significantly decreased, to 3.6% from 13.3%, the resistance rate to levofloxacin was increased to 11.7% from 3.6%.

4. Discussion

This study describes the serotype and antimicrobial resistance of *S. pneumoniae* isolates in a tertiary-care hospital in Korea. We evaluated the change in the common serotypes and antimicrobial susceptibility patterns between 2008 and 2014. The distribution of serotypes was changed after PCV7 was introduced in Korea in 2003. In our study, the common serotypes were 3, 35, 19A, 19F, 6A, and 34 among all isolates, and the major invasive serotypes were 3, 19A, 35, 22F, and 6A. Compared with the previous report of Lee et al. [23] from 1996 to 2008, both serotypes 19F and 23F decreased and serotypes 3, 35, and 22F increased. This finding suggests that the proportion of PCV7 serotypes showed a decreasing trend, whereas there was an increase in the prevalence of non-PCV7 serotype between 1996–2008 and 2008–2014.

Our study from 2008 to 2014 showed that PCV7, PCV10, PCV13, and PPSV23 covered 21.4%, 23.3%, 51.9%, and 62.4%, respectively, of all isolates. The vaccine coverage of PCV7, PCV10, PCV13, and PPSV23 was reduced from 25.8%, 28.8%,

57.6%, and 68.2% to 16.7%, 17.2%, 45.6%, and 56.1% between period I and period II. Serotype 19A was significantly increased in children worldwide after the introduction of PCV7 [7, 24]. In Korea, Choi et al. reported that serotype 19A increased from 1996 to 2006 [25]. However, we also verified the change in the serotype's distribution after the introduction of PCV10 and PCV13, including the decline in the prevalence of serotype 19A from 11.1% in 2008–2010 to 6.7% in 2011–2014. On the other hand, serotypes 3 and 6A were slightly increased between 2008–2010 and 2011–2014.

We could see differences in the distribution of serotypes between invasive and noninvasive isolates. Ten serotypes (1, 8, 37, 11B, 15A, 17A, 17F, 18C, 23B, and 23F) were detected only among noninvasive isolates (7.1%), whereas serotype 12F was detected only as an invasive isolate. Also, the prevalence of serotype 19F was higher among noninvasive (7.7%) than invasive (1.5%) isolates, and serotype 22F was more common among invasive (5.9%) than noninvasive (1.9%) isolates. We also found a difference in the serotypes of *S. pneumoniae* by age. The common serotypes in children were 19A, 11A, and 23A, whereas serotypes 3 and 35 were predominant in adults. The lower occurrence of serotype 3 among the children has been reported in another study also [26]. A limitation of this study was the small numbers (only 4.2%) of isolates from children under 5 years who are the primary target age group for PCV vaccination.

Our findings confirm the previously reported high rates of resistance to macrolides such as erythromycin (73.3%), azithromycin (72.0%), and clindamycin (56.9%). The resistance rate to penicillin was higher (9.4%) in the invasive isolates in period I than in the ANSORP study [4] in Korea from 2009 to 2010 (0.3%). Also, the nonsusceptibility rate to penicillin was high in invasive isolates (23.4%) compared with the report of Park et al. [21] (10.7%) from 2009 to 2014. However, we found that the resistance rate to penicillin declined from 9.4% in period I (2008–2010) to 3.6% in period II (2011–2014) among invasive isolates. The interesting thing was that the intermediate resistance rate to penicillin increased slightly over the course of the study, from 15.6% to 17.9% among invasive isolates. We found that the resistance rate to levofloxacin increased significantly, from 3.6% in period I to 11.7% in period II among all isolates (p value = 0.003). Therefore, we need to continuously investigate the susceptibility rates for penicillin and levofloxacin.

The resistance rates in children were higher than those in other age groups, with 20% of isolates resistant to penicillin. Resistance to levofloxacin was not detected in children, whereas resistance was common in those more than 65 years old (10.3%). We do not know the exact reason why the resistant rates to levofloxacin have increased in the older age group. However, we guess the increasing use of levofloxacin is strongly associated with the higher resistance rates because the fluoroquinolone is commonly used as a choice of drug in adults for the respiratory tract infection while that is hardly used in young children. The resistance rates of noninvasive isolates were higher than those of invasive isolates; the rate of levofloxacin resistance was twice as high.

The proportion of MDR *S. pneumoniae* isolates, 34.7%, in all isolates and serotypes 19A, 19F, and 6A showed predominant serotypes in MDR *S. pneumoniae*. In children, the proportion of MDR *S. pneumoniae* was higher (68.8%) than that in other age groups (36.5% and 29.1% for younger adults and the elderly, resp.). The rate of MDR *S. pneumoniae* was decreased from 39.4% in 2008–2010 to 29.4% in 2011–2014. The reduction of MDR *S. pneumoniae* was associated with a decline in the proportion of 19A serotypes.

In this study, we evaluated the change of serotype distribution and antimicrobial susceptibility of all *S. pneumoniae* isolates in Korea over 7 years. We found a decrease of serotypes 19A and 19F and an increase in nonvaccine serotype 35. There were characteristic findings showing a high nonsusceptibility rate to penicillin in children and high resistance rates to levofloxacin. Therefore, we need continuous monitoring for changes of serotype and appropriate main antimicrobial agents.

Competing Interests

The authors declare that they have no competing interests.

Authors' Contributions

Si Hyun Kim and Il Kwon Bae contributed equally to this work.

Acknowledgments

This research was supported by a grant of the Korea Health Technology R&D Project through the Korea Health Industry Development Institute (KHIDI), funded by the Ministry of Health & Welfare, Republic of Korea (Grant no. HI14C1005).

References

[1] E. AlonsoDeVelasco, A. F. M. Verheul, J. Verhoef, and H. Snippe, "*Streptococcus pneumoniae*: virulence factors, pathogenesis, and vaccines," *Microbiological Reviews*, vol. 59, no. 4, pp. 591–603, 1995.

[2] S. Ogihara, R. Saito, T. Akikura et al., "Characterization of mucoid and non-mucoid *Streptococcus pneumoniae* isolated from outpatients," *Annals of Laboratory Medicine*, vol. 35, no. 4, pp. 410–415, 2015.

[3] T. S. Oh, Y. S. Nam, Y. J. Kim et al., "Trends in bloodstream infections at a Korean University Hospital between 2008 and 2013," *Annals of Clinical Microbiology and Antimicrobials*, vol. 18, no. 1, pp. 14–19, 2015.

[4] S. H. Kim, J.-H. Song, D. R. Chung et al., "Changing trends in antimicrobial resistance and serotypes of Streptococcus pneumoniae isolates in Asian countries: an Asian Network for Surveillance of Resistant Pathogens (ANSORP) study," *Antimicrobial Agents and Chemotherapy*, vol. 56, no. 3, pp. 1418–1426, 2012.

[5] H. B. Konradsen and M. S. Kaltoft, "Invasive pneumococcal infections in Denmark from 1995 to 1999: epidemiology, serotypes, and resistance," *Clinical and Diagnostic Laboratory Immunology*, vol. 9, no. 2, pp. 358–365, 2002.

[6] "Direct and indirect effects of routine vaccination of children with 7-valent pneumococcal conjugate vaccine on incidence of invasive pneumococcal disease—United States, 1998–2003," *Morbidity and Mortality Weekly Report*, vol. 54, no. 36, pp. 893–897, 2005.

[7] C. G. Whitney, M. M. Farley, J. Hadler et al., "Decline in invasive pneumococcal disease after the introduction of protein-polysaccharide conjugate vaccine," *The New England Journal of Medicine*, vol. 348, no. 18, pp. 1737–1746, 2003.

[8] M. R. Moore, R. E. Gertz Jr., R. L. Woodbury et al., "Population snapshot of emergent Streptococcus pneumoniae serotype 19A in the United States, 2005," *Journal of Infectious Diseases*, vol. 197, no. 7, pp. 1016–1027, 2008.

[9] S. R. Williams, P. J. Mernagh, M. H. T. Lee, and J. T. Tan, "Changing epidemiology of invasive pneumococcal disease in Australian children after introduction of a 7-valent pneumococcal conjugate vaccine," *Medical Journal of Australia*, vol. 194, no. 3, pp. 116–120, 2011.

[10] L. A. Hicks, L. H. Harrison, B. Flannery et al., "Incidence of pneumococcal disease due to non-pneumococcal conjugate vaccine (PCV7) serotypes in the United States during the era of widespread PCV7 vaccination, 1998–2004," *Journal of Infectious Diseases*, vol. 196, no. 9, pp. 1346–1354, 2007.

[11] K. P. Klugman, "Pneumococcal resistance to antibiotics," *Clinical Microbiology Reviews*, vol. 3, no. 2, pp. 171–196, 1990.

[12] M. R. Jacobs, H. J. Koornhof, and R. M. Robins-Browne, "Emergence of multiply resistant pneumococci," *The New England Journal of Medicine*, vol. 299, no. 14, pp. 735–740, 1978.

[13] A. Azadegan, A. Ahmadi, A. R. Lari, and M. Talebi, "Detection of the efflux-mediated erythromycin resistance transposon in *Streptococcus pneumoniae*," *Annals of Laboratory Medicine*, vol. 35, no. 1, pp. 57–61, 2015.

[14] J.-H. Song, N. Y. Lee, S. Ichiyama et al., "Spread of drug-resistant *Streptococcus pneumoniae* in Asian countries: Asian Network for Surveillance of Resistant Pathogens (ANSORP) Study," *Clinical Infectious Diseases*, vol. 28, no. 6, pp. 1206–2011, 1999.

[15] K. Shibayama, H. Lee, and S. Kim, "Comparison of antibiotic resistance rate of medically important microorganisms between Japan and Korea," *Annals of Clinical Microbiology*, vol. 18, no. 4, pp. 111–118, 2015.

[16] H. Goossens, "European strategies to control antibiotic resistance and use," *Annals of Clinical Microbiology*, vol. 17, no. 1, pp. 1–8, 2014.

[17] Clinical Laboratory Standard Institute, "Performance standards for antimicrobial susceptibility testing; 18th informational supplement," CLSI Document M100-S18, CLSI, Wayne, Pa, USA, 2008.

[18] M. Imöhl, R. R. Reinert, P. M. Tulkens, and M. van der Linden, "Penicillin susceptibility breakpoints for *Streptococcus pneumoniae* and their effect on susceptibility categorisation in Germany (1997–2013)," *European Journal of Clinical Microbiology and Infectious Diseases*, vol. 33, no. 11, pp. 2035–2040, 2014.

[19] A. R. Golden, M. Rosenthal, B. Fultz et al., "Characterization of MDR and XDR *Streptococcus pneumoniae* in Canada, 2007–13," *Journal of Antimicrobial Chemotherapy*, vol. 70, no. 8, pp. 2199–2202, 2015.

[20] Y. Lee, S. K. Hong, S. H. Choi, W. Im, D. Yong, and K. Lee, "In vitro activity of tedizolid against gram-positive bacteria in patients with skin and skin structure infections and hospital-acquired pneumonia: a Korean multicenter study," *Annals of Laboratory Medicine*, vol. 35, no. 5, pp. 523–530, 2015.

[21] M. Park, H.-S. Kim, K. S. Shin et al., "Changes in the incidence of Streptococcus pneumoniae bacteremia and its serotypes over 10 years in one hospital in South Korea," *Vaccine*, vol. 32, no. 48, pp. 6403–6407, 2014.

[22] S. D. Brown, D. J. Farrell, and I. Morrissey, "Prevalence and molecular analysis of macrolide and fluoroquinolone resistance among isolates of *Streptococcus pneumoniae* collected during the 2000-2001 PROTEKT US study," *Journal of Clinical Microbiology*, vol. 42, no. 11, pp. 4980–4987, 2004.

[23] S. Lee, S. Bae, K.-J. Lee, J.-Y. Yu, and Y. Kang, "Changes in serotype prevalence and antimicrobial resistance among invasive *Streptococcus pneumoniae* isolates in Korea, 1996–2008," *Journal of Medical Microbiology*, vol. 62, no. 8, pp. 1204–1210, 2013.

[24] A. Fenoll, J. J. Granizo, L. Aguilar et al., "Temporal trends of invasive streptococcus pneumoniae serotypes and antimicrobial resistance patterns in Spain from 1979 to 2007," *Journal of Clinical Microbiology*, vol. 47, no. 4, pp. 1012–1020, 2009.

[25] E. H. Choi, S. H. Kim, B. W. Eun et al., "*Streptococcus pneumoniae* serotype 19A in children, South Korea," *Emerging Infectious Diseases*, vol. 14, no. 2, pp. 275–281, 2008.

[26] M. Imöhl, R. R. Reinert, C. Ocklenburg, and M. D. van der Linden, "Association of serotypes of *Streptococcus pneumoniae* with age in invasive pneumococcal disease," *Journal of Clinical Microbiology*, vol. 48, no. 4, pp. 1291–1296, 2010.

Hindawi Publishing Corporation
BioMed Research International
Volume 2016, Article ID 4124263, 7 pages
http://dx.doi.org/10.1155/2016/4124263

Research Article

Identification of a Large *SLC25A13* Deletion via Sophisticated Molecular Analyses Using Peripheral Blood Lymphocytes in an Infant with Neonatal Intrahepatic Cholestasis Caused by Citrin Deficiency (NICCD): A Clinical and Molecular Study

Qi-Qi Zheng,[1] Zhan-Hui Zhang,[2] Han-Shi Zeng,[1] Wei-Xia Lin,[1] Heng-Wen Yang,[3] Zhi-Nan Yin,[3] and Yuan-Zong Song[1]

[1]*Department of Pediatrics, The First Affiliated Hospital, Jinan University, Guangzhou 510630, China*
[2]*Core Laboratory, The First Affiliated Hospital, Jinan University, Guangzhou 510630, China*
[3]*Biomedical Translational Research Institute, Jinan University, Guangzhou 510630, China*

Correspondence should be addressed to Yuan-Zong Song; songyuanzong@vip.tom.com

Received 3 January 2016; Accepted 23 February 2016

Academic Editor: Patrizia Cardelli

Background. Neonatal intrahepatic cholestasis caused by citrin deficiency (NICCD) is a Mendelian disorder arising from biallelic *SLC25A13* mutations, and *SLC25A13* genetic analysis was indispensable for its definite diagnosis. However, conventional *SLC25A13* analysis could not detect all mutations, especially obscure large insertions/deletions. This paper aimed to explore the obscure *SLC25A13* mutation in an NICCD infant. *Methods.* Genomic DNA was extracted to screen for 4 high-frequency *SLC25A13* mutations, and then all 18 exons and their flanking sequences were analyzed by Sanger sequencing. Subsequently, cDNA cloning, SNP analyses, and semiquantitative PCR were performed to identify the obscure mutation. *Results.* A maternally inherited mutation IVS16ins3kb was screened out, and then cDNA cloning unveiled paternally inherited alternative splicing variants (ASVs) featuring exon 5 skipping. Ultimately, a large deletion c.329-1687_c.468+3865del5692bp, which has never been described in any other references, was identified via intensive study on the genomic DNA around exon 5 of *SLC25A13* gene. *Conclusions.* An NICCD patient was definitely diagnosed as a compound heterozygote of IVS16ins3kb and c.329-1687_c.468+3865del5692bp. The large deletion enriched the *SLC25A13* mutation spectrum, and its identification supported the concept that cDNA cloning analysis, along with other molecular tools such as semiquantitative PCR, could provide valuable clues, facilitating the identification of obscure *SLC25A13* deletions.

1. Introduction

Human citrin deficiency is an autosomal recessive disease due to dysfunction of citrin, the liver-type calcium-stimulated aspartate-glutamate carrier isoform 2 (AGC2) encoded by the *SLC25A13* gene [1, 2]. Up to now, three age-dependent clinical phenotypes had been reported for this disorder, that is, adult-onset citrullinemia type 2 (CTLN2) in adolescents and adults, neonatal intrahepatic cholestasis caused by citrin deficiency (NICCD) in neonates or infants, and failure to thrive and dyslipidemia caused by citrin deficiency (FTTDCD) in older children [3–8]. Although most reported patients were Asian [9–14], citrin deficiency has been recognized as a worldwide panethnic disorder nowadays [15–19].

Due to the lack of well-recognized clinical/biochemical diagnostic criteria for NICCD, *SLC25A13* genetic analysis has been regarded as reliable tool for the definite diagnosis of such patients. However, routine *SLC25A13* genetic analyses, such as polymerase chain reaction (PCR), long and accurate-PCR (LA-PCR), PCR-restriction fragment length polymorphism (RFLP), and Sanger sequencing, could not detect all *SLC25A13* mutations, especially large deletions or insertions

of an obscure nature. It has been estimated that approximately 15% of compound heterozygotes or homozygotes carrying *SLC25A13* mutations in both alleles could not be definitely diagnosed just by the above conventional approaches [20]. In such cases, other molecular tools, although usually labor-intensive and cost-expensive, were needed to identify the obscure mutations.

In this study, a large *SLC25A13* deletion was identified via sophisticated molecular analyses using peripheral blood lymphocytes (PBLs) in an NICCD patient, who responded well to a lactose-free and medium-chain triglycerides- (MCTs-) enriched formula. We herein reported the clinical and molecular findings.

2. Subjects and Methods

2.1. Subjects and Ethics. The research subjects in this study were a male patient suspected to have NICCD and his parents as well. With the informed consent from the parents and the ethical approval by the medical ethical committee of our hospital, we performed intensive clinical and genetic study on this family.

2.2. Conventional DNA Analysis. The DNA was extracted from the peripheral venous blood following the genomic DNA extraction kit (Omega, USA) instructions. Four high-frequency *SLC25A13* mutations, c.851_854del, c.1638_1660dup, IVS6+5G>A, and IVS16ins3kb, were screened by PCR, LA-PCR, and PCR-RFLP procedures, and then Sanger sequencing of all the 18 exons and their flanking sequences was undertaken, using direct sequencing of DNA fragments amplified by genomic DNA-PCR to identify novel mutation in the gene *SLC25A13* [21].

2.3. Reverse Transcriptional PCR (RT-PCR) and Nested PCR. PBLs were separated using lymphocyte separation medium (LSM, MP) from 2-3 milliliters of ethylene diamine tetraacetic acid- (EDTA-) anticoagulant peripheral venous blood [20]. PBLs were cracked with ribonucleic acid (RNA) trizol reagent (The Life Technologies) and total RNA was extracted using a variety of organic solvents, as described previously [12, 22–25]. The cDNAs were synthesized from total RNA by Moloney murine leukemia virus (MMLV) reverse transcriptase (TaKaRa). Nested PCR was used to amplify *SLC25A13* open reading frame (ORF), and the primers and PCR temperature profile were described in detail as in previous references [21, 22]. The two primer pairs in Nested PCR were RAS2 and RACEA1 in the first PCR and RAS3 and Ex18R in the second one, with expected PCR products of 3107 bp and 2191 bp in size, respectively. Both of them contained the citrin-coding sequence (CDS).

2.4. Molecular Cloning and Alternative Splicing Variants (ASVs) Analyses. The Nested PCR products of paternal origin were purified by using a gel extraction kit (Omega) and then connected with the sequence of the pMD 18-T vector (TaKaRa) and transformed into DH5α *Escherichia coli* competent cells, as in our previous publications [12, 22, 24, 25].

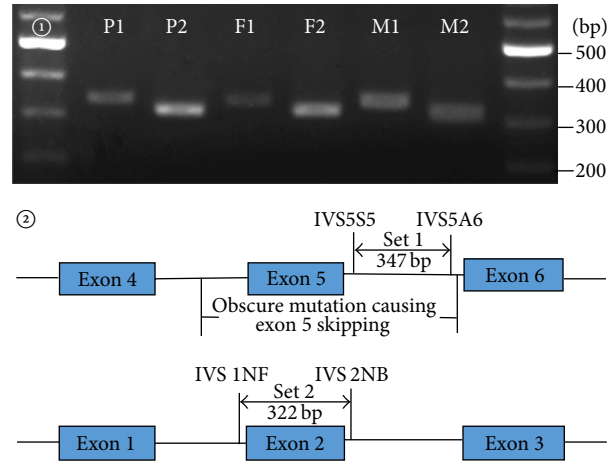

Figure 1: Semiquantitative PCR in positioning analysis of the novel large deletion. Figure 1① was a representative electrophoresis of the semiquantitative PCR products. Compared with the mother (M1), the patient (P1) and the father (F1) had less signal intensity of the PCR products when using primer Set 1, while this is not the case when using primer Set 2; note that the signal intensity of the PCR products in the patient (P2) and the father (F2) was similar to that in the mother (M2). Figure 1② depicted the positions of the primer Sets 1 and 2. The primer sequences in Set 1 were 5′-GAGCTTCTTAGAAACCACCATGTGG-3′ (IVS5S5) and 5′-TCCAATGAGG AAGAAGACTACAGGAAG-3′ (IVS5A6), while in Set 2, 5′-TTTATGCACTGGGGCAACATG-3′ (IVS 1NF) and 5′-TGCCGGGCTGACACTTTGG-3′ (IVS 2NB), respectively. The results suggested that the patient (P) and the father (F) might harbor an obscure large deletion around the primer Set 1 but not Set 2.

Following that, the transformed cells were cultured in the shaking table for 4 h and then coated on plates after centrifugation on 1000 rpm for 5 min. After cultivation in 37°C for 16 hours, the positive clones which had the targeted bands after PCR amplification were selected and sequenced. The ASV sequences were analyzed by using the ContigExpress and DNAMAN software, and their designation was according to the nomenclature guidelines [26, 27].

2.5. Further Location and Identification of the Obscure Mutation. According to the ASV structures, to further locate the DNA span around exon 5 that might contain the obscure mutation, semiquantitative PCR was performed in a total volume of 50 μL, containing 5 μL of 10x Buffer (Mg^{2+} plus) (TaKaRa), 4 μL of dNTP (10 mM), 37.75 μL of sterilized distilled water, 0.25 μL of Taq (TaKaRa), 2 μL of the forward and reverse primers together, and 1 μL of DNA template. Then, all tubes were placed into a thermal cycler and the parameters were set in 94°C for 5 minutes followed by 28 to 30 cycles of 94°C for 30 seconds, 60°C for 40 seconds, 72°C for 40 seconds, and a final extension step at 72°C for 10 minutes. The two primer pairs were IVS5S5 and IVS5A6 in Set 1 and IVS 1NF and IVS 2NB in Set 2, whose sequences and locations were displayed in Figure 1, respectively.

Based on the findings above, a PCR approach using the primers IVS4S3 and J5.6KbDelR1 (Set 3) was carried out

Table 1: Biochemical changes over time in the NICCD infant.

Biochemical indices	2.0M	2.3M	2.4M	2.5M	2.6M	2.8M	3.0M	3.7M[a]	4.8M	8.8M	17.7M
ALT (5–40 U/L)	46.00	29.80	40.39	34.48	33.00	30.00	19.23	20.00	174.00	63.00	27.00
AST (5–40 U/L)	83.00	127.50	116.92	73.47	72.00	62.00	45.02	37.00	172.00	54.00	30.00
GGT (8–50 U/L)	—	—	131.13	139.63	183.00	185.00	475.33	211.00	109.00	54.00	26.00
ALP (20–500 U/L)	—	—	246.65	205.63	259.00	201.00	269.91	385.00	418.00	243.00	251.00
TP (60.0–83.0 g/L)	33.90	66.20	67.53	66.32	62.80	63.70	65.39	54.40	61.70	66.00	62.80
Alb (35.0–55.0 g/L)	21.30	36.94	39.66	39.23	35.00	37.60	40.87	37.50	41.80	45.80	43.80
Glb (20.0–30.0 g/L)	—	29.26	27.87	27.09	27.80	26.10	24.52	16.90	19.90	20.20	19.00
Tbil (2–19 μmol/L)	178.60	163.09	172.99	92.56	56.50	60.90	63.61	38.40	44.70	3.20	6.20
Dbil (0–6 μmol/L)	70.70	66.76	79.86	48.95	35.10	31.90	35.04	31.00	36.30	1.00	2.00
Ibil (2.56–20.9 μmol/L)	107.9	96.33	93.13	43.61	21.40	29.00	28.57	7.40	8.40	2.20	4.20
TBA (0–10 μmol/L)	—	33.86	39.35	54.43	—	73.50	44.45	173.60	169.7	11.30	8.80
AFP(0–12 ng/mL)	—	—	—	—	—	—	—	10709.20	887.20	—	1.90

ALT, alanine aminotransferase; AST, aspartate aminotransferase; GGT, γ-glutamyl transpeptidase; ALP, alkaline phosphatase; TP, total protein; Alb, albumin; Glb, globulin; Tbil, total bilirubin; Dbil, direct bilirubin; Ibil, indirect bilirubin; TBA, total bile acid; AFP, alpha-feto protein. M, months of age. —, not tested.
[a]When the breast milk feeding was stopped while a galactose-free and MCT-enriched therapeutic formula was introduced.

to identify the obscure mutation. The reaction mixture was a total volume of 50 μL, containing 5 μL of 10x LA Buffer (Mg^{2+} plus) (TaKaRa), 8 μL of dNTP (10 mM), 30.3 μL of sterilized distilled water, 0.2 μL of Taq, 0.5 μL of LA Taq (TaKaRa), 4 μL of the forward and reverse primers together, and 2 μL of DNA template. The temperature profile was 95°C for 5 minutes followed by 40 cycles of 94°C for 40 seconds, 55°C for 40 seconds, 68°C for 10 minutes, and a final extension step at 68°C for 10 minutes.

2.6. Statistical Analysis. The proportions of the ASVs with exon 5 skipping in all ASVs from the patient and 8 healthy volunteers were statistically assessed using SPSS (Version 13.0) chi-square test, and a P value of less than 0.05 was considered statistically significant.

3. Results

3.1. Clinical Findings. A male infant at the age of 2 months was referred to the local hospital with the chief complaint of jaundiced skin over 10 days. Physical examination at referral revealed a mildly pale face and hemorrhagic spots scattered on the skin of whole body. The lungs were clear on auscultation. No abnormal sound or murmur was heard on heart auscultation. An enlarged liver, 5.0 cm below the right costal margin, was palpated. No pathological reflexes could be found on nervous system examination. Slightly visible pitting edema could be found in both lower extremities.

Biochemical test demonstrated elevated aspartate aminotransferase (AST), gamma-glutamyl transpeptidase (GGT), total bilirubin (Tbil), direct bilirubin (Dbil), indirect bilirubin (Ibil), and total bile acids (TBA), which indicated intrahepatic cholestasis. The albumin level was decreased while that of alpha-feto protein (AFP) elevated markedly (Table 1). Ultrasonography revealed hepatomegaly, ascites, and abdominal bloating, along with a patent oval foramen of the heart. The urinary gas chromatography mass spectrometry (GC-MS) analysis discovered large quantity of hexanedioic acid and 4-hydroxyphenyl lactate (4HPL), and on tandem mass spectrometry (MS-MS) analysis, elevated levels of citrulline and arginine were detected.

NICCD was thus suspected based on the above clinical and biochemical findings, and according to the pediatrician's advice, breast feeding was stopped and a lactose-free and MCT-enriched therapeutic formula was introduced immediately. In the subsequent follow-up, the clinical manifestations were alleviated gradually. At his age of 3.7 months, the infant was referred to our hospital to confirm the NICCD diagnosis by *SLC25A13* gene analyses.

3.2. Screening and Sequencing Results. Screening of the 4 high-frequency mutations proved that the patient harbored a maternally inherited mutation IVS16ins3kb, but another mutation was not detected. Even after Sanger sequencing of all the 18 exons and their flanking sequences, the *SLC25A13* mutation of paternal origin remained obscure. Therefore, cDNA cloning analysis was undertaken to facilitate the identification of the obscure mutation.

3.3. Findings of cDNA Cloning Analysis. As the maternal mutation IVS16ins3kb led to production of an aberrant mRNA molecule with a new exon 17, losing the normal exons 17 and 18 [21], only the ASVs transcribed from the paternal *SLC25A13* allele were amplified by the Nested PCR approach using the two reverse primers both within the normal exon 18 of *SLC25A13* gene. In other words, the 26 ASVs in Table 2 all resulted from the paternally inherited *SLC25A13* allele.

Similar to our previous findings [22], these ASVs demonstrated remarkable structural heterogeneity. However, all these ASVs featured exon 5 skipping (*r*.329_468del), as shown in Table 2. When compared with the ASVs in the 8 healthy volunteers which had been reported previously [24], exon 5 skipping was a unique structural feature of the ASVs in this patient ($\chi^2 = 129.2$ and $P < 0.01$ as in Table 3), strongly suggesting the existence of a large insertion or deletion around exon 5 at the DNA level.

Table 2: The *SLC25A13* ASVs detected by cDNA analysis in the NICCD patient.

Clones	Alternative splicing variants (ASVs)	Annotations
C0282-1	*r*.213_468del; *r*.1194A>G	Exons 4 and 5 skipping
C0282-2	*r*.70_468del; *r*.1194A>G	Exons 3, 4, and 5 skipping
C0282-3	*r*.70_468del; *r*.1194A>G	Exons 3, 4, and 5 skipping
C0282-4	*r*.213_468del; 1311_1312ins1311+102_1312+176; *r*.1194A>G	Exons 4 and 5 skipping
C0282-5	*r*.213_468del; *r*.616_848del; *r*.1194A>G	Exons 4, 5, 7, and 8 skipping
C0282-6	*r*.70_468del; *r*.1194A>G	Exons 3, 4, and 5 skipping
C0282-7	*r*.329_468del; *r*.1194A>G	Exon 5 skipping
C0282-8	*r*.213_468del; *r*.755_848del; *r*.1194A>G	Exons 4, 5, and 8 skipping
C0282-9	*r*.329_468del; *r*.1194A>G	Exon 5 skipping
C0282-10	*r*.70_468del; *r*.1194A>G	Exons 3, 4, and 5 skipping
C0282-11	*r*.70_468del; *r*.1194A>G	Exons 3, 4, and 5 skipping
C0282-12	*r*.213_468del; 1311_1312ins1311+102_1312+176; *r*.1194A>G	Exons 4 and 5 skipping
C0282-13	*r*.213_468del; *r*.993_1018del; *r*.1194A>G	Exons 4 and 5 skipping
C0282-14	*r*.213_468del; *r*.1194A>G	Exons 4 and 5 skipping
C0282-15	*r*.213_468del; *r*.1194A>G	Exons 4 and 5 skipping
C0282-16	*r*.70_468del; *r*.1194A>G	Exons 3, 4, and 5 skipping
C0282-17	*r*.213_468del; *r*.755_848del; *r*.1194A>G	Exons 4, 5, and 8 skipping
C0282-18	*r*.213_468del; *r*.1194A>G	Exons 4 and 5 skipping
C0282-19	*r*.70_468del; *r*.1194A>G	Exons 3, 4, and 5 skipping
C0282-20	*r*.213_468del; 1311_1312ins1311+102_1312+176; *r*.1194A>G	Exons 4 and 5 skipping
C0282-21	*r*.213_468del; *r*.1194A>G	Exons 4 and 5 skipping
C0282-22	*r*.213_468del; *r*.755_848del; *r*.1194A>G	Exons 4, 5, and 8 skipping
C0282-23	*r*.213_468del; *r*.755_848del; *r*.1194A>G	Exons 4, 5, and 8 skipping
C0282-24	*r*.213_468del; *r*.1194A>G	Exons 4 and 5 skipping
C0282-25	*r*.213_468del; *r*.1194A>G	Exons 4 and 5 skipping
C0282-26	*r*.213_468del; 1311_1312ins1311+102_1312+176; *r*.1194A>G	Exons 4 and 5 skipping

The ASVs in this table were described according to the nomenclature guidelines [26, 27]; nucleotide numbering was based on cDNA sequence (GenBank: NM_014251), with +1 indicating the A of the ATG-translation initiation codon.

Table 3: *SLC25A13* ASVs harboring *r*.329_468del in the patient C0282 and 8 healthy volunteers.

Subjects	*SLC25A13* ASVs		χ^2	P
	With *r*.329_468 skipping	Without *r*.329_468 skipping		
C0282	26 (100%)	0 (0.0%)	129.2	<0.01
Volunteers	1 (0.9%)	115 (99.1%)		

Correction for continuity was performed for χ^2 calculation in this table.

3.4. Positioning and Sequencing Analysis of the Obscure Mutation. Based on the findings above, a diversity of primers was designed and PCR amplification conducted to analyze a variety of SNPs within the DNA fragment around exon 5 in all 3 family members. Although no clues suggestive of the obscure mutation could be detected by these analyses, semiquantitative PCR had positive findings—when amplified using the primer Set 1 near exon 5, the DNA samples of the patient (P1) and the father (F1) had less PCR products in comparison to that of the mother (M1), but this is not the case when using the primer Set 2 covering the entire exon 2 (Figure 1), indicating that the patient and the father might have a large deletion or insertion involving the positions of the primer Set 1. According to this result, LA-PCR amplification using the primer Set 3 (Figure 2) yielded an unexpected band of 632 bp in size in the patient and father, besides the expected 6324 bp product as in the mother, and subsequent Sanger sequencing of the unexpected product uncovered a large deletion c.329-1687_c.468+3865del5692bp.

4. Discussion

Although a maternally originated *SLC25A13* mutation IVS16ins3kb had been discovered as a high-frequency mutation in this study, conventional genetic analyses, such as PCR/LA-PCR, PCR-RFLP, and Sanger sequencing, could not unveil the paternally inherited mutation in the infant with typical clinical and biochemical features of intrahepatic cholestasis, making the definite diagnosis of NICCD a challenge. It was by using cDNA cloning along with SNP

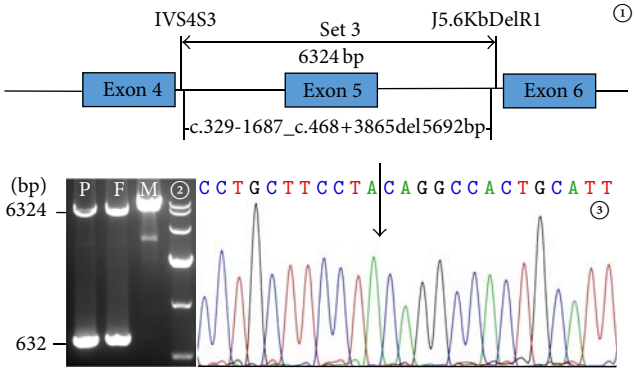

Figure 2: The large deletion mutation in *SLC25A13* gene of the infant and his father. Figure 2① depicted the positions of the primer Set 3 and the novel large deletion. The primer sequences were 5′-AAGATTGTTGTTTATGGTGAGAC-3′ for IVS4S3 and 5′-ATGGTTTGCCCGACATGAGTAATC-3′ for J5.6KbDelR1, respectively. In Figure 2②, LA-PCR with the primer Set 3 revealed that the patient (P) and his father (F), but not the mother (M), had an unexpected band of 632 bp in size besides the normal product of 6324 bp. Figure 2③ was a segmental sequencing result of the unexpected PCR product. The arrow indicated the breakpoint arising from the large deletion.

analysis and semiquantitative PCR in all family members that c.329-1687_c.468+3865del5692bp, a large deletion, was finally identified, which has never been described in any other references. Although time- and cost-consuming, the identification of this novel deletion confirmed the feasibility of *SLC25A13* cDNA cloning analysis using PBLs as a molecular tool facilitating the identification of large deletions and provided reliable evidence for the definite diagnosis of NICCD in the patient along with the mutation IVS16ins3kb of maternal origin. This was important not only for the proband himself but also for future genetic counseling and antenatal diagnosis in the family.

This 5692 bp deletion resulted in exon 5 skipping at mRNA level, as described in Table 2, theoretically yielding a truncated citrin protein of 127 amino acids—the exon 5 skipping gave rise to a frameshift at codon 110, continued to translate 17 amino acids, and then encountered a terminator codon at the position of 127, eventually producing an aberrant citrin molecule p.E110fs127X. Interestingly, this truncated citrin molecule was the same as the one arising from the large insertion IVS4ins6kb which had been reported very recently by our group [24]. The aberrant mRNA with exon 5 skipping could be a target for nonsense-mediated mRNA decay (NMD). Moreover, according to the molecular structural feature of mitochondrial AGCs (aspartate/glutamate carriers) [28], such a truncated citrin molecule predictively lost the entire mitochondrial carrier domain and had no AGC2 function to export aspartate and import glutamate together with a proton into the mitochondrial matrix, thus causing a series of metabolic disturbances and finally leading to the formation of the laboratory and clinical presentations in the patient.

The lactose-free and MCT-enriched formulas have been reported to be clinically and biochemically effective for NICCD patients in increasing clinical cases [12, 25, 29–31]. The clinical process in this study further supported this concept. Overall, the increased cytosolic NADH/NAD^+ ratio in hepatocytes has been well-recognized as a key biochemical alteration for citrin deficiency [6]. Breast milk or common formula contained high carbohydrate in the form of lactose, a well-known disaccharide that was easily digested by lactase on the intestinal mucosa into glucose and galactose, both of which were then rapidly absorbed into the blood flow. In hepatocytes, galactose was conversed via Leloir pathway into glucose [32], the metabolism of which produced NADH, and thus increased the cytosolic NADH/NAD^+ ratio in the liver and caused liver damage in patients with citrin deficiency [6, 31]. Moreover, secondary galactosemia due to citrin deficiency might be involved in the NICCD pathogenesis—the increased cytosolic NADH/NAD^+ ratio in citrin-deficient hepatocytes might inhibit the activity of uridine diphosphate-(UDP-) galactose-4-epimerase [33], leading to accumulation of a large quantity of galactitol and galactonate [34], and galactitol has been suggested as one of the substrates causing jaundice, hepatosplenomegaly, hepatocellular insufficiency, and cataracts [30, 35, 36].

Energy shortage in the liver caused by an impairment of glycolysis due to an increased NADH/NAD^+ ratio has been proposed as an important pathophysiology in citrin deficiency [31, 37]. Since the galactose kinase reaction in Leloir pathway was energy-consuming [32], the galactose metabolism in hepatocytes inevitably exacerbated such a pathophysiology. On the other hand, the absorption of MCTs was not bile acid-dependent, which might reduce the burden of the liver to synthesize and excrete bile salt into the gut [30]. Of particular note, MCTs can be better absorbed and transported via the portal vein into the liver and were mainly metabolized to acetyl-CoA along with $FADH_2$ and NADH, which could supply more such substrates to hepatic cells as energy sources [31]. Taking all these factors together, it was not surprising for the NICCD infant in this study to respond well to the lactose-free and MCT-enriched therapeutic formula.

In summary, by sophisticated molecular analysis using PBLs, this study definitely diagnosed an NICCD patient who was a compound heterozygote of the IVS16ins3kb mutation and a novel deletion c.329-1687_c.468+3865del5692bp in the *SLC25A13* gene. The large deletion constituted a novel component in the *SLC25A13* mutation spectrum, and its identification lent further support to the concept that *SLC25A13* cDNA cloning analysis using PBLs, along with other molecular tools such as semiquantitative PCR, could provide valuable clues, facilitating the identification of unknown large deletions.

Abbreviations

NICCD:	Neonatal intrahepatic cholestasis caused by citrin deficiency
SLC25A13:	Solute carrier family 25, member 13
DNA:	Deoxyribonucleic acid
cDNA:	Complementary deoxyribonucleic acid
SNP:	Single nucleotide polymorphism

PCR:	Polymerase chain reaction
ASVs:	Alternative splicing variants
CTLN2:	Adult-onset citrullinemia type 2
FTTDCD:	Failure to thrive and dyslipidemia caused by citrin deficiency
LA-PCR:	Long and accurate-polymerase chain reaction
PCR-RFLP:	Polymerase chain reaction-restriction fragment length polymorphism
PBLs:	Peripheral blood lymphocytes
MCTs:	Medium-chain triglycerides
RT-PCR:	Reverse transcriptional polymerase chain reaction
LSM:	Lymphocyte separation medium
EDTA:	Ethylene diamine tetraacetic acid
RNA:	Ribonucleic acid
MMLV:	Moloney murine leukemia virus
ORF:	Open reading frame
CDS:	Coding sequence
AST:	Aspartate aminotransferase
GGT:	Gamma-glutamyl transpeptidase
Tbil:	Total bilirubin
Dbil:	Direct bilirubin
Ibil:	Indirect bilirubin
TBA:	Total bile acids
AFP:	Alpha-feto protein
GC-MS:	Gas chromatography mass spectrometry
4HPL:	4-Hydroxyphenyl lactate
MS-MS:	Tandem mass spectrometry
NMD:	Nonsense-mediated mRNA decay
AGC:	Aspartate/glutamate carrier
NADH:	Reduced form of nicotinamide adenine dinucleotide
NAD^+:	Nicotinamide adenine dinucleotide
UDP-galactose-4-epimerase:	Uridine diphosphate-galactose-4-epimerase.

Competing Interests

The authors declare that they have no competing interests.

Acknowledgments

The authors would like to express their deep appreciation to all research subjects for their kind cooperation. The research was financially supported by the Cultivation Foundation for Scientific Research (nos. 2014208 and A2014101) approved by the First Affiliated Hospital, Jinan University, the Medical Scientific Research Foundation of Guangdong Province (A2014385), the Fundamental Research Funds for the Central Universities (no. 21615470), and the projects supported by the National Natural Science Foundation of China (nos. 81270957 and 81570793).

References

[1] K. Kobayashi, D. S. Sinasac, M. Iijima et al., "The gene mutated in adult-onset type II citrullinaemia encodes a putative mitochondrial carrier protein," *Nature Genetics*, vol. 22, no. 2, pp. 159–163, 1999.

[2] L. Palmieri, B. Pardo, F. M. Lasorsa et al., "Citrin and aralar1 are Ca^{2+}-stimulated aspartate/glutamate transporters in mitochondria," *The EMBO Journal*, vol. 20, no. 18, pp. 5060–5069, 2001.

[3] T. Ohura, K. Kobayashi, Y. Tazawa et al., "Neonatal presentation of adult-onset type II citrullinemia," *Human Genetics*, vol. 108, no. 2, pp. 87–90, 2001.

[4] Y. Tazawa, K. Kobayashi, T. Ohura et al., "Infantile cholestatic jaundice associated with adult-onset type II citrullinemia," *The Journal of Pediatrics*, vol. 138, no. 5, pp. 735–740, 2001.

[5] T. Tomomasa, K. Kobayashi, H. Kaneko et al., "Possible clinical and histologic manifestations of adult-onset type II citrullinemia in early infancy," *The Journal of Pediatrics*, vol. 138, no. 5, pp. 741–743, 2001.

[6] T. Saheki and K. Kobayashi, "Mitochondrial aspartate glutamate carrier (citrin) deficiency as the cause of adult-onset type II citrullinemia (CTLN2) and idiopathic neonatal hepatitis (NICCD)," *Journal of Human Genetics*, vol. 47, no. 7, pp. 333–341, 2002.

[7] Y.-Z. Song, M. Deng, F.-P. Chen et al., "Genotypic and phenotypic features of citrin deficiency: five-year experience in a Chinese pediatric center," *International Journal of Molecular Medicine*, vol. 28, no. 1, pp. 33–40, 2011.

[8] K. Kobayashi, T. Saheki, and Y. Z. Song, "Citrin deficiency," in *GeneReviews®*, R. A. Pagon, M. P. Adam, H. H. Ardinger et al., Eds., University of Washington, Seattle, Wash, USA, 1993–2015.

[9] M. K. Thong, C. C. M. Boey, J. S. Sheng, M. Ushikai, and K. Kobayashi, "Neonatal intrahepatic cholestasis caused by citrin deficiency in two Malaysian siblings: outcome at one year of life," *Singapore Medical Journal*, vol. 51, no. 1, pp. e12–e14, 2010.

[10] B. H. Lee, H. Y. Jin, G.-H. Kim, J.-H. Choi, and H.-W. Yoo, "Nonalcoholic fatty liver disease in 2 siblings with adult-onset type II citrullinemia," *Journal of Pediatric Gastroenterology and Nutrition*, vol. 50, no. 6, pp. 682–685, 2010.

[11] A. Kikuchi, N. Arai-Ichinoi, O. Sakamoto et al., "Simple and rapid genetic testing for citrin deficiency by screening 11 prevalent mutations in SLC 25A13," *Molecular Genetics and Metabolism*, vol. 105, no. 4, pp. 553–558, 2012.

[12] Z.-H. Zhang, W.-X. Lin, M. Deng et al., "Clinical, molecular and functional investigation on an infant with neonatal intrahepatic cholestasis caused by citrin deficiency (NICCD)," *PLoS ONE*, vol. 9, no. 2, Article ID e89267, 2014.

[13] M.-H. Zhang, J.-Y. Gong, and J.-S. Wang, "Citrin deficiency presenting as acute liver failure in an eight-month-old infant," *World Journal of Gastroenterology*, vol. 21, no. 23, pp. 7331–7334, 2015.

[14] S. Bijarnia-Mahay, J. Häberle, V. Rüfenacht, Y. Shigematsu, R. Saxena, and I. Verma, "Citrin deficiency: a treatable cause of acute psychosis in adults," *Neurology India*, vol. 63, no. 2, pp. 220–222, 2015.

[15] D. Dimmock, K. Kobayashi, M. Iijima et al., "Citrin deficiency: a novel cause of failure to thrive that responds to a high-protein, low-carbohydrate diet," *Pediatrics*, vol. 119, no. 3, pp. e773–e777, 2007.

[16] T. Hutchin, M. A. Preece, C. Hendriksz et al., "Neonatal intrahepatic cholestasis caused by citrin deficiency (NICCD) as a cause of liver disease in infants in the UK," *Journal of Inherited Metabolic Disease*, vol. 32, no. 1, supplement, pp. S151–S155, 2009.

[17] G. Fiermonte, G. Parisi, D. Martinelli et al., "A new Caucasian case of neonatal intrahepatic cholestasis caused by citrin deficiency (NICCD): a clinical, molecular, and functional study," *Molecular Genetics and Metabolism*, vol. 104, no. 4, pp. 501–506, 2011.

[18] I. Vitoria, J. Dalmau, C. Ribes et al., "Citrin deficiency in a Romanian child living in Spain highlights the worldwide distribution of this defect and illustrates the value of nutritional therapy," *Molecular Genetics and Metabolism*, vol. 110, no. 1-2, pp. 181–183, 2013.

[19] D. M. Avdjieva-Tzavella, M. B. Ivanova, T. P. Todorov et al., "First bulgarian case of citrin deficiency caused by one novel and one recurrent mutation in the SLC25A13 gene," *Genetic Counseling*, vol. 25, no. 3, pp. 271–276, 2014.

[20] D. Tokuhara, M. Iijima, A. Tamamori et al., "Novel diagnostic approach to citrin deficiency: analysis of citrin protein in lymphocytes," *Molecular Genetics and Metabolism*, vol. 90, no. 1, pp. 30–36, 2007.

[21] A. Tabata, J.-S. Sheng, M. Ushikai et al., "Identification of 13 novel mutations including a retrotransposal insertion in SLC25A13 gene and frequency of 30 mutations found in patients with citrin deficiency," *Journal of Human Genetics*, vol. 53, no. 6, pp. 534–545, 2008.

[22] Z.-H. Zhang, W.-X. Lin, M. Deng, X.-J. Zhao, and Y.-Z. Song, "Molecular analysis of SLC25A13 gene in human peripheral blood lymphocytes: marked transcript diversity, and the feasibility of cDNA cloning as a diagnostic tool for citrin deficiency," *Gene*, vol. 511, no. 2, pp. 227–234, 2012.

[23] W.-X. Lin, Z.-H. Zhang, M. Deng, X.-R. Cai, and Y.-Z. Song, "Multiple ovarian antral follicles in a preterm infant with neonatal intrahepatic cholestasis caused by citrin deficiency: a clinical, genetic and transcriptional analysis," *Gene*, vol. 505, no. 2, pp. 269–275, 2012.

[24] Y.-Z. Song, Z.-H. Zhang, W.-X. Lin et al., "SLC25A13 gene analysis in citrin deficiency: sixteen novel mutations in East Asian patients, and the mutation distribution in a large pediatric cohort in China," *PLoS ONE*, vol. 8, no. 9, Article ID e74544, 2013.

[25] H.-S. Zeng, S.-T. Zhao, M. Deng et al., "Inspissated bile syndrome in an infant with citrin deficiency and congenital anomalies of the biliary tract and esophagus: identification and pathogenicity analysis of a novel SLC25A13 mutation with incomplete penetrance," *International Journal of Molecular Medicine*, vol. 34, no. 5, pp. 1241–1248, 2014.

[26] J. T. den Dunnen and S. E. Antonarakis, "Mutation nomenclature extensions and suggestions to describe complex mutations: a discussion," *Human Mutation*, vol. 15, no. 1, pp. 7–12, 2000.

[27] J. T. den Dunnen and E. Antonarakis, "Nomenclature for the description of human sequence variations," *Human Genetics*, vol. 109, no. 1, pp. 121–124, 2001.

[28] C. Thangaratnarajah, J. J. Ruprecht, and E. R. S. Kunji, "Calcium-induced conformational changes of the regulatory domain of human mitochondrial aspartate/glutamate carriers," *Nature Communications*, vol. 5, article 5491, 2014.

[29] T. Ohura, K. Kobayashi, Y. Tazawa et al., "Clinical pictures of 75 patients with neonatal intrahepatic cholestasis caused by citrin deficiency (NICCD)," *Journal of Inherited Metabolic Disease*, vol. 30, no. 2, pp. 139–144, 2007.

[30] Y. Z. Song, F. Wen, F. P. Chen, K. Kobayashi, and T. Saheki, "Neonatal intrahepatic cholestasis caused by citrin deficiency: efficacy of therapeutic formulas and update of clinical outcomes," *Japanese Journal for Inherited Metabolic Diseases*, vol. 26, no. 1, pp. 57–69, 2010.

[31] K. Hayasaka, C. Numakura, K. Toyota, and T. Kimura, "Treatment with lactose (galactose)-restricted and medium-chain triglyceride-supplemented formula for neonatal intrahepatic cholestasis caused by citrin deficiency," in *JIMD Reports—Case and Research Reports, 2011/2*, SSIEM, Ed., vol. 2 of *JIMD Reports*, pp. 37–44, 2012.

[32] P. A. Frey, "The Leloir pathway: a mechanistic imperative for three enzymes to change the stereochemical configuration of a single carbon in galactose," *The FASEB Journal*, vol. 10, no. 4, pp. 461–470, 1996.

[33] T. Saheki, K. Kobayashi, M. Iijima et al., "Pathogenesis and pathophysiology of citrin (a mitochondrial aspartate glutamate carrier) deficiency," *Metabolic Brain Disease*, vol. 17, no. 4, pp. 335–346, 2002.

[34] Y.-Z. Song, B.-X. Li, F.-P. Chen et al., "Neonatal intrahepatic cholestasis caused by citrin deficiency: clinical and laboratory investigation of 13 subjects in mainland of China," *Digestive and Liver Disease*, vol. 41, no. 9, pp. 683–689, 2009.

[35] C. Ning, R. Reynolds, J. Chen et al., "Galactose metabolism by the mouse with galactose-1-phosphate uridyltransferase deficiency," *Pediatric Research*, vol. 48, no. 2, pp. 211–217, 2000.

[36] A. M. Bosch, "Classical galactosaemia revisited," *Journal of Inherited Metabolic Disease*, vol. 29, no. 4, pp. 516–525, 2006.

[37] K. Hayasaka, C. Numakura, and H. Watanabe, "Treatment and pathomechanism of citrin deficiency," *Brain and Nerve*, vol. 67, no. 6, pp. 739–747, 2015.